# Acid based recovery of PGMs from spent autocatalytic convertors using $AlCl_3$ and HOCl

**Collins Tatenda Saguru**

A dissertation submitted to the Faculty of Engineering and the Built Environment, University of the Witwatersrand, Johannesburg, in fulfilment of the requirements for the degree of Master of Science in Engineering.

Johannesburg,

03 December 2018

## Declaration

I declare that this dissertation is my own unaided work which is being submitted for the degree of Master of Science in Engineering to the University of the Witwatersrand, Johannesburg, South Africa.

It has not been submitted before for any degree or examination to any other University.

……...

(Signature of Candidate)

……day of……2018

(Day) (Month) (Year)

## Abstract

The environmental importance of the platinum group metals (PGMs) for catalytic reduction and oxidation of toxic gases emitted by internal combustion engines has been responsible for the increasing demand for these metals. Consequentially, the majority of PGMs have been reporting to end-of-life autocatalytic convertor scrap, providing an opportunity for recycling, to recover the PGMs. A combination of pyrometallurgy and hydrometallurgy is employed in most of the current global industrial recycling centres. However, an exclusively hydrometallurgical process has some advantages over the current industrial establishments, chief amongst them being the lower energy consumption as a result of eliminating the smelting step. The aim of this study was to investigate the leaching of the PGMs via a purely hydrometallurgical process, using readily available and environmental friendly reagents. Platinum (Pt), palladium (Pd) and rhodium (Rh) were leached into a chloride solution under acidic, oxidizing conditions. $AlCl_3$ and HOCl obtained after $Ca(OCl)_2$ dissolution, were used as the complexing/acidifying and oxidising agent respectively. Maximum leaching efficiencies of 15%, 78% and 86% for Rh, Pt and Pd respectively were obtained from preliminary experiments designed using the central composite methodology. A second battery of experiments using the one factor at a time methodology and compounding on insights obtained from the preliminary set of experiments was conducted. Recoveries of Pt, Pd and Rh were improved to 99%, 99% and 68% under optimised conditions of 100 $^oC$, 1.2 M $AlCl_3$, 0.15 M $Ca(OCl)_2$ and S/L ratio of 3g : 10ml.

Solvent extraction of both Pt and Pd was conducted to illustrate the feasibility of co-extracting the 2 PGMs into a tri-iso octyl amine (Alamine 308) in Kerosene with n-Decanol organic phase. Recoveries from pregnant leach liquor of 99.6% and 87% for Pd and Pt were recorded, using a 4 stage batch simulation process for a continuous counter current solvent extraction process. There was negligible co-extraction of other metals except for Fe, which had an extraction into the organic phase of 98 %. Pt and Pd could then be selectively stripped using 0.5 M HCl with 2 different concentrations of thiourea. An exclusively hydrometallurgical process was therefore developed with overall recoveries for Pt, Pd and Rh of 85 %, 97 % and 67 % respectively. A preliminary cost benefit analysis based on operating costs alone was conducted, which revealed that the process could attain an operational profit margin of approximately 9.9 % / oz. (3E).

## Acknowledgements

First of all, I would like to express a lot of gratitude to my family; my parents, sisters Tanaka and Lisa snr and most importantly my daughter Lisa Saguru, jnr.; for all the support and inspiration they gave to me in the last 2 years. Clearly, this would not have been an easy road without their support.

I would also love to acknowledge my supervisor, Professor Sehliselo Ndlovu, for the support and direction she gave during the research period. Special mention goes to Professor Marek Dwornazowski as well, for his efforts in improving the quality and industrial relevance of the project.

Many thanks also go to the Metal Extraction and Recovery Research group under Professor Ndlovu for their invaluable input throughout the different stages of the research. The support staff in the school of Chemical and Metallurgical Engineering is also acknowledged for the very important roles they played towards the success of this research project.

Lastly, I would like dedicate this research to the prospect of a better African future premised on engineering for sustainability.

## Publications

Saguru, C., Ndlovu, S., 2017. *Preliminary study on PGM leaching from used autocatalytic convertors using $AlCl_3$ and HOCl*, in: Production and Recycling of Non-Ferrous Metals: Saving Resources for a Sustainable Future. European Metallurgical Conference 2017, GDMB, Leipzig, Germany, pp. 55–70.

Collins Saguru, Sehliselo Ndlovu, Desiree Moropeng, *A review of recent studies into hydrometallurgical methods for recovering PGMs from used catalytic converters*, **Hydrometallurgy**, Volume 182, 2018, Pages 44-56, ISSN 0304-386X, https://doi.org/10.1016/j.hydromet.2018.10.012.

Makua, L., Saguru, C., Ndlovu, S., 2017. PGM recovery using Alamine 308 from used autocatalytic converter leach solution, *(manuscript under review)*

# Table of contents

## List of figures

# List of tables

## Nomenclature

[Bmim][$Tf_2N$] - 1-butyl-3-methylimidazolium bis(triflouro-methylsulfonyl)imide

[$C_4$mim][$PF_6$] - 1-butyl-3-methylimidazolium hexafluorophosphate

[Hmim][$Tf_2N$] - 1-hexyl-3-methylimidazolium bis(triflouro-methylsulfonyl)imide

[Omim][$Tf_2N$] - 1-octyl-3-methylimidazolium bis(triflouro-methylsulfonyl)imide

A/O – aqueous solution to organic solution volume ratio

Cyphos®IL 101 - trihexyl(tetradecyl)phosphonium chloride

Cyphos®IL 102 - trihexyl(tetradecyl)phosphonium bromide

Cyphos®IL 105 - trihexyl(tetradecyl)phosphonium dicyanamide

MRT – Molecular recognition technology

MSCs – Metallic Supported Converters

PGMs – Platinum Group Metals

SAC – Spent Autocatalytic Converter

SX – Solvent Extraction

# Chapter 1 : Introduction

## 1.1 Motivation and background

The autocatalytic converter is a device that was first designed and patented by Eugene Houdry in the 1950s (Houdry, 1956). It was designed as a response to the increasing amount of polluting gaseous emissions from the rising global fleet of automobiles and increasing industrial activity. Shortly afterwards, the Clean Air Act was revised in 1970 to address the growing contribution of automobiles and other sources of air pollutants (McCarthy et al., 2011). Legislation elsewhere was enacted later, e.g. the Euro Standards of 1993, to address the same problem of industrial and vehicular air pollution. This intervention at policy level may have been largely responsible for the decreasing amounts of global pollutants as illustrated in Figure 1.1, consequently fuelling the growth of the autocatalytic manufacturing industry.

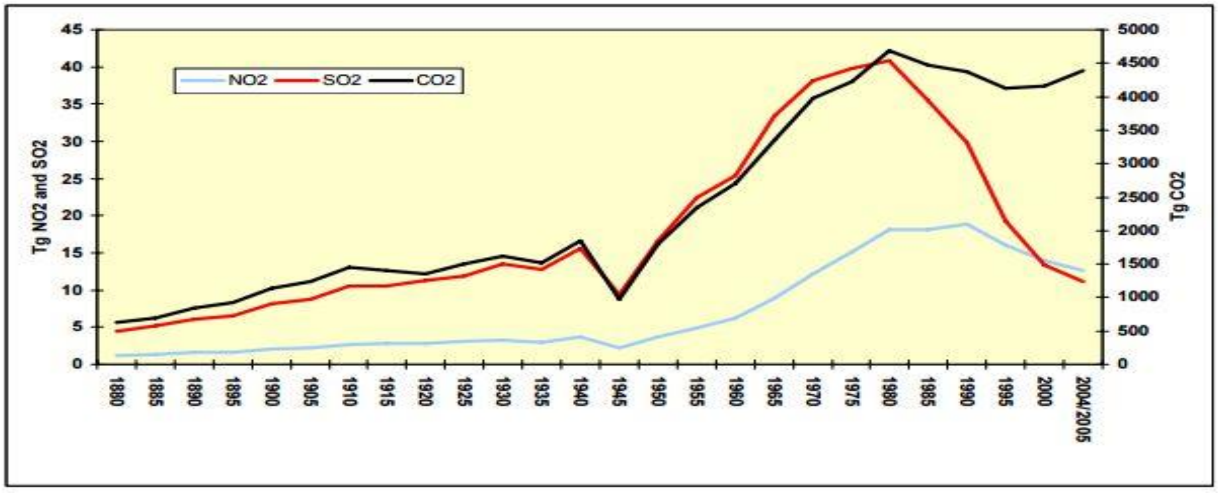


Figure 1.1: Variation of of NOx, $SO_2$ and $CO_2$ in the atmosphere from 1850 to 2015

In line with global trends to promote environmentally sustainable development, these pieces of legislation have consistently been tightened and revised over the years. The US Clean air act has been revised 3 times, the latest revision being in 1990, and the European Emission standards, a total of 6 times since the Euro 1 standard of 1993, with each revision providing stricter emission tolerances. The active and proven technology to meet these tolerances has been the autocatalytic converter containing different amounts of the PGMs: Platinum (Pt), Palladium (Pd) and Rhodium (Rh) as active catalysts to convert toxic emissions to less toxic gases. In South Africa,

the autocatalytic manufacturing industry was instituted in the 1990s and grew substantially due to government support via the Motor Industry and Development Program (MIDP). The industry has grown at an average of 14% per annum since its initiation. At its peak, it generated ZAR 20 Billion for the country, representing 15% global production of autocatalytic converters (Dewar, 2012). It has also been a major consumer of locally produced steel and a major direct and indirect employer of both skilled and unskilled labour.

The growth of this industry has subsequently increased the global demand for platinum, palladium and rhodium, which are used in the manufacture of catalytic convertors. The demand trend for the three PGMs is illustrated in Figure 1.2 for the period 2010 to 2014. The figure illustrates the dominant contribution of auto catalyst converter manufacture on global PGM demand. The manufacturing of autocatalytic converters has consistently contributed over 70 % to global demand for the 3 PGMs.

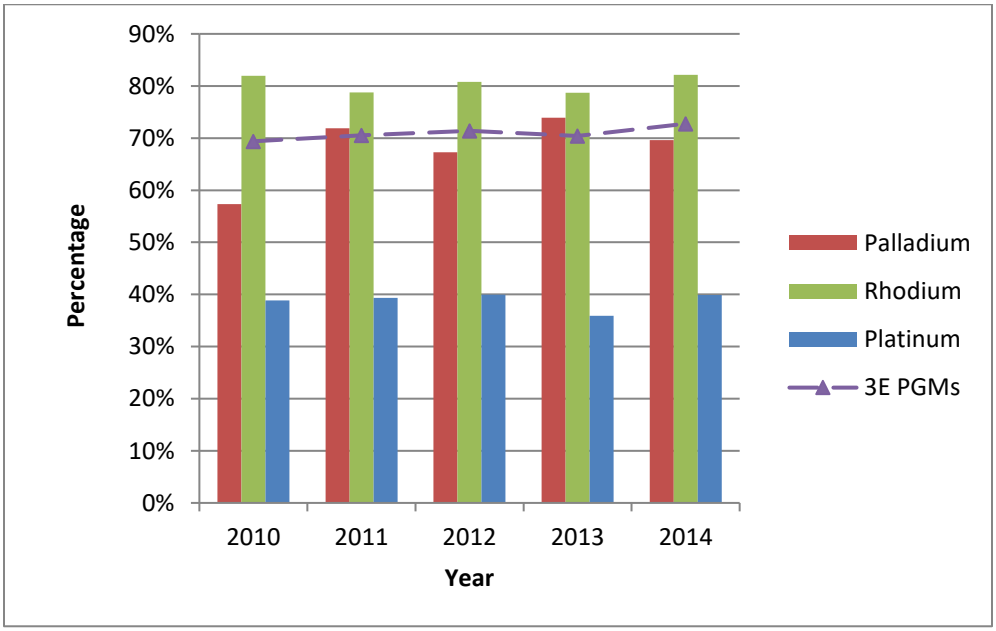


Figure 1.2: Percentage consumption of PGMs in the manufacture of autocatalytic converters (2010 – 2014) (Johnson Matthey, 2016)

This growth in demand for PGMs has consistently been satisfied by supply from mining and pyrometallurgical recycling. In response to the growing PGM demand and increasing PGM

prices, academia has also directed research efforts into development of alternative materials that can perform the same catalysis reactions as PGMs in autocatalytic converters. The purpose was to develop or identify cheaper PGM substitutes of comparable catalytic efficiency, so as to reduce the demand on PGMs for autocatalysis. Very little progress has however, been registered on this front as reported by Watts et al., (2008). Sherif, (1995) patented a method for synthesizing transition metal carbides to replace PGMs as catalysts; however, no commercial application could be identified for these carbides. Significant research under the NextGenCat initiative funded by the EU was also directed towards the replacement of PGMs by employing efficient nanostructured catalysts that incorporate lower costing nanoparticles within the supporting structure ("NextGenCat Overview," n.d.). Using this funding instrument, Glisenti et al., (2014) published a new process for the synthesis of titanates dopped with Cu and Co whose efficiency for CO oxidation and NO reduction were evaluated. Schön et al., (2015) also published an evaluation of the efficiency of a surface-modified perovskite based catalyst for 3 way catalysis. Notwithstanding all these strides to replace PGMs, the unparalled efficiency of the PGMs as catalysts for reducing emissions makes it highly unlikely that they will be replaced as the automotive catalysts of choice in the near future. As a result of the slow progress in reducing demand for PGMs by finding suitable alternatives, mining and recycling are therefore, the only sources of PGMs that are available for meeting the demand.

Global PGM supply from mining activities is controlled by South Africa and Russia (Johnson Matthey, 2016). South Africa has an estimated 80% of the global platinum reserves and contributed 70% of platinum supply, 35% of palladium supply and 75% of rhodium supply in 2014 (Johnson Matthey, 2016). However, mining activity in South Africa has encountered numerous challenges. Erratic energy supply negatively impacted mining economics when a two week power outage from 25 January 2008 reduced annual production by 3% (Yang, 2009). Labour constraints also negatively impacted the supply dynamics from platinum mining as evidenced by the 2014, five month strike that reduced overall production by about 29%, (KPMG, 2015). Declining ore grades in the BushVeld complex have also been negatively impacting the industry supply economics. KPMG (2015) reported that historically, 10 tons had to be processed to produce 1 ounce of platinum, a number that has recently grown to around 20 - 40 tons. Kolesnikova, (2013) reported that Russia's palladium base was also dwindling, meaning that

supply from palladium mining alone can no longer be depended on. Stringent environmental protection laws and calls for sustainable mining have also increased the operation costs of the mining companies. The combined effect of all the stated factors is an increase in operating costs, which have made PGM mining commercially strenuous.

The lack of alternative materials for the catalysis reactions taking place in autocatalytic converters and challenges currently being faced by the mining industry thereby demands that recycling be considered as a potential source of PGMs. As a result, recycling end of life autocatalytic converters has been contributing to the supply of PGMs since the early 2000s and has consequently been on a steady growth pattern as illustrated in Figure 1.3.

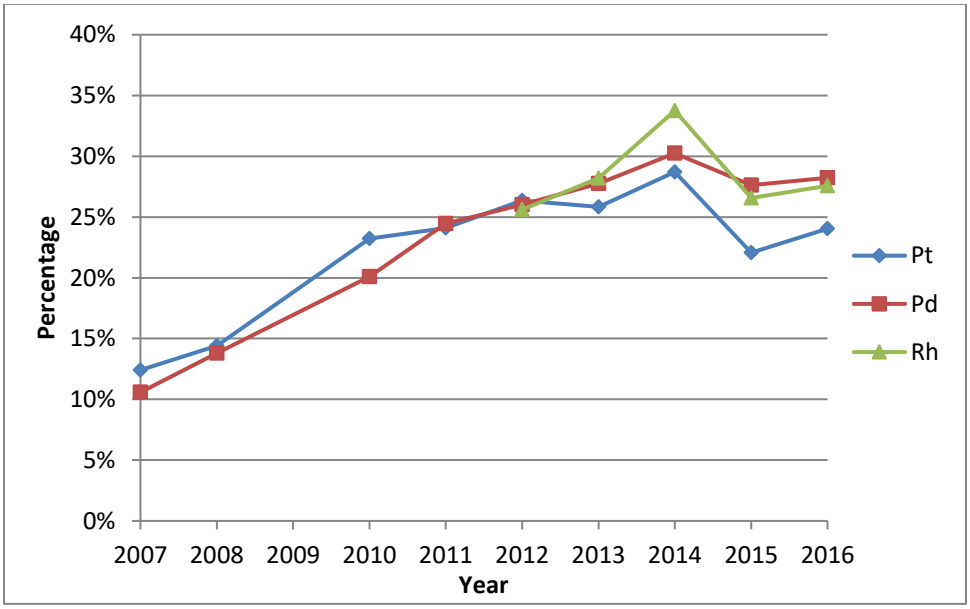


Figure 1.3: Contribution of PGM recycling to global supply (2007 - 2016)

Despite the global growth of the PGM recycling industry, South Africa's adoption for PGM recycling has been rather slow. There is also no support at policy level for PGM recycling in the country. This could be because there are still major underground reserves that are still being exploited by the mining sector. However, in the interest of long term sustainable mineral exploitation, it is imperative that recycling of PGMs be seriously considered. Recycling autocatalytic converters would add to the PGM resource base of South Africa and reduce the

load on PGM mining, thereby ensuring sustainability of the economic benefits that have accrued from PGM supply.

Current global PGM recycling activities are dominated by pyrometallurgical processes. In fact, not a single commercial process was identified that employs purely hydrometallurgy for PGM recycling. However, pyrometallurgical processing has some operational demerits, chief amongst them being the high energy costs and high particulate matter discharges. Other disadvantages for pyrometallurgical operations include increased capital and operating costs and the inability to tailor them for recovering other values contained in autocatalytic converters. In light of these disadvantages, a hydrometallurgical processing route may prove beneficial if it attains comparable extraction efficiencies, consumes less energy, and is operationally safer and more environmentally friendly. Moreover, because autocatalytic converters contain a significant amount of valuable metals that may also leach into solution, recovery of these co-leached metals could also improve the economics of the developed hydrometallurgical process.

Consequently, much research has been accorded to hydrometallurgical recycling of PGMs. A hydrometallurgical recycling process would typically go through crushing and/or grinding, leaching, extraction, purification, precipitation and reduction. The spent, PGM depleted solution may then be sent for extraction of any other co-leached species. Leaching PGMs has been investigated using different ligands e.g. chloride, iodide and cyanide. However, chloride leaching seems to be the more promising leaching route from an operational and economic perspective. Some of the major problems associated with PGM leaching using chlorides are operational safety and environmental sustainability, when using a chlorine generating species. Furthermore, chloride based media may also require expensive effluent disposal and could result in increased costs due to corrosion of vessels. All these challenges could be overcome by varying the parameters of the leaching environment; by using less harsh conditions that generate minimum chlorine but still maintain high recoveries. If such an approach is used, it would be imperative to identify how the PGM leaching efficiencies respond to these changing leaching environment conditions. A consistent observation within the chloride PGM leaching literature has been that there are lower recoveries obtained for Rh leaching when compared to Pt and Pd. However, the heavy reliance of both diesel and gasoline engines on Rh means that an understanding of the Rh

leaching mechanism will be imperative to improve recoveries of the metal from hydrometallurgical recycling. Rh is extensively used in both types of engines because of the three PGMs; i.e. Pt, Pd and Rh, it is the only one that performs the catalytic role of reducing nitrogen oxide emissions in the engine exhaust gases.

In order to recover PGMs from the leach solution, solvent extraction, ion exchange, and direct precipitation have also been investigated. Solvent extraction however, seems to have attained more favourable results and is quite established in PGM refining. The challenge with solvent extraction is to identify a suitable solvent for extraction of the PGMs. A suitable solvent refers to one that is less toxic, preferably has a higher flash point and can attain favourable extraction efficiencies.

The ultimate goal of investigating a hydrometallurgical process would therefore be the development of a flow sheet, performance of mass balances across the different units and conducting a preliminary cost benefit analysis of the proposed flow sheet. This flow sheet would be expected to inform any future investments in developing the process any further.

### 1.2 Problem statement

The increasing demand of PGMs for emissions control requires that new sources of PGMs be identified and exploited. Currently, supply of the 3 PGMs is mainly from conventional mining and pyrometallurgical recycling. However, both pyrometallurgical recycling and conventional mining have demerits that may be potentially overcome by the development of an efficient and economical hydrometallurgical process for PGM recycling. Such a process would employ a combination of chloride leaching followed by amine solvent extraction for Pt and Pd, and direct precipitation for Rh. Identification of optimal leaching conditions could reduce the amount of gaseous chlorine generated, making the process more environmentally friendly and inherently safer. Recovery of other co-leached values has the potential to improve process economics and make the recycling more profitable. Ultimately, recycling precious metals is expected to increase the South African national metal resource base and also reduce environmental damage due to disposal of spent convertors. In light of depressed commodity prices and dwindling ore grades, the recovery of PGMs from end of life autocatalytic converters is expected to buffer the PGM supply dynamics in the future.

## 1.3 Research approach and methodology

The research approach entailed investigating the variation in leaching efficiency for the PGMs with changing parameters by using central composite design to identify leaching trends. Insights that were obtained from this preliminary analysis were then used to design a one factor at a time experimental methodology, focusing on the optimum region. This was used to obtain an optimum set of conditions for leaching. A single solvent extraction run was eventually conducted to illustrate the potential for extracting PGMs from the leach solution.

## 1.4 Research Objectives

### 1.4.1 General objective

- To develop a cost effective, environmentally friendly hydrometallurgical process route to leach and recover platinum, palladium and rhodium from spent autocatalytic convertors.

### 1.4.2 Specific objectives

The specific aims are:

a. To determine the qualitative and quantitative constitution and structure of autocatalytic convertors,
b. To conduct leaching tests and model the influences of temperature, solids: liquid ratio, $AlCl_3 \cdot 6H_2O$ and HOCl concentrations and predict conditions to attain optimal PGM leaching,
c. To determine potential post-treatment methods that increase process economics by identifying routes for co-extraction of other values,
d. To do a preliminary run for recovery of PGMs using solvent extraction from the leach solution,
e. To develop a process flow sheet, and use it to perform mass balances and a subsequent cost evaluation analysis specifically on the leaching and solvent extraction sections.

## 1.5 Scope of the study

The research work was limited to the development of a leaching process for PGMs and optimisation of the variables to obtain an optimum set of conditions for the leaching. This was followed by a single solvent extraction run to illustrate the viability of PGM extraction. The

detailed development of a process for solvent extraction of PGMs, or a method for recovering any other co-leached metals was beyond the scope of the research.

## 1.6 Research questions

The academic inquiry attempted to answer the following questions:

1) What are the optimum conditions for leaching Pt, Pd and Rh from used autocatalytic converters?
2) How does the leaching efficiency for the 3 metals vary with changing parameters, and why is Rh leaching efficiency always lower than that of Pt and Pd?
3) Can solvent extraction be used to separate the PGMs efficiently?
4) Can a flow sheet, with mass balances be drawn and used for a cost benefit analysis of the entire PGM recovery process?

## 1.7 Research Outcomes

The following outcomes were obtained:

### 1.7.1 Publications

- A conference proceeding on the preliminary investigation into the leaching of PGMs from used autocatalytic converters using $AlCl_3$ and HOCl.
- A journal review paper on the current state of the PGM recycling industry, focusing on hydrometallurgical recycling.
- An intention to patent the developed process was submitted to the University for preliminary evaluation of proof of innovation.

### 1.7.2 Conference presentations

- The results from the preliminary investigation were presented at the European Metallurgical Conference (EMC), in Liepzig, Germany (June 25 – 28; 2017)

## 1.8 Organisation of the thesis

This thesis is organised as follows:

*Chapter 1 Introduction:* The chapter presents the rationale for the research and sets the objectives.

*Chapter 2 Literature review*: This chapter reviews related work that has been carried out before.

*Chapter 3 Research Methodology:* The chapter outlines the experimental work conducted.

*Chapters 4 and 5: Results and discussion:* The chapters present and discuss the results obtained from experimental work.

*Chapter 6 Flow sheet development:* This chapter presents the development of the flow sheet, and performance of a cost benefit analysis.

*Chapter 7: Conclusions and recommendations:* This chapter summarises the findings of the research and suggests further work that can be conducted on the process.

# Chapter 2 : Literature Review

## 2.1 Introduction

A significant amount of research attention has been accorded to the recycling of metal bearing end of life material. This trend is inspired by the emergence and realisation of secondary metal containing materials as a growing resource base of precious metals. This chapter will briefly introduce the rationale for metal recycling, give an overview of the chemical characteristics of platinum, palladium and rhodium and consider pre-treatment and PGM recycling using pyrometallurgical methods in brief. Major attention will be given to hydrometallurgical methods of PGM recycling. Various complexing ligands, e.g. $Cl^-$, $I^-$ and $CN^-$ have been investigated in literature as suitable options for hydrometallurgical PGM recycling. An associated review of required conditions for leaching using these complexing agents will therefore, be investigated and a scientific basis for this inquiry set-up.

## 2.2 Justification for Platinum Group Metal reclamation

Metal reclamation from end of life materials is beneficial for the environment because it reduces metal bearing waste discharges into the environment. When PGMs are deposited into the environment, they can solubilise due to the presence of naturally occurring complexing agents like humic acids and triphosphates. If these soluble PGMs are consumed e.g. in drinking water by humans, they may have detrimental health consequences, such as cell sensitization, mutagenesis and tumour formation (Rauch and Morrison, 2008). Dudka and Adriano, (1997) mentioned that the greatest contribution to soil contamination globally is actually neither mining nor smelting, but contamination from disposed end of life material. It is therefore, quite essential that the amount of metals disposed of into the environment, where they may subsequently leach into water bodies or into soils, is kept to a minimum to avoid these deleterious health hazards.

Besides the health concerns associated with metal leaching into potential water bodies, sustainable development is also a motivation for PGM recycling. The world has been moving towards adoption of green technologies and environmentally friendly processes. As a consequence, a lot of effort has been put into efficient use of resources, or recycling of resources to reduce demand from primary sources like mining. Mining and mineral processing is largely

responsible for increased loss of biodiversity and increased soil erosion. It generally produces 3 types of waste; tailings' dumps, mine waste water and overburden. Furthermore, smelting, which usually follows mining along the mineral processing chain, also produces a lot of toxic noxious volatile emissions and slags that need to be safely disposed of (Dudka and Adriano, 1997). After concentration, mineral processing usually ends up with metal refining to produce metals of desired commercial purity. Metal refining is usually hydrometallurgy based, which results in production of large volumes of liquid effluent discharges. Supply of metals from mining therefore results in production of waste along all stages of mineral extraction, from mining to metal refining. In light of this, recycling metals from end of life material therefore reduces the load on mining to supply the growing demand of the metals, which leads to lesser environmental damage as a result of less mining activities.

The greatest motivation when dealing with precious metal recycling may as also be the economics involved. PGMs in the ores exist as sulphides, requiring long pre-treatment flow sheets after mining to concentrate them. On the other hand PGMs in autocatalytic converters are in their elemental form, although a small potion may become oxidised during their service life. This means recovering PGMs from end of life materials, specifically from autocatalytic converters, requires very few pre-treatment steps because most of the PGMs are already in their elemental state. Processing these scrap materials is therefore, expected to be less costly which would translate to increased profit margins. Figure 2.1 illustrates that a mining operation for PGMs typically goes through more stages, with higher metal losses at each stage, increased capital and operating expenditure and increased cost of pollution abatement measures, when compared to a typical hydrometallurgy based PGM recycling operation. Furthermore, PGMs in autocatalytic converters are more concentrated than in their native ores, which also translates to better process economics. Figure 2.2 shows a comparison of PGM content for typical autocatalytic converters that have been investigated in literature, with PGM ores and PGM concentrates currently being exploited in the mining and refining industry. Evidently, virgin autocatalytic material is of higher grade when compared to the current mining and refining feed grades.

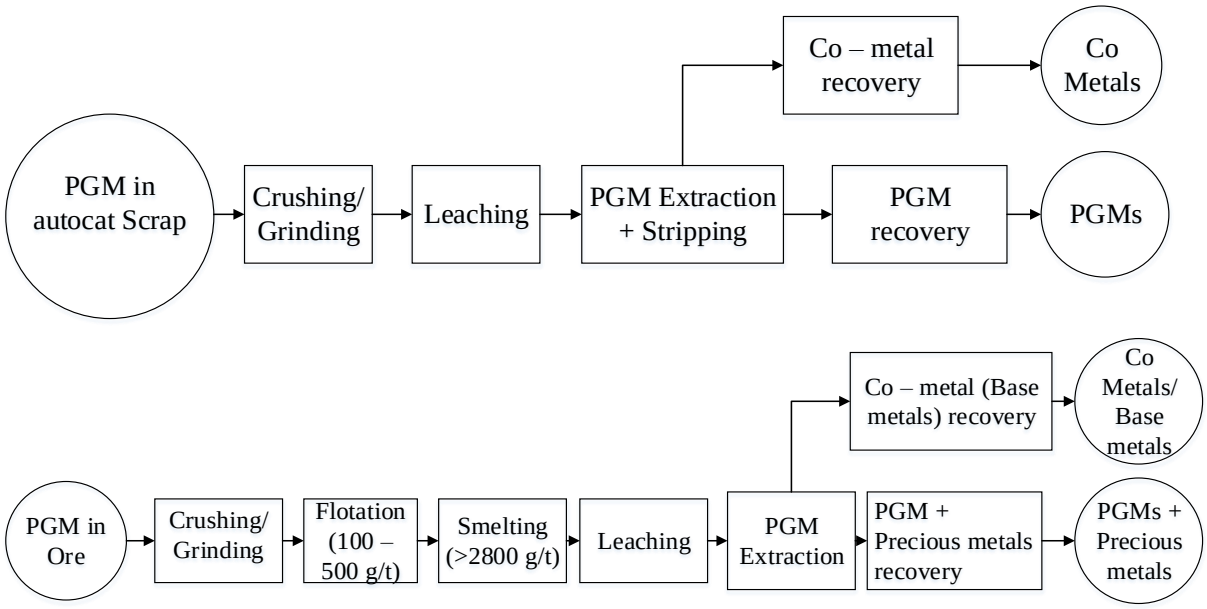


Figure 2.1: PGM extraction routes from used autocatalytic converters and PGM ores

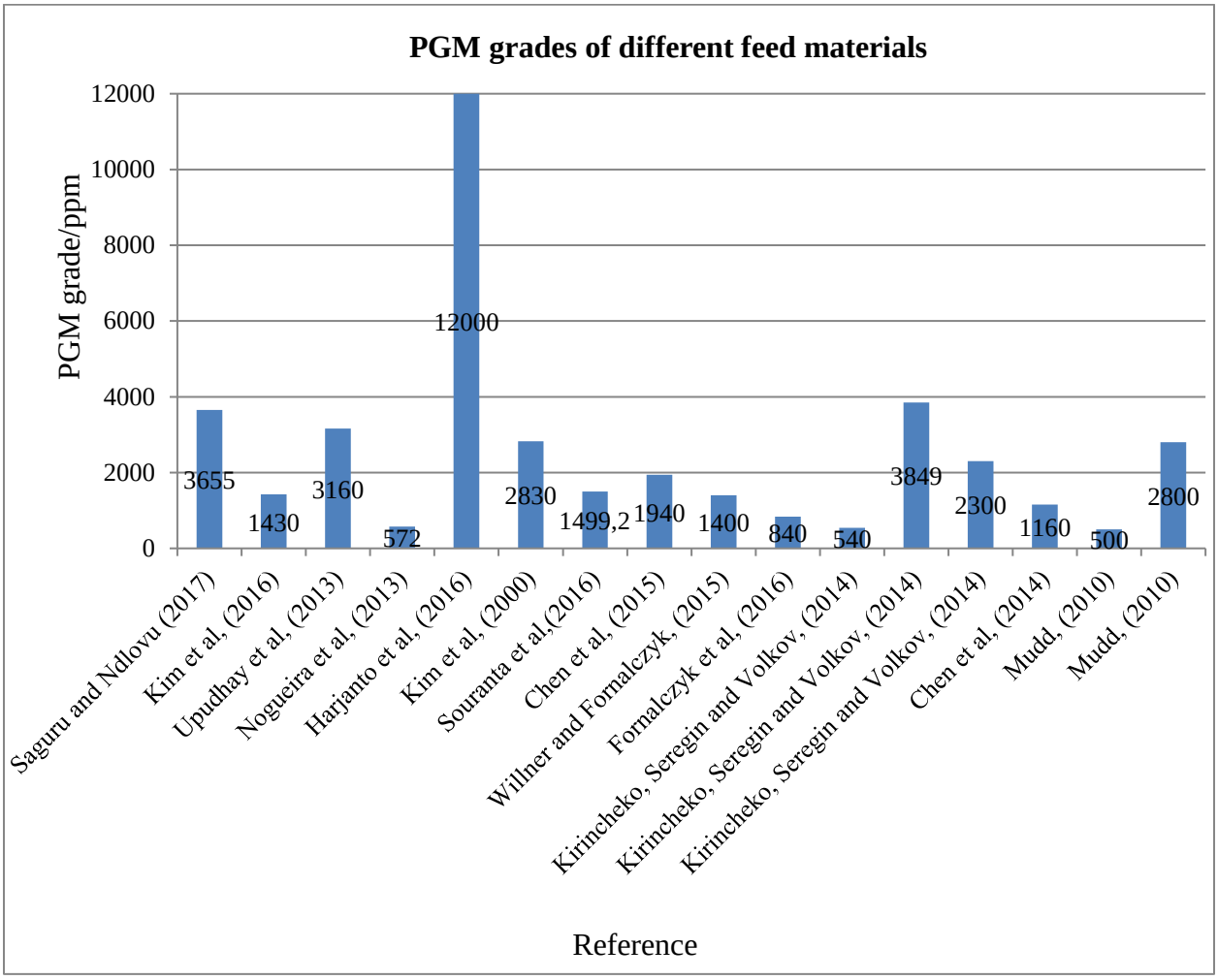


Figure 2.2: A comparison of PGM grades of different feed materials

Despite the health effects associated with PGMs leaching into water bodies, the need for meeting metal demand sustainably, and the higher concentrations of PGMs in autocatalytic converters, another motivation for PGM recycling is the possibility of recovering other valuable metals from end of life converters. Ores and scrap autocatalytic converters both have other metals that may (in the case of autocatalytic converters) or are (in the case of ore concentrates) being co-extracted to increase revenues. Base and precious metals in ores are currently being recovered to improve process economics. The recovery of other metals present in autocatalytic converters may also improve the economics of PGM recycling from autocatalytic converters, which would also add to revenue generation for the recycling entity.

Stringent environmental legislation requirements on primary metal producers, dwindling natural reserves of metals, decreasing ore grades and depressed commodity prices all contribute to

decreasing profitability margins. Secondary metal sources, however, provide rich sources of relatively more concentrated metals. It is therefore, economically prudent to process secondary sources of metals for precious PGM recovery. As such, the recycling of PGMs has been steadily growing.

### 2.2.1 Global trends in PGM recycling

Global PGM recycling has been on a steady increase due to the realisation of its importance to PGM supply dynamics. In 2010, Pt, Pd and Rh recycling contributed just 12%, 11% and 0% to global PGM supply. In 2016, 24%, 28% and 28% of Pt, Pd and Rh supply came from recycling (Johnson Matthey, 2016). Table 2.1 presents some major global PGM recyclers and their recycling capacities. Current recycling operations all employ pyrometallurgical processes. Despite the numerous investigations on hydrometallurgical recycling, no commercial operation could be identified that employs hydrometallurgy for PGM recycling.

Challenges faced within the PGM recycling industry

PGM recycling has, however, not been without its challenges. Chief amongst them is the formulation of a suitable supply model for the end of life material. End of life material is sourced via two main supply models; a closed loop and an open loop supply model.

Closed loop supply is a consequence of the Business to Business (B2B) model whereby companies that develop PGM products e.g. catalysts, sell them directly to business that utilise these products (Meyer, 2007). When these catalysts have reached the end of their service life, they are sold to recyclers via established business to business agreements. The amount of metals that are recovered from consumers in this model is consequently high; usually around 90% (Hageluken, 2017). This is because the supply model is essentially a closed loop which is driven by market forces, i.e. (business) consumers have an incentive to sell end of life material like used catalysts to recyclers, because it presents a revenue source for their operations.

Table 2.1: Some major global PGM recycling entities

| Reference | Company | Location | Notes |
|---|---|---|---|
| (BASF, 2015) | BASF | New Jersey, USA | BASF recycling facility is centralised in Seneca, USA. It recycles PGMs from spent chemical and auto catalysts using a pyrometallurgical process. |
| (Johnsson Matthey, 2017) | Johnson Matthey | 2 refineries in England<br>1 in USA and 1 in China | Refining of pre-processed ceramic and metallic autocatalytic converters obtained from its network of suppliers who acquire, de-can, crush and characterize converters. JM uses the plasma arc furnace for PGM refining. |
| (Multimetco, 2017) | MultiMetco | Alabama, USA | Plasma arc furnace is used to recover PGMs from catalysts. The slag product is sold to steel manufacturers and precious metal alloy is sent for PGM recovery. |
| (Umicore, 2017) | Umicore | Hoboken, Belgium | The ISA smelter, submerged lance technology is used for precious metal refining. Secondary PGM containing material is sourced from Brazil, Belgium and Thailand through Umicore subsidiaries or independent suppliers. |
| (Sibanye Resources, 2017) | Stillwater | Colorado, USA | Bought by Sibanye Resources on 4 May 2017. In 2015, Stillwater recycled 14.6 tonnes of Pt, Pd and Rh through its smelting facility (Dick, 2016). |
| (Bergeron and Richer-Laflèche, 2011) | NovX21 | Quebec, Canada | Ressources Minieres Pro-Or Inc, filed for patents in Canada (2012), USA (2011), South Africa (2007) and Australia (2009) for a carbochlorination process that recovers 97% of PGMs from autocatalytic converters. |

The bulk of PGMs however, ends up in public consumer applications e.g. autocatalytic converters, giving rise to the business to consumer (B2C) business model. Supply of this end of life material back to recyclers is not as integrated and there is no efficient way to recover that end of life material for PGM recovery. Furthermore, it relies heavily on legislation and government interventions to promote the recovery of values from end of life materials. The amount of metals consequently recycled from such consumer goods is low, typically around 60 % – 70 % for

autocatalytic converters (Hageluken, 2017). A comparison of B2B and B2C supply models has been presented in Figure 2.3.

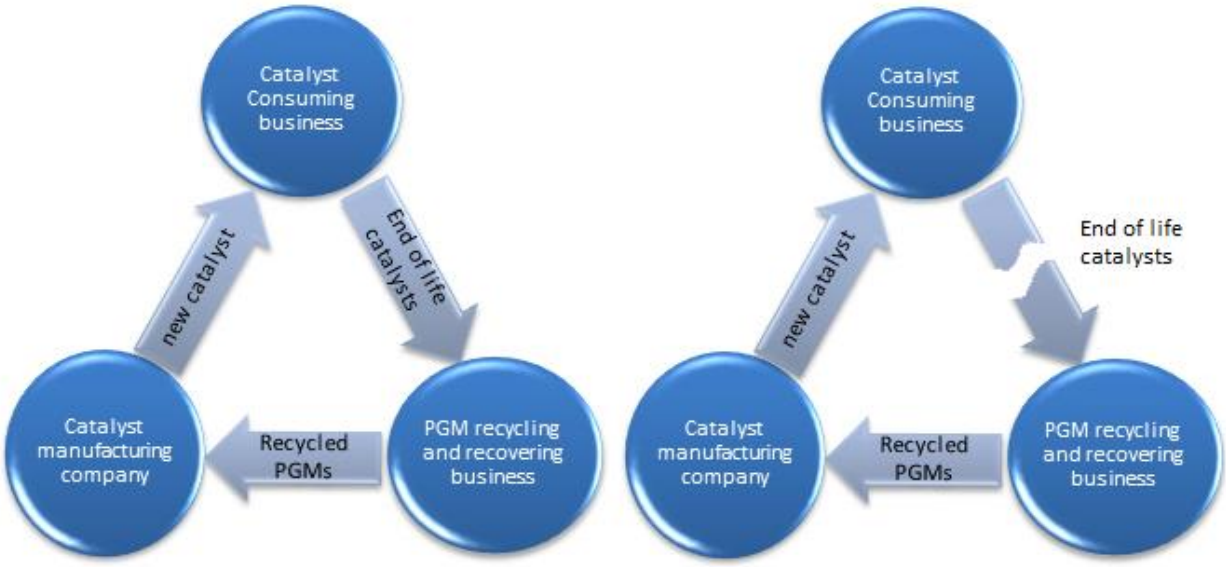


Figure 2.3: A comparison of recycling in the context of B2B and B2C business models

### 2.2.2 Current state of the South African PGM recycling industry

The South African PGM mining industry is well established and mature as a result of the vast deposits the country is endowed with. The same however, cannot be said about its PGM recycling industry which seems to be still in its infancy. Attempts to gather information on the current state of recycling in the country were largely unfruitful. Small scale operations are unwilling to engage with outside people to provide business information, and no centralised source of information on recycling could be identified. Progress in PGM recycling within South Africa may be affected by the vast deposits of PGMs in primary ore bodies that are still available. As a result, recycling of PGMs has not been accorded the required attention. There are therefore, no dedicated policies in South Africa that support PGM recycling, as is the case in other continents like Europe, Asia and North America where existing policies encourage recycling from end of life vehicles due to the unavailability of native ore bodies. However, in the interest of sustainable development, recycling in South Africa should be seriously considered as a supplement for the existing PGM supply. The potential to recover other values like cerium for example, from the autocatalytic converters, if proven to be economically feasible, also means

that the country can have a secondary source of metals that are not native to it for its vibrant autocatalytic manufacturing industry.

## 2.3 Physical and chemical properties and uses of Pt, Pd and Rh

The increasing importance of the PGMs is a direct consequence of their superior catalytic properties. Tables 2.2 and 2.3 show selected chemical and physical properties of the three most used PGMs; platinum (Pt), palladium (Pd) and rhodium (Rh).

Table 2.2: Selected chemical and physical characteristics of Pt, Pd and Rh, (Hartley, 1991)

| Property | Rh | Pd | Pt |
|---|---|---|---|
| Atomic number | 45 | 46 | 78 |
| Electronic configuration | (Kr) $4d^{10}5s^{1}$ | (Kr) $4d^{10}5s^{0}$ | (Xe) $4f^{14}5d^{10}6s^{1}$ |
| Atomic weight | 102.9055 | 106.4 | 195.09 |
| Melting point/ $^{o}$C | 1960 | 1554 | 1769 |

The PGMs are relatively stable metals that do not react readily with a variety of known strong acids. Rhodium and platinum, for example, will not react with either 36 % HCl or 65 % $HNO_3$ at 100 $^{o}$C. Palladium will also not react with 96 % $H_2SO_4$, even at a temperature of 300 $^{o}$C. In aqua regia at 150 $^{o}$C, only Pd and Pt are solubilized. In a $HCl/H_2O_2$ mixture at 100 $^{o}$C only Rh and Pt will solubilise (Hartley, 1991). This low chemical reactivity of the PGMs is attributed to their high ionization energies. The 1$^{st}$ ionisation energies for Rh, Pd and Pt are presented on the next page and for illustrative purposes, are compared to that for gold.

Table 2.3: First ionisation energies for Pt, Pd, Rh and Au, (Elements, 1980)

| Element | Rh | Pd | Pt | Au |
|---|---|---|---|---|
| First ionization Energy (kJ/mol) | 719.78 | 803.72 | 864.51 | 890.1 |

The chemical inertness of the PGMs is as a consequence of the inability of the lower lying f and s orbital electrons to successfully shield the outer d electrons from the effective pull of the nucleus. The effective pull on the outer electrons by the nucleus is therefore higher than would otherwise be expected for the atom's size (Bond, 2000). Consequently, more energy is required

to pull away the outer electrons to form cations. They are, however capable of forming complexes with a variety of ligands e.g. the halides, $CN^-$, and $SCN^-$ under suitable conditions.

Pt, Pd and Rh have therefore found applications in investments, jewellery and cancer treatment because of their inertness (Rao and Reddi, 2000), and since the 1970s, autocatalytic convertors have consumed a significant percentage of PGMs due to their catalysis reactions.

## 2.4 Auto catalytic convertors: Definition, structure and use

Autocatalytic convertors, shown in Figure 2.4 (a) are devices that are fitted to exhaust lines of fossil fuel engines (petrol, diesel, gas) to reduce emissions of environmentally harmful gases into the atmosphere. They consist of an outer protective casing made from steel, housing a ceramic or metallic substrate coated with aluminium oxide and other metal oxides on which catalytic Pt, Pd and Rh are deposited. 95% of autocatalytic convertors in commercial use employ a ceramic substrate as the support. The substrate is made from iron cordierite (Jimenez de Aberasturi et al., 2011). The remaining 5% has metallic substrates and is used in specific applications, e.g. in performance vehicles like sports cars where there's need for optimal performance under heavy loading (Fornalczyk and Saternus, 2009). The honeycomb structure is usually employed to increase the surface contact area between the exhaust gases and catalytic PGMs as shown in Figure 2.4 (b) (Fornalczyk and Saternus, 2009).

Honeycomb type monoliths contain parallel square channels forming an elliptical cross-section with a typical diameter of 0.25m and length of 0.35m (Crundwell et al., 2011). Three-way convertors contain two monoliths; the first being responsible for the reduction of nitrogen oxides and the second for oxidation of hydrocarbons and carbon monoxide. The parallel square channels make gas movement easier and enhance gas-solid contact by increasing the surface area per unit volume ratio.

Figure 2.4 (a)

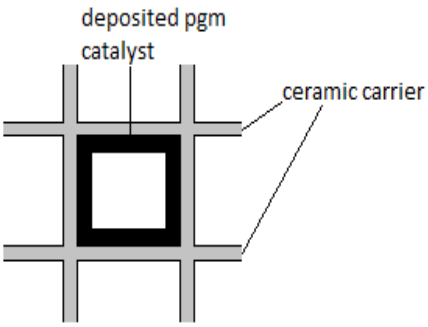


Figure 2.4 (b)

Figure 2.4 (a) and (b): Cut out cross section of autocatalytic convertor and a schematic representation of honeycomb structure of convertors

### 2.4.1 Process for manufacturing autocatalytic converters

Convertors consist of a lower ceramic (cordierite) support on which a thin layer of γ-Alumina is coated. The thin alumina layer provides a highly porous structure to which the catalytic material is deposited. Cordierite is used as a support due to its higher resistance to thermal shock. However, because of a lack in porosity, catalytic material cannot be deposited directly onto it; hence the need for an intermediate porous alumina wash coat which in turn increases the contact surface area. The process for depositing PGMs starts with immersing the cordierite support in a bath consisting of $Al_2O_3$, boehmite (AlO(OH)) and NiO and then baking at 600 $^oC$ for 5 hours. The highly porous $\gamma$ –$Al_2O_3$ wash coat which forms is typically 50 um – 200 um thick. NiO is added because it inhibits formation of $H_2S$ during the convertor's active service life. Ce and Zr oxides, which enhance the catalytic activity of the PGMs, are added by immersing in $Ce(NO_3)_3$ and $ZrO(OH)_2$ followed by baking. Cerium oxide is necessary for maintaining a suitably oxygenating environment by absorbing excess oxygen during the reduction of nitrogen in the autocatalytic converter, and releasing this stored oxygen during the oxidation of CO and hydrocarbons. Cerium oxide thereby acts as an oxygen sink; absorbing oxygen to create a reducing environment and then releasing this oxygen to form an oxidising environment. The coated support is then baked for 5 hour at 600 $^oC$ before the final coating of catalytic material is added. Pt, Rh and/or Pd are added by immersing the coated support in one or more of $H_2PtCl_6{\cdot}6H_2O$, $Pt(NH_3)_2(NO)_2$, $PdCl_2$ and/or $RhCl_3$ depending on the manufacturer's desired PGM ratios. The metals are finally reduced to their metallic form (Jimenez de Aberasturi et al.,

2011). A schematic representation of a cross sectional cut out is given in Figure 2.5. Figure 2.6 is a visual summary of the process for manufacturing autocatalytic converters.

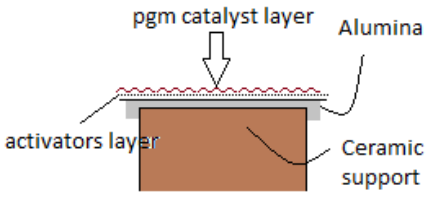


Figure 2.5: Cross sectional representation showing the layering of material on the catalyst

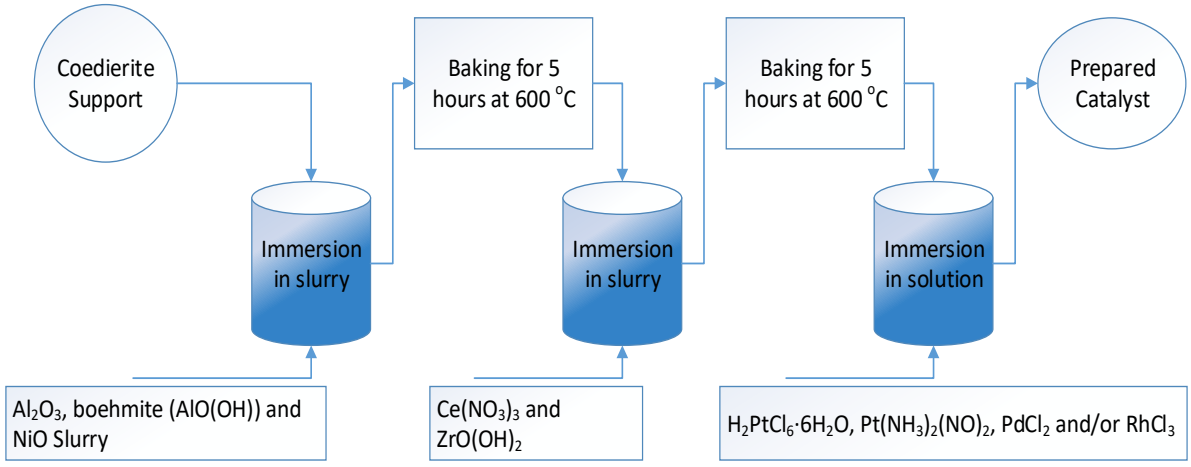


Figure 2.6: Summary of the autocatalytic converter manufacturing process

### 2.4.2 Types of autocatalytic converters

There are three types of autocatalytic convertors in commercial production. These are the two-way oxidation, three-way oxidation/reduction and Diesel Oxidation Catalyst convertors. The most common is the three-way oxidation/reduction convertor whose chemistry of operation is explained in the next section.

#### 2.4.2.1 Chemistry of operation of the three-way oxidation/reduction catalyst

The use of PGM metals is justified by the environmental consequences of fuel combustion products. Incomplete combustion produces CO and unburnt hydrocarbons. CO is a toxic gas, that when inhaled, binds strongly with the haemoglobin in the blood and reduces its carrying capacity

of $O_2$ to the muscles and $CO_2$ from the muscles. Unburnt hydrocarbons are responsible for the formation of low lying photochemical smog, which reduces visibility in urban cities. The combustion chamber temperature is also high enough to oxidise the $N_2$ which is drawn in with air, to different nitrogen oxides. NOx gases cause acid rain and also take part in the formation of smog. Exposure to NOx gases causes complications in individuals with existing respiratory ailments (Kerr et al., 1979). Environmental effects of excess NOx emissions also include eutrophication and uncontrolled vegetative growth in water bodies leading to biodiversity upsets.

PGMs are able to act as heterogeneous catalysts by reducing the activation energy for converting these harmful compounds into less toxic compounds. For any catalytic reaction to occur, the reacting species (e.g. CO and $O_2$) must be chemisorbed on the surface of the catalyst. The binding strength with which any species is chemisorbed on the metal surface differs from metal to metal and also with the species that is being absorbed. This difference in strength can cause one of two things below:

1. Restructuring of the reactant molecules on the surface of the catalyst due to electron interactions; or
2. Complete dissociation of the reactant molecule (Hartley, 1991).

Neither is exclusively desirable nor undesirable; for some reactions, complete dissociation of the reactant molecules is imperative and for some, only atomic restructuring is required for the formation of the desired product. In both instances however, the overall energy of activation required decreases. Pt, Pd and Rh satisfy the Volcano principle requirements for catalytic material, i.e. they are able to chemisorb the reactants with an optimum strength to promote the reaction, but not too strong so as to slow down the reaction (Hartley, 1991).

Three-way oxidation-reduction convertors contain all three PGMs over two monoliths. Platinum has the triplicate purpose of catalysing the oxidation of HCs to $CO_2$ and water, CO to $CO_2$ and reduction of $NO_x$ gases to $N_2$ and $O_2$. Rhodium catalyses the reduction of NOx gases and palladium is an oxidising catalyst. Different combinations and concentrations of PGM are therefore used after considering production economics and emission standards. Autocatalytic converters for modern gasoline engines for example, are slowly drifting away from Pt containing converters to Pd/Rh rich ratios due to the price of Pt.

Autocatalytic convertors typically operate at temperatures of about 200$^{o}$C during start-up and 800$^{o}$C during normal operation (Crundwell et al., 2011). The first of the two monoliths is responsible for the reduction of the $NO_x$ gases and it usually contains rhodium and/or platinum. NOx gases are reduced according to the following reactions (Crundwell et al., 2011):

$$2NOx\ (g) + (2 - x)\ O_2\ (g) \longrightarrow 2NO_2\ (g) \qquad \text{Equation } \mathbf{1}$$

*(Oxidized nitrogen in air)* *(Unused engine air)* *(Fully oxidized $N_2$)*

$$10NO_2\ (g) + 8\ HC\ (g) \longrightarrow 4H_2O\ (g) + 8CO_2\ (g) + 5N_2\ (g) \qquad \text{Equation } \mathbf{2}$$

*(Fully oxidized $N_2$)* *(Unburnt fuel)* *(Inert exhaust gases)*

The second monolith oxidizes hydrocarbons and CO according to the following reactions:

$$8\ HC\ (s) + 10\ O_2\ (g) \longrightarrow 4H_2O\ (g) + 8CO_2\ (g) \qquad \text{Equation } \mathbf{3}$$

*(Unburnt hydrocarbons)* *(Unused engine input)* *(Inert exhaust gases)*

$$2CO\ (g) + O_2\ (g) \longrightarrow 2CO_2\ (g) \qquad \text{Equation } \mathbf{4}$$

*(Partially combusted fuel)* *(Unused engine input air)* *(Inert exhaust gas)*

PGMs in autocatalytic convertors therefore reduce emissions of CO, unburnt hydrocarbons and toxic NOx gases by converting them to more inert $CO_2$, steam and $N_2$.

## 2.5 Technologies for PGM extraction

Processing secondary sources has its own set of technological challenges. PGMs in catalytic converters are usually finely disseminated to attain maximum surface area contact with exhaust fumes. This means that accessing the metal to extract it may become operationally challenging. Consequently, the PGM industry resorted to pyrometallurgical processes for recovering PGMs from autocatalytic converters. Pyrometallurgy only requires the melting of the entire unit and using a collector metal to recover the PGMs. However, it is also possible to recover PGMs using hydrometallurgical extraction, by providing a suitable thermodynamic environment for leaching the metals. A general comparison of hydrometallurgy and pyrometallurgy has been presented in Table 2.4. The comparison illustrates the potential for a purely hydrometallurgical route as a recycling alternative for recovering PGMs from autocatalytic converters.

Table 2.4: Pyrometallurgy vs. Hydrometallurgy comparison

| Hydrometallurgy | Pyrometallurgy |
|---|---|
| Process can be tailored to recover other values present in the feed material economically | Less selective and it may be difficult to recover valuable by-products in pyro processes |
| Operations can start off small, and then scaled up slowly, meaning hydrometallurgical processing can be used on smaller production scales without much capital injection | Operations cannot be initiated at lower production levels and scaled up progressively due to the need for specialized equipment. Scaling up production is therefore usually at the cost of high capital expenditure |
| The use of lower temperatures means that energy consumption is usually significantly low | High energy costs result in significantly increased operating and capital expenditure |
| Results in lower particulate matter discharges and emissions of combustion products | A lot of particulate matter discharges and toxic emission products which increase operating costs from emission control technologies |
| Flexible designs which can be tailored for different feed material by employing different reagent conditions, or relatively small capital modifications | Usually not very flexible, a drastic change in feed material may require significant redesigning, which is fundamentally problematic since waste material doesn't have a fixed composition |
| May result in production of large volumes of potentially toxic effluents | Usually associated with lower volumetric effluent |
| Corrosion problems may be significant, adding to the operating costs of the recycling facility | Refractory linings tend to wear off, increasing operating expenditure significantly. |
| Crushing and grinding costs for the PGM containing substrate can end up consuming a lot of energy given the relatively hard materials (Cordierite and Alumina) used in the monolith. | The use of heat resistant and stable cordierite and alumina for the manufacture of the converter monolith also requires high amounts of energy to melt the supporting structure. |

## 2.6 Current commercial pyrometallurgical technologies

Notwithstanding their disadvantages, numerous pyrometallurgical processes for PGM recycling that are currently in commercial operation have been identified. Multimetco Inc. operations located in Anniston, Alabama employs a plasma arc process at temperatures as high as 2000 $^{o}$C for the recycling of PGMs. It is based on the plasma furnace developed by Burnham et al., (1985) for Johnson Matthey. Iron or iron oxide is added as a collector material and PGMs are collected in the metal phase. The metallic phase is then subjected to leaching of the iron alloy, leaving behind a PGM concentrate. In other processes, smelting is done using a copper or nickel collector because both nickel and copper mattes are good metal collectors. Silica or lime may be

added as a flux depending on the type of smelting employed. At its Hoboken Plant, Umicore operates an Isa Smelt submerged lance furnace with a capacity of 1000 t/d, that receives a variety of feed material from different parts of Europe, via an integrated supply chain. NovX21 patented a new carbochlorination method for PGM recycling with recoveries reaching 97% (Bergeron and Richer-Laflèche, 2011). A 50 t/year plant employing this carbochlorination technology was commissioned in Quebec City, Canada.

## 2.7 Hydrometallurgical Methods

Hydrometallurgy refers to the recovery of metals by dissolution and extraction in an aqueous or liquid solution under the right set of conditions. Ideal leaching would involve the selective dissolution of a desired metal, although due to similarity of elements and their properties, a clear cut separation may not necessarily be possible. Impurities may be dissolved together with wanted material. However, the goal is always to identify a suitably selective lixiviant to minimize downstream separation processes.

Dissolution is determined by considering the thermodynamics for the maximum transfer of metal into solution. Dissolution of a metal is only possible when the overall free energy of the forward solubilisation process is negative. Thermodynamic determination of solubility is predicted using Eh - pH diagrams through consideration of stability regions for different ions in aqueous solutions, at set temperatures. Software e.g. HSC Thermodynamics, to predict regions of stability are in commercial and academic use.

Adoption of a lixiviant is not a function of thermodynamic considerations alone, as certain feasible lixiviants may not be economically viable due to corrosion of the vessels, side reactions, cost of reagents, cost of purification and recovery and/or slow kinetics. A good lixiviant will therefore, be a suitable economically determined compromise on all these considerations.
Kinetic dissolution of a metal can be represented by the following scheme in accordance with the shrinking core model (SCM) for fluid-solid reactions (Levenspiel, 1999):

1. Diffusion of active reagents from bulk solution through the film surrounding the solid to its surface
2. Adsorption of lixiviant on the surface of the solid

3. Occurrence of chemical reaction
4. Desorption of chemical products from surface of solid
5. Diffusion of reaction products into bulk solution.

Chemical dissolution kinetics is therefore determined by the rate of the slowest of these steps. A leaching operation's kinetics may be film layer controlled, product layer controlled or chemical reaction controlled. Knowledge of the rate of the determining steps allows manipulation of external factors to control the rate of reaction and hence increase throughput. The following considerations therefore impact on the design of a leaching operation:

1. Particle size

The amount of size reduction affects the degree of metal exposed to the action of the lixiviant. It is not a requirement that the entire metal should be liberated; only sufficient exposure of the desired metal is required. Particle size is therefore a trade-off between degree of dissolution and energy expended during size reduction.

2. Diffusion rate

The rate of diffusion of material to (i.e. leaching reagents) and from (i.e. products of leaching) the reaction surface impacts the rate of reaction for a diffusion controlled reaction. In such instances, increasing the agitation increases material transfer and consequently increases the rate of reaction. If however, the slowest step is movement of solvent through a porous solid to the reaction interface, or chemical reaction kinetics, increasing agitation doesn't necessarily have an effect. In such cases, increasing temperature or concentration increases the rate of reaction.

3. Rate of chemical reaction

In reaction controlled kinetics, the rate of chemical reaction at the surface controls the rate of overall reaction. In such instances, the rate can be increased by increasing temperature, pressure and/or concentration – all of which have the net effect of increasing the number of successful collisions. Introducing a catalyst can also increase the rate of the reaction by lowering the activation energy of the reaction. Another option would be to decrease the size of the solid and thus, increase its available surface area for reaction.

4. Leach agent concentration and reagent combination

Different reagents have different chemical interactions with the desired metal, impurities and additives. An ideal lixiviant is perfectly selective, attains equilibrium in the shortest possible time, achieves a high dissolution and makes subsequent recovery of desired material easy.

Increasing the concentration of the lixiviant increases the rate of successful collisions, and consequently, the rate of reaction. The lixiviant properties and concentration should however, be selected subject to considerations of operator and environmental safety, effect on piping and reactor material, and ease of waste water treatment.

5. Pulp Density

Increasing pulp density means increased amounts of solids, hindered flow of solution and localised variation of lixiviant concentration. The net effect is reduction in the rate of reaction. Higher pulp density also consumes more energy for maintaining solids in suspension. However, an optimally high solid to liquid ratio, results in a high throughput, which translates to higher production rates and more favourable operating economics.

6. Reaction Products

The thermodynamic stability regions of ions in aqueous solution change with liberation of new ions. The dissolution of unwanted material not only uses up the lixiviant, it may also introduce ions that alter thermodynamic stability regions. Formation of insoluble products during leaching may also hinder flow of the reactant to the solid surface, reducing the rate of reaction.

Leaching of PGM from secondary sources, including spent catalytic convertors has been investigated in literature. Two fundamental approaches that may be used to reclaim PGM are;

1. Transferring platinum, palladium and rhodium into aqueous solution, extraction and purification followed by recovery of the metallic form of the metal in another operation e.g. cementation or electro winning.
2. Dissolution of the supporting material (monolith), using a lixiviant which will not leach the PGMs, followed by reclamation of the metallic PGM fraction using a solid - liquid separation operation like filtration or centrifugal separation.

The majority of monoliths are manufactured using cordierite, which is resistant to acid attack. Therefore, attempting to dissolve the cordierite may be technologically challenging. Due to PGM noble nature, dissolution of PGM in acid may also be a major technological challenge. Despite this challenge, various reagent combinations and conditions have been investigated for both approaches, each attaining different recoveries. The associated literature for both will therefore be investigated in the following sections.

### 2.7.1 Leaching approach of dissolving PGMs into solution

Various complexing agents have been investigated for PGM leaching from secondary sources. Halide systems, predominantly chloride systems, seem to have enjoyed a dominant scientific interest as PGM complexing agents. A review of past advancements in PGM leaching from secondary sources is therefore presented, with more emphasis placed on halide leaching of PGMs.

#### 2.7.1.1 PGM leaching using Cyanide (CN-) complexing ions

The ability of the cyanide ion to form stable complexes with PGMs makes it a possible complexing agent in leaching of PGMs. At 25$^{o}$C, the stability constants (log $\beta_4$) of $CN^-$ with Pt and Pd are 78.00 and 63.00 respectively (Mahmoud, 2003). Chen and Huang, (2006) investigated the effect of $CN^-$ on the dissolution of PGMs from spent catalysts and flotation concentrates. Although it is thermodynamically feasible to dissolve the PGMs in $CN^-$, the kinetics at room temperature and pressure are very slow. The presence of residual carbon and hydrocarbons from fuel combustion on the catalyst inhibited efficient dissolution, warranting the need for a pre-treatment step prior to leaching. Alkaline leaching at 160$^{o}$C, 2.0 MPa $O_2$, liquid: solids ratio of 4:1 for 2 hours followed by two stages of cyanide leaching at 160$^{o}$C, 6.25g/L NaCN, 1.5MPa $O_2$, liquid: solids ratio of 4:1 for 1 hour yielded 96.0%, 97.8% and 92.0% recovery of Pt, Pd and Rh respectively. The alkaline leaching pre-treatment removed carbon and hydrocarbon impurities off the solid surface, and exposed the catalyst surface to cyanide attack. A mechanism similar to gold dissolution in cyanide was suggested as the dissolution mechanism for PGMs, represented by equations 5 and 6 (Chen and Huang, 2006).

$$2X\,(s) + 8\,NaCN\,(aq) + \,O_2(aq) + 2H_2O\,(l) \rightarrow 2Na_2[X(CN)_4](aq) + 4NaOH(aq) \quad \text{Equation } \mathbf{5}$$

Where X = Pt/Pd

$$4Rh(s) + 24\,NaCN\,(aq) + \,3O_2(aq) + 6H_2O\,(l) \rightarrow 4Na_3[Rh(CN)_6](aq) + 12NaOH(aq)$$

Equation **6**

Dissolution efficiency was in the order Pt > Pd > Rh due to the increasing complex bond strength in the order of $Rh(CN)_6^{3-}$ > $Pd(CN)_4^{2-}$ > $Pt(CN)_4^{2-}$ (Jha et al., 2013). Pilot plant work by Kuczynski et al., (1995), on leaching of 45 kg batches of used monolith catalyst using the $CN^-$

ligand achieved 78% - 88% Pd, 75% - 90% Pt, and 43% - 71% Rh recoveries. To attain environmentally acceptable $CN^-$ concentration, $CN^-$ in the residual solution was precipitated to a content less than 0.2 mg/L (Kuczynski et al., 1995).

The single biggest problem associated with cyanide use is the need to maintain strict pH control to avoid HCN formation. The operation of leaching under high pressure and temperature conditions further imposes high safety considerations, which increases operating and capital equipment costs. Furthermore, accidental discharge of cyanide or its products could have detrimental environmental implications (Hilson, 2000), and costs associated with handling of toxic effluents containing $CN^-$ ions also add to the operating costs.

### 2.7.1.2 PGM leaching using $Cl^-$ complexing systems

PGMs may also be leached using chloride complexing systems in an acidic environment. Figure 2.7 illustrates the regions of thermodynamic stability for Pt in chloride media, drawn using HSC Chemistry.

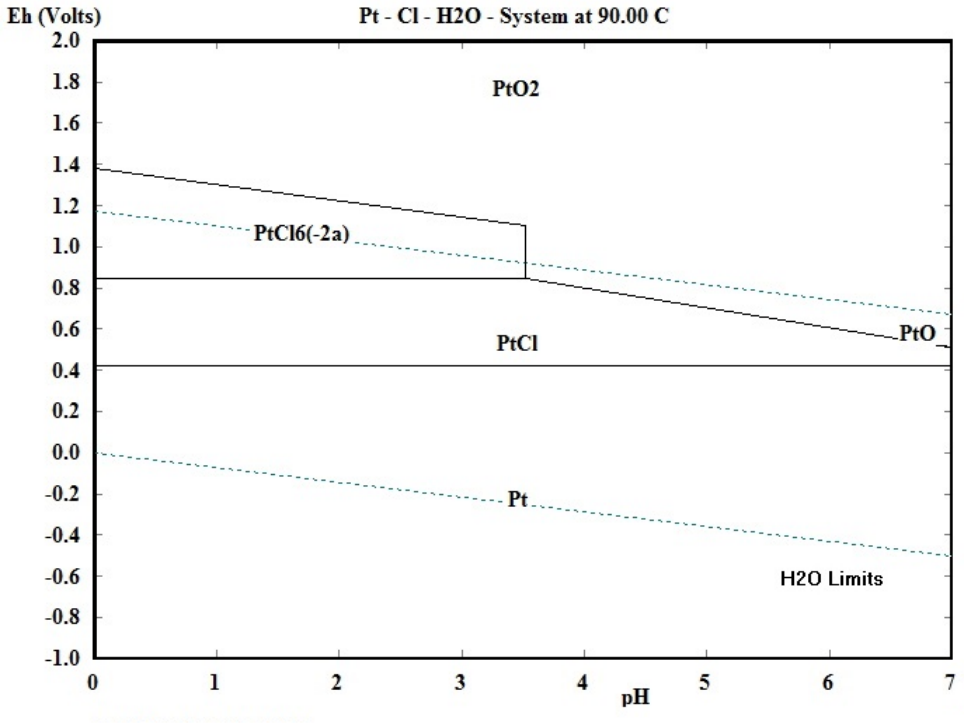


Figure 2.7: Eh – pH diagram for Pt – Cl – H2O system at 90 °C, drawn using HSC Chemistry

Studies were conducted by Kim et al., (2013) and Lillkung et al., (2013) to investigate and understand the underlying chemistry for the dissolution behaviour of Pt in different chloride media. Kim et al., (2013) investigated dissolution of pure platinum powder in electro-generated chlorine and HCl. Lillkung et al., (2013) also investigated the dissolution of 99.9% Pt, Pd and Rh wire electrodes using concentrated NaCl. These experiments reaffirmed the feasibility of using the chloride ion as a suitable leaching complexing agent for the PGMs.

Upadhyay et al., (2013) investigated the leaching of PGMs from spent autocatalytic converters (SAC) containing 0,018 wt. % Pt, 0.12 wt. % Pd and 0.016 wt. % Rh in HCl acid using electro generated chlorine. Optimum metal extraction was obtained under the conditions of 6.0 M HCl, current density of 714 A/m$^2$, 363 K, 20 g/L and agitation speed of 700 rpm. The extraction however, increased to 97%, 94% and 90% for Pt, Pd and Rh respectively after pre-reduction of spent converters in formic acid at room temperature. Chlorine gas was produced from the anode of an HCl electrolytic cell with an anionic exchange membrane and graphite electrodes. The gas was bubbled into the leaching reactor containing ground SAC (-212 mm) and 500 ml HCl (varied between 4.0 M - 8.0 M). Agitation was investigated over 500 rpm – 900 rpm, and temperature over 290 K – 370 K. According to Alkan et al., (2005) and Majima et al., (1990), PGM dissolution in HCl/$Cl_2$ media occurs as a result of the $Cl_{2(aq)}$ and ${Cl_3}^-{}_{(aq)}$ species. These are formed from the reactions shown in equations 7 to 9.

$$Cl_{2(g)} \leftrightarrow Cl_{2(aq)} \qquad \text{Equation } \mathbf{7}$$

$$Cl_{2(g)} + H_2O \leftrightarrow H^+ + Cl^- + HClO \qquad \text{Equation } \mathbf{8}$$

$$Cl_{2(g)} + {Cl^-}_{(aq)} \leftrightarrow {Cl_3}^-{}_{(aq)} \qquad \text{Equation } \mathbf{9}$$

Subsequent PGM dissolution thereby occurs according to:

$$Pt + {Cl_3^-}_{(aq)} + {Cl^-}_{(aq)} \rightarrow {PtCl_4^{2-}}_{(aq)} \qquad E^\Theta/V = 0.69V \qquad \text{Equation } \mathbf{10}$$

$${PtCl_4^{2-}}_{(aq)} + Cl_{2(aq)} \rightarrow {PtCl_6^{2-}}_{(aq)} \qquad E^\Theta/V = 0.62V \qquad \text{Equation } \mathbf{11}$$

$$Pd + {Cl_3^-}_{(aq)} + {Cl^-}_{(aq)} \rightarrow {PdCl_4^{2-}}_{(aq)} \qquad E^\Theta/V = 0.80V \qquad \text{Equation } \mathbf{12}$$

$$2Rh + 3{Cl_3^-}_{(aq)} + 3{Cl^-}_{(aq)} \rightarrow 2{RhCl_6^{3-}}_{(aq)} \qquad E^\Theta/V = 0.98V \qquad \text{Equation } \mathbf{13}$$

Increasing the $Cl^-$ (HCl) and $Cl_2$ (Current density) concentrations would favour the dissolution of PGMs, an observation that was corroborated by Upadhyay et al., (2013). A higher $Cl^-$

concentration favours the formation of the chloro-complexes e.g. $PtCl_6^{2-}$ of the PGMs over the aqua complexes (i.e. $PtCl_x(H2O)_{6-x}^{(x-2)-}$). It also increases their stability and improves dissolution efficiency, and oxidation of the metals. Optimum PGM leaching was obtained at a S: L ratio of 20 g/L. Increasing this S: L ratio any further decreased the extraction of precious metals, possibly due to their re-adsorption on the substrate material. Formic acid was used as a reducing agent to reduce any PGMs that may have been oxidised during their service life to the metallic form before subsequent extraction. Formic acid reduces PGMs according to:

$$PtO_{(s)} + HCOOH \rightarrow Pt + H_2O + CO_2 \qquad \text{Equation } \mathbf{14}$$

$$PdO_{(s)} + HCOOH \rightarrow Pd + H_2O + CO_2 \qquad \text{Equation } \mathbf{15}$$

$$Rh_2O_{3(s)} + 3HCOOH \rightarrow 2Rh + 3H_2O + 3CO_2 \qquad \text{Equation } \mathbf{16}$$

The role and importance of reductive pre-treatment was illustrated as the recoveries under optimised reducing conditions increased from 71% to 97%, 60% to 94% and 58% to 90% for Pt, Pd and Rh respectively. Reaction kinetics followed an ash diffusion model through the porous alumina wash coat.

Kim et al., (2016) employed a similar method for PGM dissolution but investigated the efficiency of incorporating a recycling step for unused chlorine gas. Spent autocatalytic converters that were investigated contained 0.128 wt. % Pt and 0.015 wt. % Rh. Unused chlorine gas was reduced in the cathodic compartment of the electrolytic cell, which was separated from the anode by an anionic exchange membrane. This approach for dissolution of PGMs is highly dependent on the ability of the electrolyte to reduce unused chlorine so as to minimise chloride losses. This reduction step was consequently investigated in three solutions:

- 35% HCl + 2.0M NaCl (+ NaOH for pH control),
- 35% HCl alone and
- 35% HCl + 0.1 M $FeCl_3$.

An optimum reduction for unused chlorine of 99.8% was obtained in 2.0 M NaCl at pH of 10. Without the chlorine recycling unit, the system was largely similar to that investigated by Upadhyay et al., (2013) and Kim et al., (2013). However, the recycling step increased extraction to about 99.6% of Pt under the optimised conditions of S: L ratio of 100 g/L, temperature of 80 $^oC$, HCl concentration of 8 M and T = 90 minutes. Increasing S: L ratio to beyond 400 g/L reduced Pt extraction to below 16%, possibly due to re-adsorption of leached out metal back onto

the substrate material. However, this effect was not registered for rhodium. This could have been because Pt may have already occupied most adsorption spaces since it was the most concentrated, or the concentration of rhodium might just have been too low. Optimum extractions of 93% Pt, and 48% Rh were obtained at a S: L ratio of 100 g/L, temperature at 80 $^{o}$C, 8.0 M HCl, current density of 22.6 mA/cm$^2$ and 30 minutes for time.

Upadhyay et al., (2013) and Kim et al., (2016) investigated the leaching of PGMs from used materials by employing an in situ chlorine generation unit. The benefits of such an approach would be the reduced cost of purchasing and transporting chlorine to the processing facility. Furthermore, the incorporation of a recycling unit could potentially result in increased revenue. The disadvantage, however, is that on site generation of chlorine increases the safety risk to chlorine exposure, which would result in increased safety and environmental costs.

Cupric chloride was investigated by Nogueira et al., (2014) as an oxidant to leach a Pd/Rh used catalyst, due to its relatively safer and more environmentally friendly nature. The full factorial design methodology to evaluate the effects of HCl and $Cu^{2+}$ concentration, temperature and time was employed to establish significance and interaction of factors. All factors were significant ($p < 0.05$) for both Pd and Rh. Concentration of HCl and $Cu^{2+}$ were the most significant factors for Pd leaching whilst temperature was significant for Rh alone. Interaction between the concentration of HCl and $Cu^{2+}$ was also significant whereas all interactions were practically not significant on Rh yield except for temperature and concentration of $Cu^{2+}$. Pd yield was always higher than Rh yield and aggressive conditions had to be employed to justify the economic leaching of Rh. Maximum yield for Rh was 80% at a HCl concentration of 6.0 M, concentration of $Cu^{2+}$ at 0.3 M and temperature at 80 $^{o}$C. Dissolution of PGMs was also observed without any oxidant ($Cu^{2+}$) added.

The dissolution of PGMs in acidic media without a dedicated oxidant has also been observed by Bolinski, (1991), Harjanto et al., (2006) and Nogueira et al., (2014). A possible explanation offered by the authors is that during their service life operation, PGMs may have been oxidized into a more reactive species that is more amenable to leaching in acidic media alone. However, no data on this state was presented by the authors through morphological or XRD

characterization of the solids prior to leaching. As a result, none of the authors presented any conclusive analysis for this dissolution.

#### 2.7.1.3 Microwave energy assisted leaching

Microwave energy has been investigated extensively in extractive metallurgy for improving many metallurgical unit operations. It has been proposed for drying operations (Pickles, 2005), carbothermic reduction of nickeliferrous laterite ores (Samouhos et al., 2012), and calcination as well as sintering of manganese carbonate ores (Amankwah and Pickles, 2005). A review has been presented that deals extensively with microwave assisted leaching of base metals by Al-Harahsheh and Kingman, (2004). As a result of these investigations, microwave leaching has also been suggested and investigated for precious metals' recycling and leaching.

Microwave assisted leaching of the PGMs Pt, Pd, Rh and Ru from two sources; an automotive catalyst and a Ru/alumina supported catalyst was investigated by Suoranta et al., (2015). 37% HCl at 120 $^{o}$C was used for the leaching process. A conventional heating block was compared to microwave heating in a pressure reactor and the results are illustrated in Figure 2.8, which show that microwave heating resulted in better leaching recoveries.

Microwave roasting and simultaneous leaching were investigated by Chen et al., (2015) to optimize leaching of Pd and Rh from a spent binary catalyst that had a respective composition of Pd and Rh of 1698 ppm and 242 ppm. 20 g sample of the auto catalyst ground to 2.12 um was placed in a thermally insulated crucible with a 1:1 solution of $NaClO_3$ and $NaHSO_4 \cdot H_2O$. The liquid to solid ratio (mass/mass) was varied from 9 to 11, roasting temperature investigated from 450$^{o}$C to 550$^{o}$C, and time investigated from 40 minutes to 80 minutes. Central composite design was employed to model the extraction of both PGMs as a function of the three investigated parameters. Under optimized conditions of L: S ratio = 10, 550 $^{o}$C roasting temperature and 60 minutes reaction time, PGM extraction was 99.33% and 95.48% for Pd and Rh respectively.

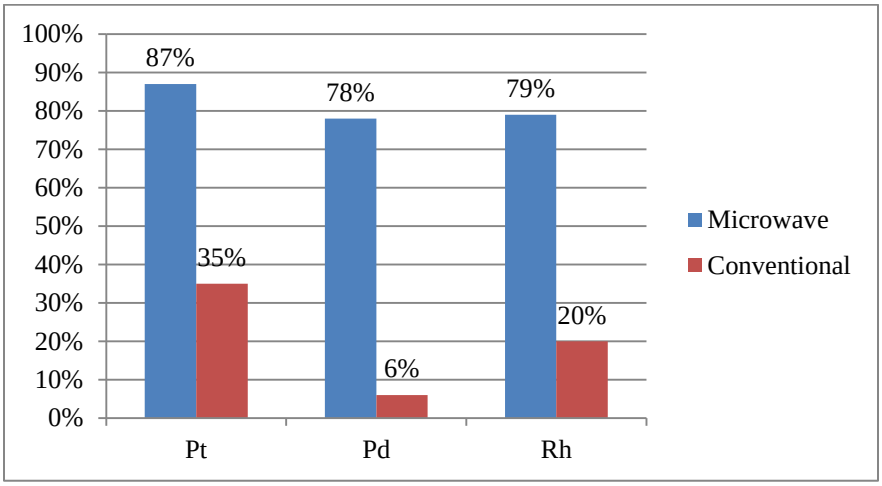


Figure 2.8: Comparison of PGM extraction from used catalyst at 120 ºC, by conventional block heating and by microwave irradiation (Suoranta et al., 2015)

The exact mechanisms by which microwave heating improves extraction, or how it works in other mineral processing units are still contentious at the very least. However, as far as leaching is concerned, the higher recoveries could be attributed to localized super-heating of the solution, which results in increased and improved extraction at certain locations within the solution. The use of microwaves for roasting aids the breakdown of surrounding oxide matrices that may have formed as a consequence of the consistent use of PGMs under high operating temperatures. Once this breakdown occurs, it increases the lixiviant - solid contact and leaching efficiency of PGMs from the SAC matrix. The high extraction of Rh observed is especially noteworthy, given the difficulty usually associated with Rh leaching.

#### 2.7.1.4 Comparison of the leaching efficiencies of the PGMs using chloride ions

A consistent observation noted in the PGM leaching chemistry has been the lower recoveries obtained for Rh leaching when compared to Pt and Pd recoveries. When hydrochloric acid and hydrogen peroxide solution was used as the leaching medium by Rumpold and Antrekowitsch, (2012) maxima of 90%, 80% and 65% were obtained for Pt, Ce and Rh. Nogueira et al., (2014) was able to reach maxima leaching efficiencies of 95% Pd and 86% Rh from a used autocatalytic converter that assayed 441 ppm and 131 ppm Pd and Rh respectively. Upadhyay et al., (2013) also attained leaching efficiencies of 71%, 68% and 60% for Pt, Pd and Rh from a used autocatalytic converter using $Cl_2$ and HCl as the leaching medium. This trend in leaching

efficiencies is replicated along numerous PGM-chloro leaching texts in literature. Chen et al., (2014) attributed this trend to oxidation; citing that during the service life of the PGMs on the autocatalytic converters and exposure to consistently high temperatures, a significant proportion of the Rh is oxidised. Oxidised PGMs are more difficult to leach than elemental state PGMs. Despite this proposed explanation, the authors did not confirm this supposition by presenting data on the state of the Rh in the used autocatalytic converter prior to leaching. However, when the used autocatalytic converter was subjected to a reducing atmosphere in hydrogen, the Rh recovery improved from 56% to 82%, which may give some level of credence to this proposed explanation of Rh oxidation.

In light of the observed PGM leaching trend in the texts reviewed and proposed explanation by Chen et al., (2014), it became imperative to compare the reactivity of the three PGMs in their elemental form under standardized conditions in acidic, oxidising chloro solutions. Hartley, (1991) compared PGM leaching efficiency in different solutions and revealed that the reactivity of the three pure PGM metals was again of the order Pt >/≈ Pd > Rh. In chlorine saturated HCl, for example, at 100 $^{o}$C the reactivity for Pt, Pd and Rh was 1 mg/cm$^{2}$·h$^{-1}$, 1 mg/cm$^{2}$·h$^{-1}$ and 0.1 mg/cm$^{2}$·h$^{-1}$. Pt and Pd reactivity was greater than that of Rh by an order of approximately 10. This analysis proved that as much as oxidation during the service life of the autocatalytic converter is probably a contributing factor as proposed by Chen et al., (2014), differences in leaching efficiencies must surely result from the mechanisms by which the individual metals are complexed as well.

This observation of PGM leaching in the magnitude of Pt >/≈ Pd > Rh has been made both in the primary refining industries and PGM hydrometallurgical recycling literature. However, a conclusive explanation for this observation could not be identified in literature. It was therefore decided that one of the objectives of this research would be to propose a plausible scientific explanation that could be further explored and evaluated for the consistently lower Rh recoveries.

### 2.7.2 PGM leaching approach of dissolving supporting structure into solution

Another approach to recover the PGMs is to dissolve the supporting structure using a lixiviant selective only to the supporting structure, i.e. strong mineral acids in the absence of an oxidant. The undissolved PGMs are then obtained using a solid - liquid separation procedure like filtration. The dissolved support is obtained in the filtrate whilst the relatively more concentrated PGM dust is obtained in the solid residue. The low solubility of Pt, Pd and Rh in mineral acids at various concentrations and temperatures has been shown by Hartley, (1991).

Table 2.5: Solubility of PGM in selected common mineral acids (Hartley, 1991).

| Mineral Acid | Concentration | Temperature/$^{o}$C | Solubility/mg·cm$^{-2}$·h$^{-1}$ | | |
|---|---|---|---|---|---|
| | | | Pt | Pd | Rh |
| HCl | 36% | 20 | - | - | - |
| | | 100 | - | 0.1 | - |
| HF | 40% | 20 | - | - | - |
| | | 100 | 0.1 | 0.1 | - |
| HI | 57% | 20 | - | 10 | - |
| | | 100 | 10 | 10 | - |
| HBr | 60% | 20 | 0.1 | 10 | 0.1 |
| | | 100 | 0.1 | 10 | 1 |
| $H_2SO_4$ | 96% | 20 | - | - | - |
| | | 100 | - | 0.1 | 0.1 |
| $HNO_3$ | 65% | 20 | 0 | 10 | - |
| | | 100 | 0 | 10 | - |

On the contrary, alumina dissolves in mineral acids, as shown in equation 17 below (Steinlechner and Antrekowitsch, 2015).

$$Al_2O_{3(s)} + 6\,H^+ \rightarrow 2Al^{3+}_{(aq)} + 3H_2O \qquad \text{Equation } \mathbf{17}$$

This approach therefore presents an opportunity for obtaining PGM from the wash coat layer by dissolving the alumina in mineral acids and recovering PGM through a solid-liquid operation. The benefits accruing from such an operation would be higher expected recoveries and fewer PGM-related beneficiation processes that could result in loss of values. However, the dissolution of the supporting matrix, which has a higher proportion by mass when compared to the PGMs, is expected to produce a high volume of highly acidic effluent, which is expensive to safely dispose.

Willner and Fornalczyk, (2015) investigated the use of 10 M acid solutions of $H_2SO_4$, HCl and $H_3PO_4$ to dissolve the supporting matrix. This study achieved the best dissolution of 26% of the matrix using 10 M $H_3PO_4$ and as expected, alumina dissolved more significantly compared to silica, which resisted acid attack. The results were not very encouraging but could, however, be improved by employing different conditions like higher temperature, autoclave/pressure digestion or multistage dissolution in different acids.

Metallic substrate converters (MSCs) were initially used only in high performance vehicles. However, Fornalczyk et al., (2016) reports an increase in the proportion of cars employing MSC in their design. The basic structure of MSCs is the same as that of the ceramic supported converters, the only difference being that in MSCs, PGM are deposited onto substrates synthesised from Fe-Cr-Al foil (Fornalczyk et al., 2016). Fornalczyk et al., (2016) investigated the dissolution of this MSC in concentrated and dilute 2 M solutions of $H_2SO_4$, $HNO_3$, $H_3PO_4$ and HCl, stirred at ambient conditions for 24 hours using a S: L ratio of 3g: 50 ml.

The metals Fe, Cr and Al react with dilute HCl and $H_2SO_4$ to evolve hydrogen and their respective aqueous ions. The concentrated acids and dilute nitric acid are strong oxidising agents that will passivate the metals and prevent further attack by the acids. Fornalczyk et al., (2016) were able to illustrate and present an alternative to recycling of metal substrate supported converters that recovers the PGM fraction in the solid residue, and the metal substrate in the filtrate. The PGM dust recovered in the solid residue component assayed 0.7% – 0.8% from its initial 0.084% in the raw autocatalytic converter. Maximum loss of platinum reporting to the filtrate solution was 0.003%, obtained after dissolution in 2 M $H_3PO_4$ and $H_2SO_4$. The dissolution of the supporting metal substrate using dilute acids may provide significant economic returns and environmental benefits when compared against PGM dissolution for MSC.

The use of dilute acids alone (without oxidants) eliminates the hazards associated with most concentrated acid/oxidant combinations such as the formation of toxic and acidic $Cl_2$, noxious nitrogen oxides or nascent nitrogen species. Dissolving the metals Fe, Cr and Al into an aqueous solution from the MSC may also provide an opportunity for recovering the metals as by-products

that may also be sold to increase revenues. Furthermore, the concentrated PGM fraction in the residue may therefore be digested using significantly smaller volumes of reagents and recovered as the main product for sale.

Willner et al., (2015) investigated acidithiobacillus ferroxidans and acidithiobacillus thiooxidans bacteria for the dissolution of the metal substrate in MSCs. Bacteria were first adapted for high metal concentrations. This was done by dosing the bacterial culture every two days for three weeks. 2.5 g sample of 2 mm metal substrate was added to 250ml distilled water in flasks containing the bacteria, which were maintained at 30 $^{o}$C, to which 10 M $H_2SO_4$ had been added.

Three sets of experiments were then conducted for a total of 96 days with sample extraction. These were a control experiment in which no bacteria were added, one with adapted bacteria and the last with un-adapted bacteria. The response variables were Fe, Cr and Al concentrations since the purpose of the bacterial culture was to facilitate the dissolution of the supporting matrix.

Fe dissolution peaked at day 14 with maxima of 235 mg/L, 211 mg/L and 1.2 mg/L for adapted, un-adapted bacteria and chemical (no bacteria) respectively, thereby illustrating the biological dependence of iron dissolution. Beyond day 14, the Fe concentration began to decrease. This was because the oxidation of $Fe^{2+}$ to $Fe^{3+}$ is an acid consuming reaction that increases the pH of the solution. Fe dissolution into solution requires acidic conditions; this therefore, resulted in the observed decrease in iron dissolution beyond day 14.

Aluminium registered a progressive increase in dissolution from the solid phase, all the way to day 96 for all three reaction conditions. The aluminium leaching efficiencies at the three test conditions (with adapted bacteria, un-adapted bacteria and with no bacteria) were quite comparable, suggesting that there was no significant contribution to Al leaching as a result of the biological oxidation. The progressive increase in Al leaching was merely a result of increased residence time in the leaching solution. The maxima Al leaching efficiencies obtained for the biological sample and for the chemical sample were 10.28 mg/L and 8.8 mg/L on day 96.

Cr concentration remained below 1 mg/L up to day 28 and only peaked at 7.66 mg/L on day 96 for adapted bacteria. This slight increase in leaching efficiency with time was attributed to cumulative adaptation due to slowly increasing metal concentration and time of bacteria exposure, thereby activating the bacteria for further dissolution activity.

The potential for biological leaching of Fe was observed, which peaked at 235 mg/L in the 96 days of leaching. However, the same cannot be concluded for both Al and Cr, which showed consistently slow leaching kinetics for biological leaching; only peaking at 10.28 mg/L and 7.66 mg/L in 96 days. Comparison data on the PGM character of the substrate before and after leaching were however, not presented, although it is expected that the PGM should not have dissolved due to either action of biological or chemical leaching.

### 2.7.3 Importance of pre and post treatment methods

Pre-treatment and post-treatment methods are important for improving metal extractions and process economics. Both are necessitated by the presence of compounds added to improve the properties of the catalytic material. Modern autocatalytic converters have a supporting structure manufactured from cordierite with a thin film of $\gamma$ - $Al_2O_3$ deposited to provide a highly porous structure for PGM deposition. Additives such as NiO are used to inhibit the formation of $H_2S$ during the operation of the convertor, and Ce and Zr compounds enhance the catalytic activity of the PGMs.

Contaminants to be expected during the operation of the convertor are carbon, soot, base metals, vanadium, moisture, phosphorous compounds and oil. Oil deposits on the convertor are a sign of a faulty engine. Oil in hydrometallurgical extraction is undesirable because it reduces the efficiency of PGM recovery by reducing the contact between the solid and the aqueous solution. If oil is present in significant proportions where thermal pre-treatment is required, it may cause local spontaneous combustion. Carbon and soot may also be present due to incomplete combustion, hard starts of the engine in cold weather and excessive oil consumption in the engine. The carbon may block catalyst surfaces and result in shielding those surfaces to lixiviant attack. Other contaminants that may be present on catalyst surfaces include phosphorous compounds, vanadium and base metal compounds. To reduce the co-dissolution of unwanted additives, pre-treatment processes may therefore be necessary.

The presence of other metals in significant quantities presents a valuable source of these metals for recovery. Post-treatment methods may therefore be employed to recover these values where the process economics are justified. The inherent benefits are that more valuable metals are obtained that may be sold to increase revenue, whilst at the same time reducing the amount of metals present in the waste streams that need to be managed.

#### 2.7.3.1 Pre-treatment methods

The different pre-treatment methods that have been investigated include metal vapour deposition (Sasaki and Maeda, 2014), reductive and oxidative pre heating (Jimenez de Aberasturi et al., 2011), (Chen et al., 2014) and formation of "complex oxides" (Kasuya et al., 2016) prior to leaching. The main motivation in most of these pre-treatment investigations has been to develop a process which leaches PGMs in acidic non-oxidising conditions. This would in turn be expected to increase operational safety, reduce formation of noxious products and reduce costs associated with effluent disposal or treatment. Sasaki and Maeda, (2014) investigated the leaching kinetics of a PGM - Zn alloy prepared by Zn vapour deposition on a used autocatalytic convertor in HCl and aqua regia. The used catalyst was obtained by heating a 1 g sample of unused catalyst in air at 1100$^{o}$C for 5 hours. After this "ageing" process, the sample was heated in a quartz tube with Zn plates to form the alloy. A Ti sponge was also added to deoxidise the air. Zn metal was always at a temperature of 15 $^{o}$C to 20 $^{o}$C below that of the SAC. The weight of the used converter test strips increased by about 0.01g, illustrating the formation of the PGM – Zn alloy. Presence of the PGM - Zn alloy was also confirmed by SEM imaging and EDX analysis. This sample was subjected to leaching in aqua regia alone, and then in HCl alone. The leaching kinetics were compared to an unalloyed used converter and another that was heated in the absence of the alloying Zn metal (the deoxidised strip). All three samples were leached in aqua regia at 60 $^{o}$C and 17 $^{o}$C and in HCl at 17 $^{o}$C for 30 minutes. Maximum Pt and Pd leaching in aqua regia at 60$^{o}$C was nearly 100% for both the deoxidised and Zn-vapour alloyed samples. The ageing process for the catalyst may have oxidised some of the PGMs. Heating in the presence of the Ti sponge, whose purpose was to maintain a reducing environment void of oxygen, may have reduced some of these PGMs back into their elemental state. This may have been the reason for the high leaching rates of the PGMs in the deoxidised used converter sample. The effects of the pre-treatment on Rh increased recoveries from <40%, to 50% and 60% for extractions without

pre-treatment, with deoxidation alone and with Zn-vapour pre-treatment respectively. Interestingly, the leaching of Pt, Pd and Rh in aqua regia at 17$^{o}$C was comparable to that at 60$^{o}$C, which would be beneficial as far as energy economics is concerned. However, these energy savings would need to be compared against the energy costs associated with temperatures needed to vaporise the Zn to form the PGM – Zn alloy.

PGMs were also leached using concentrated HCl in the absence of an oxidant by making use of "complex oxides" (Kasuya et al., 2013b), (Kasuya et al., 2013a), (Kasuya et al., 2014), (Kasuya et al., 2015), (Kasuya et al., 2016). Complex oxides are the product of calcination of Pt with a Na, K or Li salt at temperatures higher than 500 $^{o}$C. The purpose was to convert all PGMs present into their complex oxides by calcination, followed by leaching out the Na, K or Li in acidic media to expose and prime the Pt surface to chemical attack. A used autocatalytic converter which was heated at 800 $^{o}$C in the presence of 10 wt % $Li_2CO_3$ salt and then leached in 12 M HCl, achieved higher than 95 % Pt and Rh leaching efficiencies, and a rather surprising < 50% Pd leaching (Kasuya et al., 2016). Increasing $Li_2CO_3$ content to 20 wt% dropped Pt and Rh leaching to 71.2% and 28.2% and increased Pd recovery to near 100%. Pt, Pd and Rh were therefore successfully leached in a non-oxidative media by first converting them to complex oxides by calcining with $Li_2CO_3$.

During their service life, PGMs may become oxidised. According to Chen et al., (2014) the Gibbs free energies for the reaction of Rh and $Rh_2O_3$ to form the chloride (representing chloride leaching), are approximately - 140 kJ/mol and - 50 kJ/mol respectively. This shows that the chloride leaching of elemental Rh in its ground state, whose Gibbs free energy is more negative, is more spontaneous compared to that of leaching the oxide. Given the comparable chemical characteristics of the PGMs, it is also expected that leaching Pt and Pd is also more favourable compared to leaching the corresponding oxides. Consequently, a reduction step may be necessary to convert any PGMs existing in an oxide state, so as to favour the dissolution of PGMs into their respective chloride solutions.

Jimenez de Aberasturi et al., (2011) investigated hydrogen pre-treatment by heating used autocatalytic converters in a 7% $H_2$ stream for 22 hours at 80 $^{o}$C and 250 $^{o}$C . Hydrogen reductive

heating reduces any oxidised PGM fraction to its metallic form. However, the safety concerns associated with hydrogen reduction are a major concern especially at these high temperatures. Reductive leaching was also investigated as a pre-treatment step by Angelidis, (2001) using $N_2H_6SO_4$, $FeSO_4$, and KI. After reductive leaching, leaching of the PGMs in a lixiviant consisting of HCl, $AlCl_3$ and NaOCl as an oxidant was conducted. The leach solution was neutralised and PGMs obtained by reduction using aluminium foil in the presence of lead ions (Angelidis, 2001). The overall procedure achieved recoveries of between 90% and 99% of the PGMs.

Chen et al., (2014) investigated the effects of pre-treating spent autocatalytic converters in streams of oxygen, hydrogen and carbon monoxide prior to acidic sodium chlorate leaching of Rh metal. Initially, individual effects of $O_2$, $H_2$ and CO pre-treatment were investigated. After these were quantified, the authors also investigated $H_2$ and CO (reductive pre-treatment) after heating in a stream of $O_2$. In all cases, a stream of pure Ar gas was always passed at a rate of 200 mL/min for 15 minutes through the quartz tube to remove any residual gas. Leaching was conducted by adding $H_2SO_4$ and HCl to a reactor, followed by adding $H_2O_2$ and $NaClO_3$ solution and then leaching at 95 $^oC$ for 3 hours. Heating in a stream of $O_2$ prior to leaching increased the recovery of rhodium from 56% to 69% at an optimised temperature of 300 $^oC$, oxygen flow rate of 200 ml/minute and 3 hours for time, representing a 23% increase attributed to oxidation alone. Heating the auto catalyst in a stream of oxygen removes any carbon bearing material, e.g. soot, which is on the catalyst surface by oxidising it to carbon dioxide. Removing this carbon bearing material increases contact between the PGM and the leaching reagent. This was confirmed by the decrease of the carbon content from 0.18 wt. % to slightly below 0.1 wt. % with an increase in heating temperature. Chen et al., (2014) also observed an increase in specific surface area and average pore diameter with an increase in temperature, which may have also led to an increase in the contact between Rh and leaching reagents, consequently increasing the extraction of Rh.
Under optimised $H_2$ heating conditions, a paltry 7% increase in Rh extraction was observed. Similarly, with heating in the presence of CO, an increase from 56% (without pre-treatment) to 66.4% (representing an increase of just 18%) was observed under optimised CO heating conditions.

The best result of the three was obtained with $O_2$ heating alone. However, although $O_2$ heating, removes the carbon bearing waste that hinders effective contact, it may also increase the amount of oxidised PGM fraction. Leaching this oxidised PGM fraction is slower than leaching metallic PGMs, so it became imperative to investigate the potential of initially oxidative heating to remove carbon bearing waste, followed by reductive heating to reduce any oxidised PGM to their ground state. Reductive heating (in $H_2$ or CO) after oxidative heating in a stream of $O_2$ significantly increased the extraction of Rh as shown in Figure 2.11. As has already been established, oxidative heating oxidises carbonaceous material, which is removed as carbon oxides. It also increases the specific surface area and adsorption pore diameter, which results in an increase in the PGM-lixiviant contact and extraction rate. Reductive heating afterwards thus aids the reduction of any oxidised PGMs into their metallic form. This explains the increase in the Rh extraction when oxidative heating was followed by reductive heating in CO and $H_2$. The best results were oxidative heating in $O_2$ followed by $H_2$ reductive heating through which the extraction of Rh increased from 56.0 % to 82.0 %.

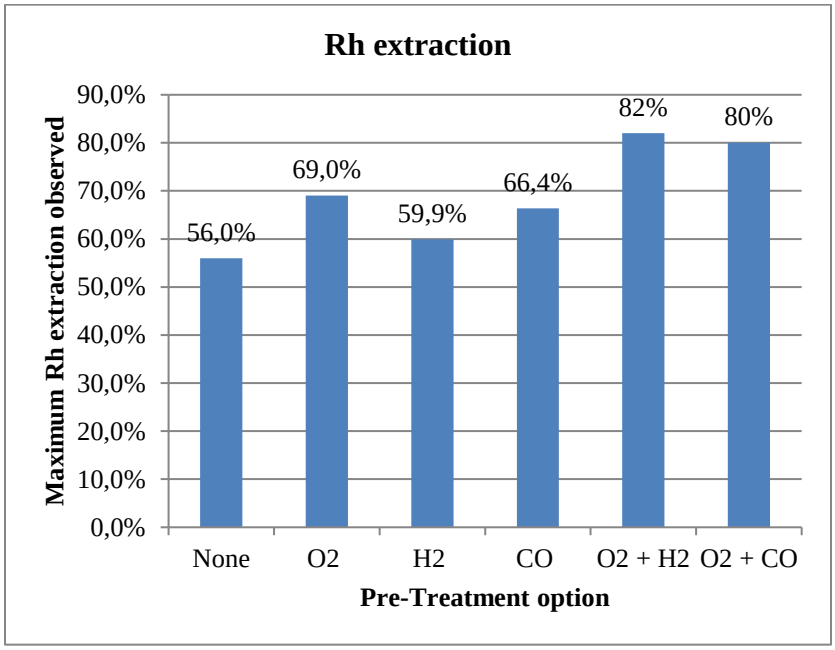


Figure 2.9: Comparison of Rh extraction after different pre-treatment methods; (Chen et al., 2014)

The use of reductive pre-treatment methods by heating in $H_2$ or oxidative pre-treatment by heating in $O_2$, poses significant safety concerns considering the flammable nature of these gases.

However, their effect on increasing leaching efficiency must not be undervalued, as clearly noted from the reviewed literature.

#### 2.7.3.2 Post-treatment methods

Post-treatment methods refer to any processes that come after PGM recovery either for reagent regeneration or co–value extraction. These are imperative for improving process economics by extracting other metallic values to increase revenue, reduce costs associated with disposal of metal bearing effluent and to reduce reagent costs where it is economically justified to regenerate and reuse them. Autocatalytic converters are often loaded with other additives such as cerium oxide, zirconium oxide and alumina; which aid in the effective catalytic activity of the PGMs. According to Steinlechner and Antrekowitsch, (2015), in acidic oxidising environments, Ce and Al undergo the following reactions:

$$Ce_{(s)} + 4.5\,H^{+} + 1.5HO_2^{-} + 4Cl^{-} \rightarrow [CeCl_4]^{-}_{(aq)} + 3H_2O \qquad \text{Equation } \mathbf{18}$$

$$Al_2O_{3_{(s)}} + 6\,H^{+} \rightarrow 2Al^{3+}_{(aq)} + 3H_2O \qquad \text{Equation } \mathbf{19}$$

PGM in the leach liquor were recovered by an aluminium cementation step to produce a PGM sponge, and both the Al and Ce were recovered by precipitation as their double sulphates through addition of sulphuric acid and potassium chloride and sulphuric acid and sodium sulphate respectively. The aim of this study was to limit residues and produce usable end products.

The Al double sulphate may be used as a bleaching agent in the paper and pulp, cosmetics and the medical industries (Steinlechner and Antrekowitsch, 2015). The Ce double sulphate can be calcined to produce an oxide, which is a feed for the glass glazing and polishing industry (Moon et al., 2014). Cerium (III)/Cerium(IV) aqueous solutions also find electrochemical applications in medicine, chemical analysis, cleaning and decontamination, gas scrubbing and environmental treatment (Arenas et al., 2016). Secondary recovery of cerium oxide or its soluble salts could have applications, which would economically justify the need for a post-treatment purpose. The ground supporting structure that is left behind from the solid-liquid separation of pregnant leach liquor may also have refractory applications due to the nature of its constituent components i.e. silica, alumina and magnesium oxide.

## 2.8 Recovery of PGMs from chloride based media

Several techniques have been reviewed in literature and adopted in the PGM refining industry for recovering PGMs from chloride solutions. These are premised on solvent extraction (Nguyen et al., 2016a), (Nguyen et al., 2016b), (Gandhi et al., 2015), cloud point extraction (Suoranta et al., 2015), ion exchange membranes, organic precipitation and inorganic precipitation/crystallisation (Crundwell et al., 2011). More recently, ionic liquids have also been adopted for recovering PGMs from solutions (Cieszynska and Wiśniewski, 2012), (Yang et al., 2014), (Regel-Rosocka et al., 2015), (Nguyen et al., 2016c). The thrust within the PGM recycling industry has been to develop a PGM recovering process whose products may be easily integrated into current PGM refining processes. A review of the related literature for PGM recovery follows in the next section.

### 2.8.1 The classical precipitation approach

Figure 2.10 summarises the precipitation approach for precious metals' refining according to Crundwell et al., (2011). Rh is obtained after extraction of Au and Ru by increasing the pH to 5 using sodium bicarbonate to form $Rh(OH)_3$ precipitates. Platinum is then recovered by adding $NH_4Cl$, HCl and $H_2O_2$ (Eh = 0.9V - 1V vs. Saturated Calomel electrode) to obtain the precipitate $(NH_4)_2PtCl_6$. After Pt recovery, the pH of the remaining solution is increased to 0.9 using NaOH, and then boiled until it reaches 3. Ammonium acetate is added, the solution is boiled again until the pH is 4.2, cooled to 30$^{o}$C and $(NH_3)_2PdCl_2$ precipitates out of solution, which is recovered by filtration. All salts are then sent to secondary treatment (Crundwell et al., 2011).

The PGM leach liquor from spent autocatalytic converters may contain a lot of leached out aluminium. Recovering Rh by increasing the pH may therefore be difficult due to the dissolved aluminium, which at that pH range (around 5) starts to form gelatinous aluminium hydroxide. However, removing the Al prior to Rh precipitation may mean that a similar extraction mechanism may be employed. The inherent advantage would be that existing refineries that incorporate PGM recovery by precipitation may easily introduce the PGM leach liquor from autocatalytic converter leaching without significant engineering restructuring.

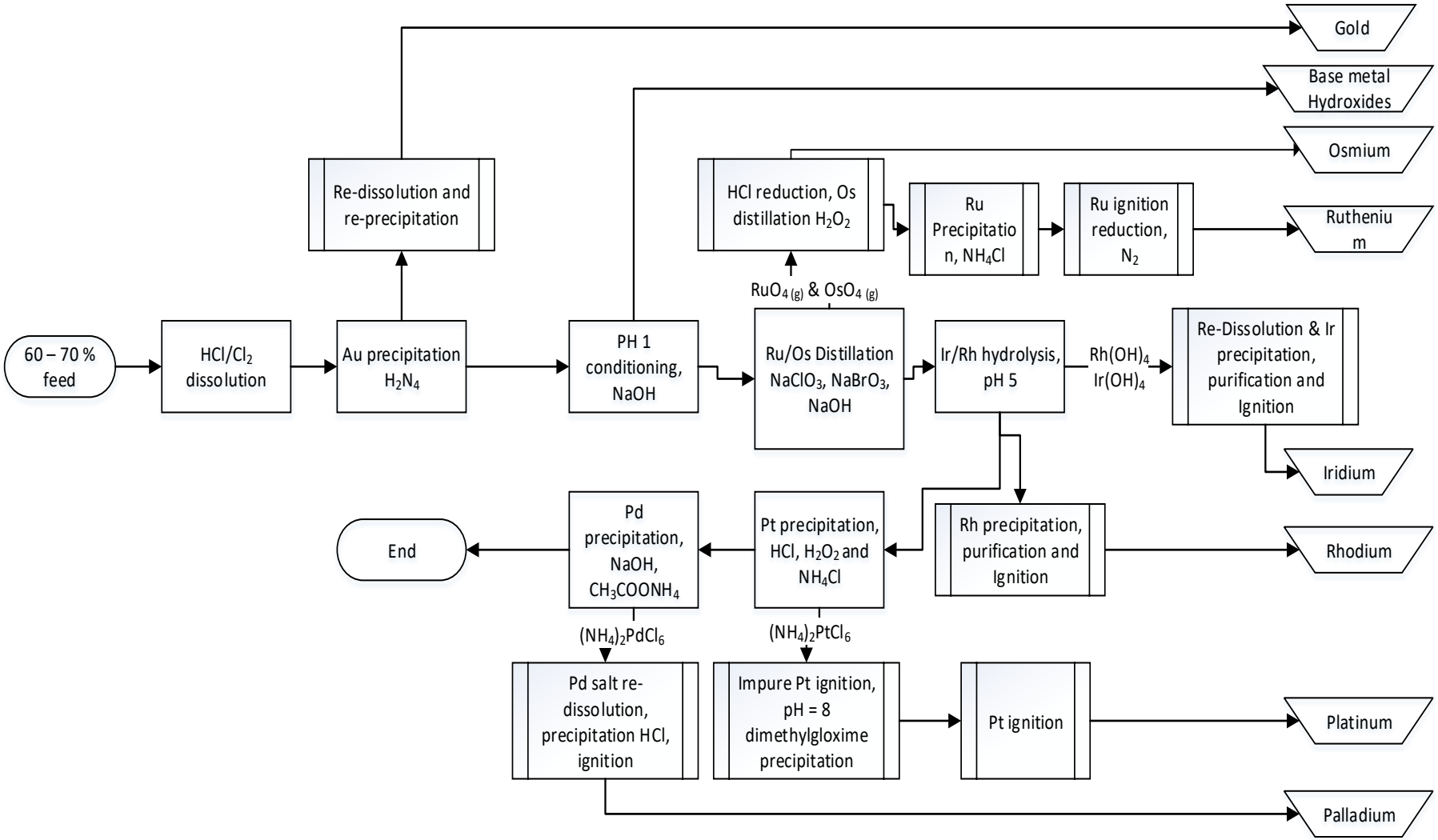


Figure 2.10: Classical precipitation method for refining of PGMs from precious metal concentrates (Crundwell et al., 2011)

### 2.8.2 The solvent extraction method

In the Johnson Matthey/Anglo American process, Pd is extracted using LIX 84A and stripped by 6 M HCl (Crundwell et al., 2011). The stripped solution is contacted with $NH_4Cl$ to precipitate Pd. Pt is extracted using a secondary amine which is stripped using 11 M HCl and precipitated using $NH_4Cl$ as well. Ir and Rh are removed by increasing the pH to 5.8 and precipitating them as impure hydroxides, which are dissolved in HCl and $H_2O_2$. Rhodium is recovered from the solution using diethylene triamine (DETA) and also precipitated using $NH_4Cl$ (Crundwell et al., 2011). Figure 2.11 illustrates the solvent extraction scheme as employed by Johnson Matthey and Anglo American refineries. The Vale refinery in Acton recovers Pd by first using di-n-octylsulfide followed by stripping using aqueous ammonia and precipitation as a result of an addition of HCl (Crundwell et al., 2011). Pt is extracted using tributyl phosphate, scrubbed using water and precipitated using $NH_4Cl$ (Crundwell et al., 2011). Rh is recovered by direct cementation using formic acid (HCOOH) to form Rh black (Crundwell et al., 2011).

### 2.8.3 The ion exchange process

At the Impala Springs refinery, Pd is extracted selectively using molecular recognition technology, before Ir and Rh are removed as hydroxides by raising the pH of the solution to around 6 (Crundwell et al., 2011). The Ir and Rh hydroxides go through an elaborate process of re-dissolution and selective organic precipitation to retain the base metals in solution as illustrated in Figure 2.12. The obtained Ir and Rh organic precipitate is again re-dissolved before ion exchange is used to remove Ir. Rh in solution is then precipitated using the same organic amine as in the first precipitation step, and ignited to produce pure Rh. Pt is essentially obtained via a precipitation process using $NH_4Cl$ (Crundwell et al., 2011).

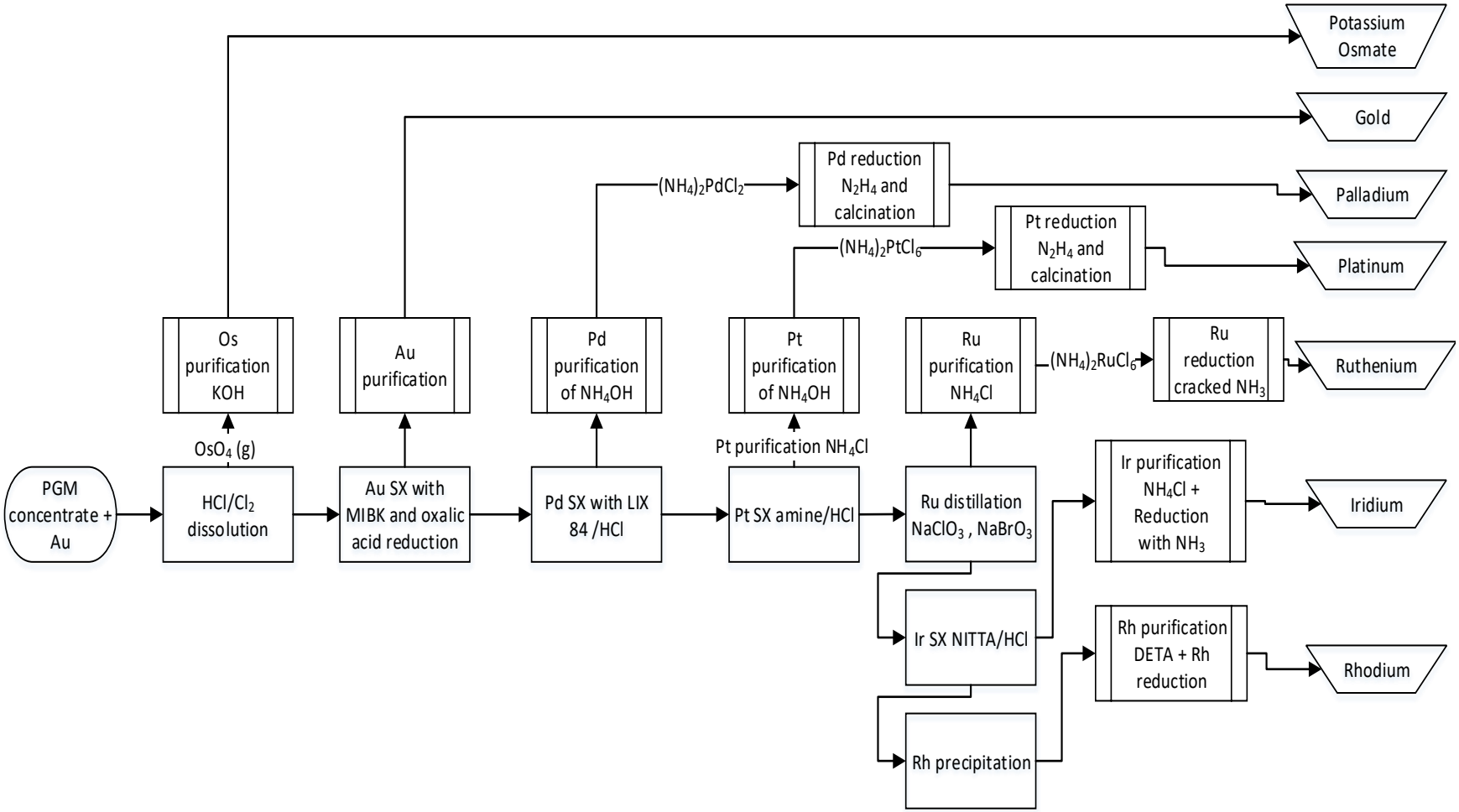


Figure 2.11: Solvent extraction method for recovery of PGMs from precious metal concentrates (Crundwell et al., 2011)

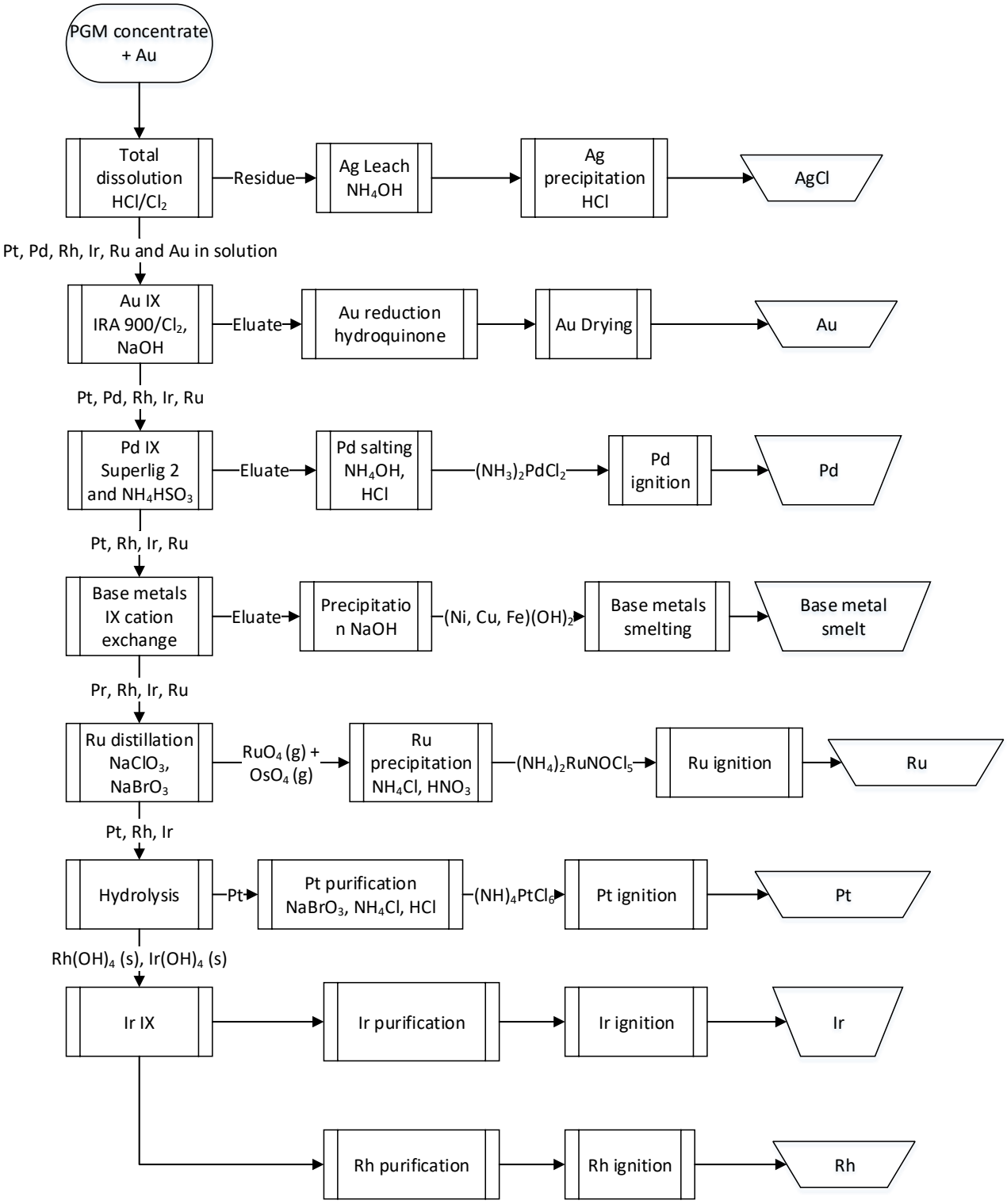


Figure 2.12: Ion exchange method for recovery of PGMs from precious metal concentrates (Crundwell et al., 2011)

### 2.8.4 Recent advances in solvent extraction (SX) of PGMs from chloride leach liquor

The solvent extraction (SX) method for recovering PGMs from leach liquor seems to be the more preferred route due to its compromise between cost and efficiency. The cheapest and relatively safest method is direct precipitation; however it has very low PGM recoveries and requires numerous re-dissolution steps that translate to a longer PGM lock up. In such instances, SX becomes a better alternative. SX is premised on the preferential distribution of the dissolved metal ions between two immiscible phases, an aqueous phase and an organic phase. Most organic solvents used for solvent extraction are however, quite toxic, mostly volatile, and can even be outright expensive. Some recent investigations are present in the literary works. These have investigated the potential for using SX in recovering PGMs from SAC leach liquor. However, most of these investigations have been on synthetic leach liquors. Synthetic leach liquor refers to a solution in which the metal ions that would be expected in the actual leach liquor are obtained by dissolving pure laboratory grade salts of the ions. Nguyen et al., (2016b) and Nguyen et al., (2016a) investigated the potential for using a variety of organic extractants for recovering and separating PGMs from simulated SAC leach liquors. Their findings have been tabulated and summarised in Tables 2.6 and Table 2.7. Of particular interest is the potential for the use of tri-iso octylamine, which is commercially known as Alamine 308, for combined Pt and Pd recovery as illustrated by Nguyen et al., (2016a). The use of a single extractant in a single step to recover both Pt and Pd has a lot of economic benefits associated with it and may make the entire recycle operation significantly cheaper.

Table 2.6: Extraction of Pd (II), Pt (IV), Ir (IV) and Rh (III) from concentrated HCl solution (Nguyen et al., 2016b)

| Metals in solution | Pt(IV) | Pd (II) | Ir (IV) | Rh (III) |
|---|---|---|---|---|
| Type of Solution | Synthetic solution was prepared from 99.5 % $H_2IrCl_6$ (99.5 %), 99.9 % $RhCl_3.xH_2O$, 99.9 % $PtCl_4$ and 99.9 % $PdCl_2$ dissolved in concentrated HCl | | | |
| Extractant | tributylphosphate (TBP) | 5,8-diethyl-7-hydroxydodecan-6-oxime (marketed as LIX 63) | Tricaprylylmethyl ammonium chloride (marketed as Aliquat 336) for Ir (IV). | *Left in raffinate* |
| *Optimum extraction* | 6 M HCl, 2 M TBP, extraction efficiency = 80 % | 6 M HCl, 0.06 M Lix 63 extraction efficiency = 80 % | 6 M HCl, 0.01 M Aliquat 336; extraction efficiency = 80 % | *N/A* |
| Stripping reagent | HCl | Thiourea | $NaClO_3$ | *N/A* |
| *Optimum stripping* | Complete at 0.01 M HCl | Complete at 0.1 M thiourea | 99.5 % at 1 M | *N/A* |
| Order of PGM recovery | Pd → Pt → Ir → Rh | | | |
| Notes | Ir extraction had to be preceded by an oxidation step. Ir (III) was oxidised to Ir (IV) using 0.0008 M $NaClO_3$. To prevent the formation of a third phase during the Ir separation, 5 % v/v TBP was added to the solution. | | | |

The flow sheet developed by Nguyen et al., (2016b) for PGM recovery separation is illustrated in Figure 2.13 below.

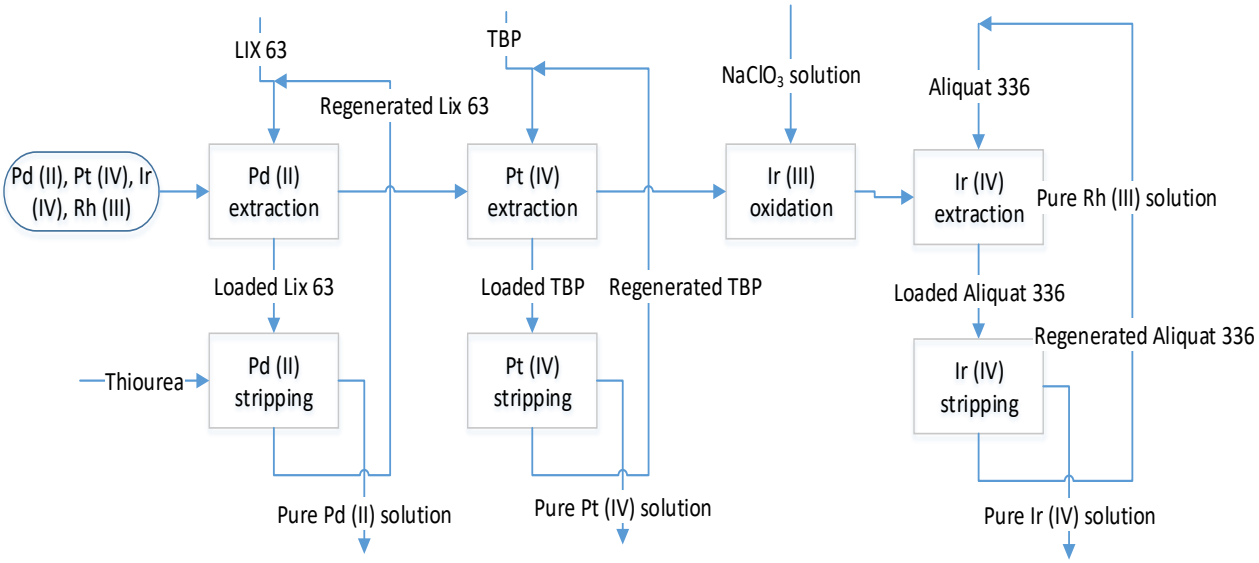


Figure 2.13: Extraction scheme for Pd (II), Pt (IV), Ir (IV) and Rh (III) (Nguyen et al., 2016a).

Table 2.7: Extraction of Pd (II), Pt (IV), Ir (IV) and Rh (III) from concentrated HCl solution (source of data Nguyen et al., (2016a)

| Metals in solution | Fe(III) | Pd (II) | Pt (IV) | Ce(III) | Rh (III) |
|---|---|---|---|---|---|
| Extractant | tributylphosphate (TBP) | tri-isooctylamine (Alamine 308) | tri-isooctylamine (Alamine 308) | *Left in raffinate* | Zn cementation |
| *Optimum extraction* | 0.3 M TBP, 6 M HCl, complete extraction | 0.1 M Alamine, A/O ratio = 2/3, 4 stages, 5 % v/v Decanol | 0.1 M Alamine, A/O ratio = 2/3, 1 stage, 5 % v/v Decanol | *N/A* | 0.4 mg was added to 20 mL raffinate to cement 83 % Rh and leave Ce (III) in solution. |
| Stripping agent | Water | HCl + Thiourea | HCl + Thiourea | *N/A* | |
| *Optimum extraction* | 3 stages, A/O ratio = 2, stripping = 100 % | 3 stages, A/O ratio = 2, 0.5 M HCl + 0.01 M thiourea; stripping = 100 % | 3 stages, A/O ratio = 2, 0.5 M HCl + 1 M thiourea stripping = 100 % | *N/A* | |
| Type of Solution | A synthetic solution was prepared by dissolving the salts $PtCl_4$, $PdCl_2$, $RhCl_3 \cdot xH_2O$, $CeCl_3$, and $FeCl_3 \cdot 6H_2O$ in HCl and mixing equal volumes of the solutions | | | | |
| Order of PGM recovery | Fe → Pt → Pd → HCl → Rh | | | | |
| Notes | A 5 stage counter current separation of HCl using TEHA was employed to reduce the concentration of HCl to 0.5 M so that Zn powder could be used to precipitate Rh out. This particular process would definitely have significant economic implications in a full scale plant as it adds to the cost of the operation. | | | | |

The extraction scheme developed by the authors is presented in Figure 2.14.

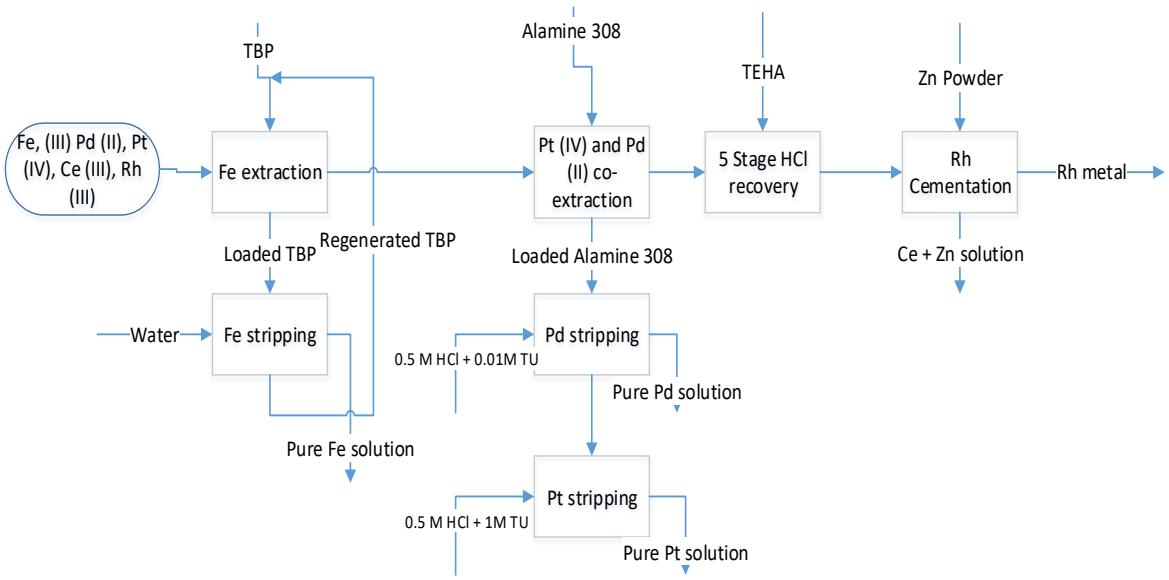


Figure 2.14: Extraction scheme for Pd (II), Pt (IV), Fe (III), Rh (III) and Ce (III) from synthetic leach liquor Nguyen et al., (2016a)

### 2.8.5 New and emerging technologies for PGM recovery from chloride leach liquors

Despite the conventional processes that have been used in the recovery of PGMs, new and emerging technologies have also been investigated. Chief amongst these is the emergence of ionic liquids and their potential application for metal recovery. Despite their widespread attention, ionic liquids still tend to have numerous challenges. However, this may be because ionic liquids are still a relatively new technology and further exploration of their potential means that they could be adopted commercially in the more near future.

Of the three metals, Pd (II) extraction using ionic liquids has been investigated the most. A new methodology for three-phase systems in which the metals are separated into an aqueous phase, ionic liquid phase and an organic solvent phase has been suggested in literature (Zhang et al., 2013). The practical, engineering applicability of such an approach is, however, still to be investigated. Notwithstanding these advances, most of the studies currently being conducted are still preliminary investigations using synthetic solutions.

Cieszynska and Wiśniewski, (2012) recovered Pd (II) using Cyphos®IL 104 diluted in toluene and observed very fast equilibrium times in the magnitude of around 5 minutes. 96% Pd (II) was

extracted at 0.1 M HCl followed by room temperature stripping using 0.5 M $NH_4OH$ which achieved 90% stripping in about 5 minutes. The IL could be used five more times before recoveries began to decrease. Yang et al., (2014) investigated the effect of extracting Pt (IV) and Pd (II) from HCl solution using undiluted [Bmim][Tf2N], [Hmim][Tf2N] and [Omim][Tf2N]. [Omim][Tf2N] attained recoveries of approximately 80% for Pt (IV) whilst Pd (II) recovery was consistently lower than 5%. No information was presented about stripping. Regel-Rosocka et al., (2015) also attained high (≈ 100 %) and fast (1 minute extraction equilibrium) Pd (II) recoveries using Cyphos®IL 102 in toluene. 0.5 M $NH_4OH$ was used for stripping, achieving equilibrium in 5 minutes with efficiencies in the range of 84% to 90% . NaCl was employed to improve phase separation. Svecova et al., (2016) investigated separation of Rh (III) and Pd (II) in HCl using Cyphos®IL 101. At 8 M HCl, extraction efficiency into Cyphos®IL 101 of Rh (III) was 0% whilst it was 89.7% for Pd (II) at the same HCl concentration. The variation in extraction as a function of HCl concentration could therefore, be used to separate Pd (II) from Rh (III). The separation factor at 6 M HCl for Cyphos®IL 101 was quite high at 4250. Nguyen et al., (2016c) also investigated the use of Cyphos®IL 101 for separation of Pt (IV) and Pd (II) followed by stripping using thiourea in 5% HCl. The authors attained a stripping efficiency of 100 % Pd (II) and 10.5% Pt (IV) using 0.02 M thiourea. Thiourea could therefore be used for selective separation of Pt (IV) over Pd (II). Zhang et al., (2013) designed a three phase system to separate Pt (IV), Pd (II) and Rh (III). The ionic liquid $[C_4mim][PF_6]$ was used for Pt (IV) extraction, di-iospentylsulfide ($S_2O_1$) in nonane for Pd (II) extraction; thereby leaving the Rh in aqueous solution. Two-stage stripping was conducted using $NH_4OH$ for Pd (II) with a recovery of 90%. Pt (IV) was stripped using concentrated HCl or $HNO_3$, attaining a maximum of only 68.5% at 3 M $HNO_3$. However, the use of concentrated acid degraded the ionic liquid, meaning it could no longer be reused.

### 2.8.6 Appraisal of recovery methods

The solvent extraction route has enjoyed a relatively widespread adoption in the PGM and precious metals refining industries. Typically, solvent extraction has high extraction efficiencies and high production throughputs, but also employs flammable and toxic solvents for the organic extractants. The use of ionic liquids as extractants may have the potential to overcome some of the challenges associated with organic solvents. However, ionic liquids are still an emerging

technology, synthesis of which is still relatively expensive. Data regarding equilibrium isotherms for both extraction and stripping using ionic liquids is also still relatively unavailable.
Precipitation, although relatively safer, and cheaper, results in lower purification levels. To attain commercially acceptable purities, numerous steps of re-dissolution and re-precipitation are therefore required, which ultimately translates to PGM lock up.

## 2.9 Research approach and proposed hypotheses

In this study, the approach for dissolving PGMs into solution is investigated. This is because the majority of auto convertors are manufactured using acid resistant cordierite, which is technologically challenging to digest. Furthermore, since the substrate structure is the dominant phase, dissolution of this phase requires a lot of reagents and produces a lot of liquid waste. It therefore, makes more economic sense to leach out the PGMs from the supporting matrix, using a lixiviant that is suitably selective to the PGMs.

The PGMs are a group of noble metals, dissolution of which requires acidic and oxidising conditions in the presence of a complexing agent as shown in Figure 2.15. Under these prevailing conditions, cerium may also dissolve into an aqueous solution of $CeCl^{2+}$. Recovering cerium as a by-product may present another revenue generating stream for a recycling entity employing this process. PGMs will then leach into a solution according to equations 20 to 22, provided the leaching solution has a potential above + 0.744 V. A suitable oxidant is therefore required to achieve this minimum solution potential.

$$PtCl_6^{2-} + 4e \rightarrow Pt + 6Cl^- \; E^\theta(V) = +0.744\,V \qquad \text{Equation } \mathbf{20}$$

$$PdCl_4^{2-} + 2e \rightarrow Pd + 4Cl^- \; E^\theta(V) = +0.615\,V \qquad \text{Equation } \mathbf{21}$$

$$RhCl_6^{3-} + 3e \rightarrow Rh + 6Cl^- \; E^\theta(V) = +0.44\,V \qquad \text{Equation } \mathbf{22}$$

### 2.9.1 Complexing and acidifying agent

$AlCl_3 \cdot 6H_2O$ will be investigated as the source of the chloride ions for complexing. $AlCl_3 \cdot 6H_2O$ dissociates in solution to produce 3 chloride ions per molecule as illustrated in equation 23.

$$AlCl_3 \cdot 6H_2O(aq) + H_2O(l) \rightarrow Al(H_2O)_6{}^{3+}(aq) + 3Cl^-(aq) + H_2O(l) \qquad \text{Equation } \mathbf{23}$$

This is expected to provide a ready excess of chloride ions, which would improve leaching kinetics and increase the stability of the PGM complexes that are formed. An excess of chloride ions is also expected to favour the forward complexing reaction of the PGMs as shown in equations 20 to 22. The addition of $Al^{3+}$ ions would also reduce the amount of aluminium that leaches out of the supporting matrix as a consequence of the common ion effect, whereby an excess of $Al^{3+}$ in solution would discourage further dissolution of $Al^{3+}$. Moreover the $Al^{3+}$ ion has a high charge density due to the large positive charge and small ionic size. This high charge density thereby results in protonation of the water molecules surrounding the $Al^{3+}$ ion. This equilibrium is illustrated in equation 24, with a pKa value of 5 at 25 $^{o}$C (Chemical Rubber Company and Lide, 2003).

$$Al(H_2O)_6{}^{3+} \leftrightarrow Al(H_2O)_5(OH)^{2+} + H^+ \qquad \text{Equation } \mathbf{24}$$

The release of the $H^+$ ions thus makes the solution acidic. A solution of $AlCl_3$ has the dual purpose of providing the required complexing ions and also giving the solution the required acidity.

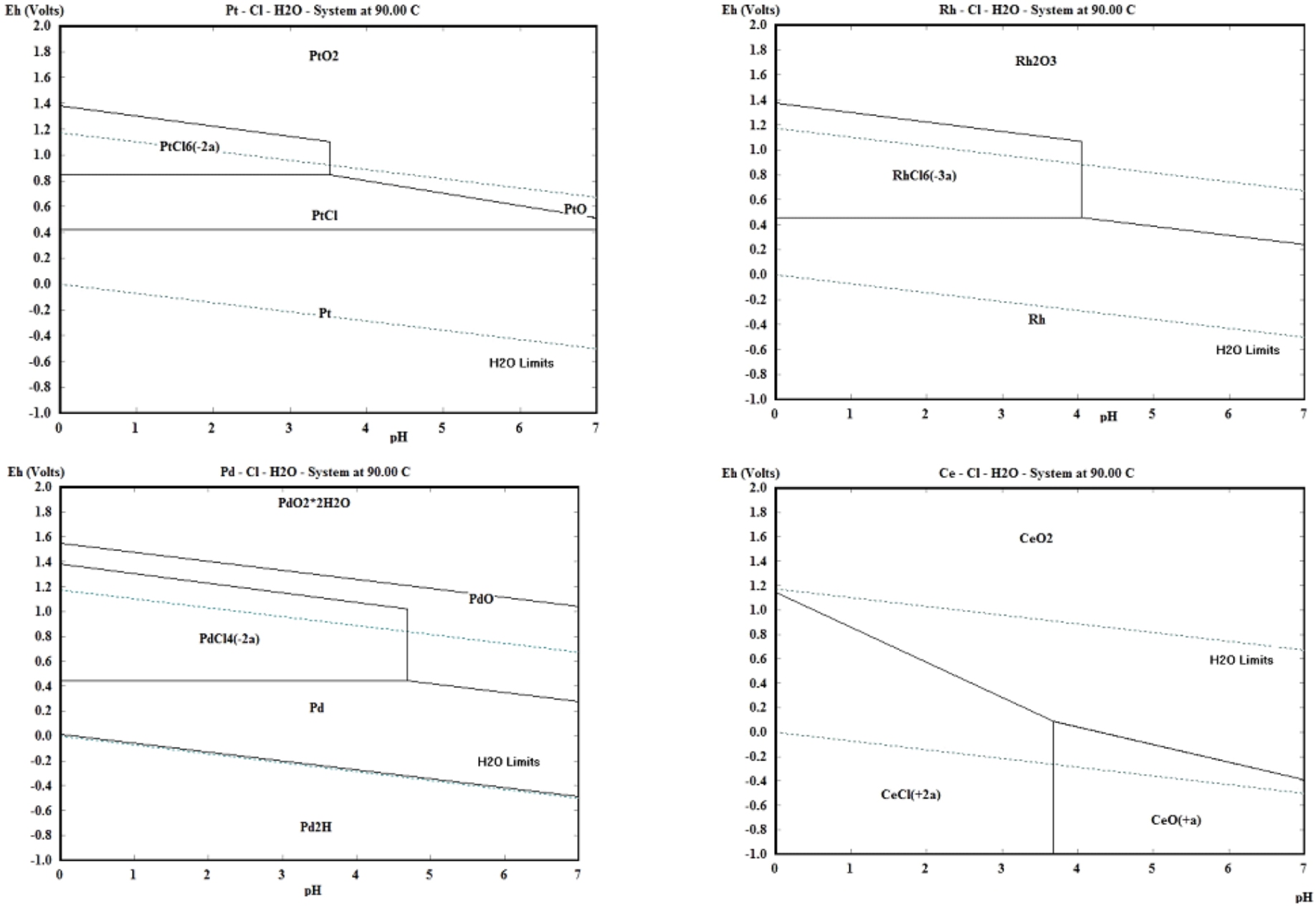


Figure 2.15: Eh – pH diagrams for Pt, Pd, Rh and Ce in Cl – $H_2O$ system (drawn using HSC Chemistry Software)

### 2.9.2 Oxidant

Equations 20 to 22 have already illustrated the need for an oxidant with a minimum oxidising potential of + 0.744 V to solubilize the PGMs. HOCl was chosen as the oxidant because of all the chloro-oxidising species, it has the highest oxidising potential as shown in equations 25 to 27 (Cotton, 1997) and ("The Cell Potential," 2013). According to equation 25, the oxidising potential for the HOCl/Cl system is +1.630 V.

$$HClO + H^+ + e^- \leftrightarrow {}^1/_2\, Cl_2 + H_2O\ ;\ E^\theta(V) = +1.630\,V \qquad \text{Equation } \mathbf{25}$$

$$ClO^- + H_2O + 2e^- \leftrightarrow Cl^- + 2OH^-\ ;\ E^\theta(V) = +0.89\,V \qquad \text{Equation } \mathbf{26}$$

$$Cl_2 + 2e^- \leftrightarrow 2Cl^-\ ;\ E^\theta(V) = +1.3604\,V \qquad \text{Equation } \mathbf{27}$$

HOCl however, has a short shelf life and is commercially unavailable in solution. Hypochlorite salts dissolve into a complex mixture of HOCl, $OCl^-$ and $Cl_2$, depending on pH, as shown in Figure 2.16.

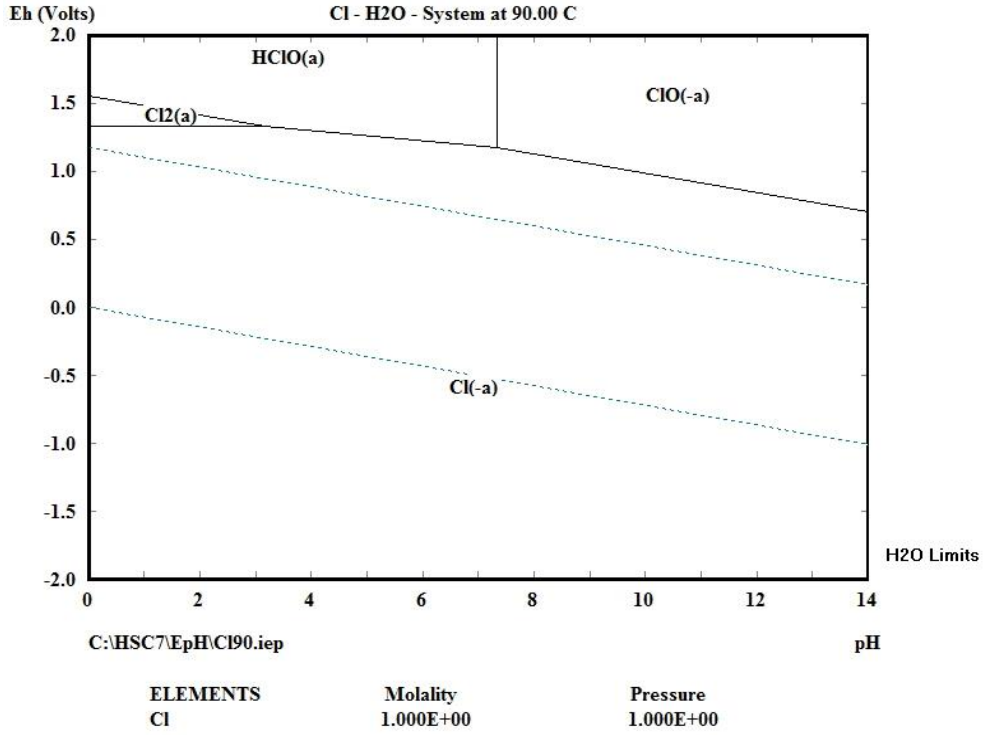


Figure 2.16: Cl- $H_2O$ Eh- pH diagram (drawn using HSC Chemistry)

$Ca(OCl)_2$ in the presence of $H_2SO_4$ and NaCl was investigated for gold processing from sulfidic refractory ores by Hasab et al., (2013). Given the comparable nobility of the PGMs to that of gold,

$Ca(OCl)_2$ was identified for investigation as the source of hypochlorous acid species. Calcium hypochlorite dissolves in water according to equation 28.

$$Ca(OCl)_2 + H_2O \rightarrow HOCl + Ca(OH)_2 \qquad \text{Equation } \mathbf{28}$$

The HOCl acid species is a weak acid that has an acid dissociation constant of $3.0 * 10^{-8}$ at 25 $^oC$, (Lister, 1952). $Ca(OH)_2$, on the other hand, is a strong base that has a solubility product of $5.02 * 10^{-6}$ (Chemical Rubber Company and Lide, 2003) at 25 $^oC$. Because HOCl only partially dissociates, the dissolved $Ca(OH)_2$ makes the solution of calcium hypochlorite strongly alkaline with a pH greater than 10. Under these conditions, the HOCl/$OCl^-$ equilibrium represented by equation 29 strongly lies to the right as shown in Figure 2.16, with more of the $OCl^-$ present at equilibrium.

$$HOCl \leftrightarrow H^+ + OCl^- \qquad \text{Equation } \mathbf{29}$$

To shift the equilibrium to the left in order to have more of the hypochlorous acid species at equilibrium, there is need to add some $H^+$ ions. Addition of $H^+$ ions shifts the equilibrium to the left which stabilises HOCl, a better oxidant than both the hypochlorite ion and chlorine as shown by their oxidising potentials.

A solution consisting of dissolved $AlCl_3 \cdot 6H_2O$ and HOCl could therefore be used to leach the PGMs out of the supporting matrix. This investigation therefore aims to identify and explain how the PGM leaching efficiencies vary with changing concentrations of aqueous $AlCl_3$ and HOCl. It is also of interest to identify the effect of temperature on the PGMs' leaching efficiency and also identify a suitable optimum set of conditions for leaching the PGMs into solution.

### 2.9.3 Method of PGM recovery

The recovery of PGMs from the leach solution is to be investigated by using solvent extraction with tri-isooctylamine, commercially sold as Alamine 308. Work done by Nguyen et al., (2016a) illustrated the potential for using the tertiary amine for recovering the 2 PGMs and individually stripping them using a combination of HCl and thiourea at different concentrations of thiourea. Nguyen et al., (2016a) investigated the recovery of Pt and Pd from a synthetic solution, and obtained impressive results. The performance of tri iso octylamine is to be investigated in a real leach solution containing the PGMs in combination with a lot more ions in solution. However, for

this works' scope, the recovery is only limited to a single illustrative run, duplicated, without detailed equilibrium isotherm determination and calculation of the total number of stages.

Tri iso octylamine is a tertiary amine with three (- $C_8H_{17}$) groups surrounding a single nitrogen atom. It has an amine characteristic odour, is water insoluble, boils between 350 ºC and 370 ºC and is inflammable. Metal extraction using tri iso octylamine occurs via protonation and anion exchange. Consequently, tri iso octylamine will only extract PGMs in acidic solutions. In the presence of an acid solution, the basic N atom in the amine structure reacts with the excess protons and forms an amine salt according to equation 30.

$$[R_3N]_{(org)} + HA_{(aq)} \leftrightarrow R_3NH^+A^-{}_{(org)} \qquad \text{Equation } \mathbf{30}$$

This amine salt has the ability to exchange its anion for another anion group depending on the relative affinity and solvation energies of the anions as shown in equation 31.

$$R_3NH^+A^-{}_{(org)} + B^-{}_{(aq)} \leftrightarrow R_3NH^+B^-{}_{(org)} + A^-{}_{(aq)} \qquad \text{Equation } \mathbf{31}$$

The solvation energy is the energy associated with the dissolution of a solute in a solvent. It is a comparison of the amount of energy absorbed during bond breaking within the solute crystal lattice to the amount of energy released during bond forming between the solute and solvent. A single illustrative run was therefore conducted for this research work to identify if extraction of the Pt and Pd from a real PGM leach solution was feasible with tri iso octylamine.

## 2.10 Summary

PGM recycling from used autocatalytic converters has been investigated in numerous texts and it has been established from thermodynamic calculations and experimental work that PGM chloride leaching requires acidic and oxidising conditions. Different combinations of these reagents have already been investigated to attain the required lixiviant conditions for leaching out the PGMs. This research will focus on leaching the ground spent autocatalytic converter in an aqueous solution of $AlCl_3$ and HOCl. A single illustrative run to investigate the feasibility of PGM extraction from solution will be conducted using tri iso octylamine as the extractant for Pt (IV) and Pd (II).

# Chapter 3 Methodology

## 3.1 Introduction

The experimentation phase was divided into three stages. The first experimental stage consisted of characterizing a homogenized representative sample of the autocatalytic convertor, and performing a preliminary investigation of leaching efficiency using the central composite design methodology. The second stage entailed using the insights gained from the preliminary experiments to optimise leaching conditions. The last stage consisted of performing solvent extraction to recover Pt and Pd from the solution. Characterisation of the residual solution was also conducted at this stage. Figure 3.1 illustrates the experimental plan and its relation to the 5 objectives presented in chapter 1.

## 3.2 Materials and Equipment used

The following equipment and materials were used for the experiments:

- Identical 1000 ml and 500 ml spherical, glass leach reactors with three arms for a sampling syringe, variable speed overheard stirrer, and one to support a reflux condenser, and channel insoluble gases to a collection syringe were used.
- XRF, ICP-OES and ICP – MS analysis was used for analytical determination. Mintek Laboratories SA was outsourced to do analysis for all samples.
- Common laboratory ware e.g. beakers, flasks, condensers, syringes etc., were also used.
- The spent autocatalytic converter that was used was purchased from a scrap auto dealer in Soweto, Johannesburg.
- Analytical grade $H_2SO_4$ (97 wt. %), $AlCl_3{\cdot}6H_2O$ (99 wt. %), $Ca(OCl)_2$ (67 % available chlorine), HCl (32 wt %), thiourea ( 99.99 wt %), kerosene ( 99 wt %), tri-isooctylamine (Alamine 308, 99 wt %) and aqueous ammonia (25 %) acquired from Sigma Aldrich, were used for the experiments. Solutions were diluted with distilled water as necessary.

## 3.3 Experimental Plan

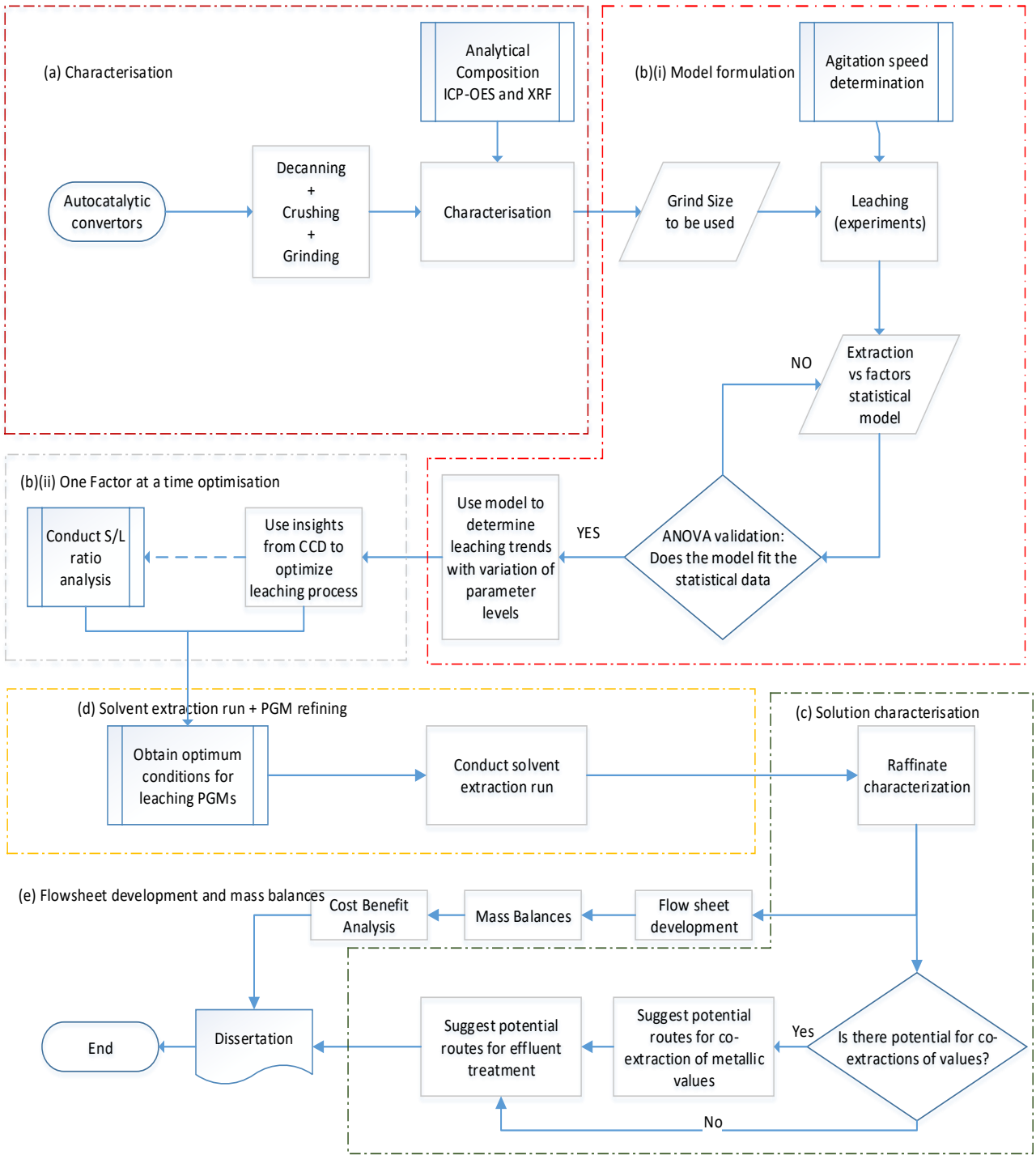


Figure 3.1: Experimental plan

## 3.4 Characterisation

The sample was prepared for characterisation and leaching by stripping the PGM bearing monolith from the bulk structure at the Richard Ward; School of Chemical and Metallurgical Engineering workshop. The ceramic wash coat bearing the PGM was crushed and pulverized to 100 % passing 104 um. 20 g (±0.001 g) of homogenised solid sample was sent to Mintek laboratories for elemental characterisation.

## 3.5 Leaching experiments

The leaching operation is affected by leach time, leach temperature, size of solids, agitation speed, $AlCl_3 \cdot 6H_2O$ concentration and $Ca(OCl)_2$ concentration. The size of the solids, solid to liquid volume ratio and agitation speed were fixed at 100% passing 104 um, 1 g/ 20 ml and 500 rpm respectively. This was meant to reduce the number of factors to be investigated and also eliminate mass transfer limitations due to lack of efficient solid to liquid contact. Parameters were thus fixed based on ranges used by Nogueira et al., (2014) and Upadhyay et al., (2013).

### 3.5.1 Preliminary run 1

The initial methodology that was proposed made use of $H_2SO_4$, $AlCl_3$ and dissolved $Ca(OCl)_2$. Based on the findings from this first preliminary run, it was later decided to drop $H_2SO_4$ and use only $AlCl_3$ and dissolved $Ca(OCl)_2$. The justification will become apparent as the methodology is explained. 26.396 g of $Ca(OCl)_2$, corresponding to 0.6 M $Ca(OCl)_2$, was added to a conical flask containing 200 ml of water, dissolved using a magnetic stirrer for 20 minutes at 300 rpm and then vacuum filtered to obtain a yellow green solution (HOCl). 150 ml of 1.5 M $AlCl_3$ solution was then added to the reactor inside the water bath whose temperature was set to 60 $^oC$. When the temperature of the $AlCl_3$ solution reached 55 $^oC$, 150 ml of 2.5 M $H_2SO_4$ was also added to the reactor, followed by slow addition of 150 ml of the filtrate that was obtained from $Ca(OCl)_2$ dissolution. At 60 $^oC$, the Eh and pH were recorded, 22.5 g of used autocatalytic converter was added, time was set to t = 0, and reaction allowed to proceed for 150 minutes, with sample collection at every 15 minutes in the first hour, every 20 minutes in the second hour, followed by the last sample collection at 150 minutes. The experimental setup used was as presented in Figure 3.2. PGM recovery was calculated using equation 32 below:

$$Yield_M = \frac{Conc\ of\ PGM\ in\ Solution/(mg/L)}{Conc\ of\ PGM\ in\ SAC/(mg/kg)} * \frac{Volume\ of\ leach\ solution(L)}{mass\ of\ SAC\ (kg)} * 100\ \%$$

Equation **32**

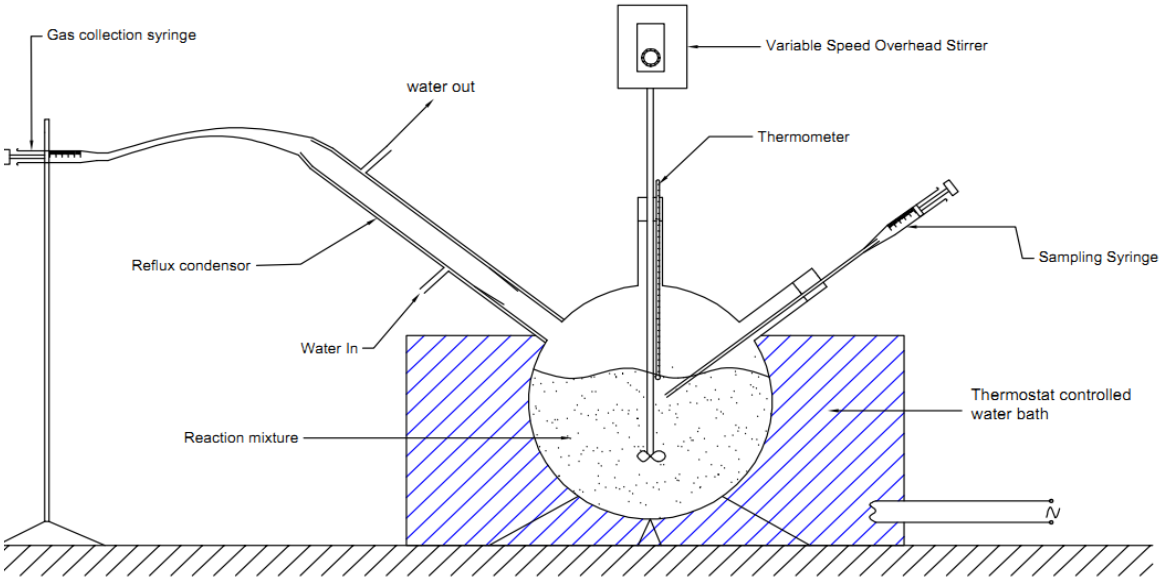


Figure 3.2: Schematic for leaching setup employed for Preliminary run 1, 2 and Central Composite Experiments

### 3.5.2 Experiments to determine [$Ca(OCl)_2$] and [$AlCl_3$] range

The operating conditions with $H_2SO_4$ were observed to be unfavourable. A lot of chlorine was generated, pH was consistently below 0, and the oxidising potential of the solution was also low, potentially due to loss of oxidant. Although PGMs were leached under stated conditions, the practical industrial adoption of such conditions was quickly deemed to be unfeasible. Robust chlorine handling mechanisms would have to be installed, worker safety would be greatly compromised, the effluent would be too acidic, and expensive materials would have to be employed to manufacture the reactor vessels and pipelines to withstand corrosion under such conditions, all of which would add to the cost of the cost of the recycling operation.

Consequently, a decision was taken to use a combination of $AlCl_3$ and dissolved $Ca(OCl)_2$ only for PGM leaching in subsequent experiments. However, because the combination of aluminium chloride and dissolved calcium hypochlorite (HOCl solution) for PGM leaching could not be

identified in literature, a new approach had to be developed to set possible concentration ranges, which was based on titration. This was also used to identify a suitable $AlCl_3$ to HOCl volume ratio that could be fixed for all subsequent experiments. The methodology was premised on titrating a known aluminium chloride concentration against a known volume of a determined dissolved $Ca(OCl)_2$ concentration.

$AlCl_3$ solutions of concentrations between 0.4 M and 1.9 M were obtained by dissolving a calculated mass of $AlCl_3 \cdot 6H_2O$ in distilled water. The pH and Eh of the solutions were recorded at the different $AlCl_3$ concentrations. Aluminium chloride hexahydrate is a very soluble salt which dissolved in less than a minute with a slight increase in the temperature of the solution. Calcium hypochlorite solutions of concentrations 0.4 M, 0.6 M and 0.8 M were also obtained by dissolving a specified mass of the calcium hypochlorite in distilled water for 30 minutes on a magnetic stirrer. The solutions obtained were then vacuum filtered to obtain a yellow-green solution. The Eh and pH of the three solutions obtained after $Ca(OCl)_2$ dissolution and filtration were also recorded.

10 ml of the yellow green solution (HOCl) was then placed in a 50 ml Erlenmeyer flask. The $AlCl_3$ solution was placed in a 50 ml burette and titrated into the Erlenmeyer flask containing 10 ml of the HOCl acid solution. The end point was recorded as the point at which pH fell within the ranges 3.8 to 4.5, at which point, the Eh was also recorded. The pH range 3.8 to 4.5 corresponded to the region of thermodynamic stability for the PGM-chloro complexes and the HOCl species as obtained according to their individual Eh - pH diagrams. The volume of $AlCl_3$ (according to Table 3.1) at different concentration levels was recorded and titrations were repeated in triplicate. A white gel which formed for some of the titrations was collected and sent for analysis.

Table 3.1: Volume of $AlCl_3$ vs. 10 ml of hypochlorous acid (HOCl)

| | | | [$AlCl_3$] | | |
|---|---|---|---|---|---|
| | | | 0.6 M | 0.8 M | 1 M |
| Volume of $Ca(OCl)_2$ = 10 ml | 0.4 M | Volume | | | |
| | | Eh | | | |
| | | pH | | | |
| | 0.6 M | Volume | | | |
| | | Eh | | | |
| | | pH | | | |
| | 0.8 M | Volume | | | |
| | | Eh | | | |
| | | pH | | | |

A suitable ratio for $AlCl_3$ solution to $Ca(OCl)_2$ solution volume ratio was therefore obtained by averaging the volumes obtained for all the titrations. This was then fixed for all subsequent experiments. The pH and Eh of pure $AlCl_3$ solution and $Ca(OCl)_2$ solution prior to any titrations were also plotted against their concentrations.

### 3.5.3 Preliminary run 3 – Using the new methodology for determination of leaching time

A third preliminary run employing the new methodology without sulphuric acid was then conducted. 0.6 M $Ca(OCl)_2$ and 0.8 M $AlCl_3$ solution were used for this reaction. The $AlCl_3$/ $Ca(OCl)_2$ volume ratio obtained from the previous section was employed. S/L ratio was maintained at 1g / 20 ml. Based on previous work in literature, temperature was fixed at 60 $^oC$. The setup presented in Figure 3.1 was employed.

29.036 g of $Ca(OCl)_2$ was added to a conical flask placed on a magnetic stirrer. 220 ml of distilled water was then added to the flask. Calcium hypochlorite was dissolved in the water for 20 minutes, after which the solution was filtered using a vacuum pump, and a clear yellow-green solution (HOCl) was obtained. The white residue obtained was dried at 105 $^oC$ in an oven for 2 hours, and its mass was recorded. 200 mL of the clear yellow-green solution, whose initial Eh and pH where recorded, was added to the reaction flask, followed by slow addition of 136.4 ml of the 0.8 M $AlCl_3$ solution. The resulting solution was heated to 60 $^oC$. At 60 $^oC$, the solution Eh and pH were recorded, time was set to t = 0 and 16.820 g of ground used autocatalytic converter was

added. The reaction was allowed to proceed for 240 minutes. 10 ml samples were drawn at 15 minute intervals and immediately placed in an ice chilled bath to stop the reaction. The samples were then centrifuged; the solids collected and sent for PGM analysis at Mintek SA. To evaluate whether it was more accurate to use solid or solution analysis, solutions at t = 15 minutes, 90 minutes, 180 minutes and 240 minutes were also sent for ICP-OES analysis. At each sampling point, the Eh and pH were measured and recorded. A white gel was still obtained and sent for analysis, together with the same gel obtained in the previous experiment. PGM yield was calculated using equation 32 as in the earlier experiments. A graph of PGM leach yield vs. time was drawn up and used to fix the time of reaction for subsequent experiments.

### 3.5.4 Central composite design experiments

Insights obtained from the previous sections were then used to design the central composite experiments. The methodology was largely similar to that described in section 3.5.3 above. The fixed parameters were S/L ratio = 1 g/ 20 mL, agitation of 500 rpm, $AlCl_3$ to HOCl volume ratio of 0.724 and time of 140 minutes. The factors that were to be varied were concentration of $AlCl_3$ over 0.8 M to 1.2 M, HOCl concentration over 0.2 M to 0.4 M, and temperature from 60 $^oC$ to 90 $^oC$. HOCl concentration range was reduced after identifying that the gel collected in previous experiments formed at concentration of calcium hypochlorite above 0.6 M. The gel was undesirable because it hindered efficient contact between the solution and the solids, and also made filtration extremely slow when separating the PGM solution from the solids.

The volumes used were also now lower, based on the amount of effervescence and chlorine generation that were observed in preceding experiments. The time for calcium hypochlorite dissolution was increased to 30 minutes to allow for complete dissolution. A determined mass of $Ca(OCl)_2$ was dissolved in 160 ml distilled water for 30 minutes using a bar magnetic stirrer at room temperature, to make the desired concentration according to Table 3.2. The solution was filtered and 150 ml of the filtrate was added to the 1 L 3 neck spherical flat bottomed flask immersed in the water bath as shown in Figure 3.2. The overhead stirrer and reflux water were immediately turned on and once the solution reached about 10 $^oC$ less the required temperature, 108.6 ml $AlCl_3$ solution at the desired concentration was slowly added to avoid loss of lixiviant due to excessive effervescence. Just before the addition of 12.63 g of the spent autocatalytic

converters, the Eh and pH were measured and recorded. The agitator was turned on and time set at t = 0. The reaction proceeded for 140 minutes after which the agitator was stopped. Eh and pH were measured and recorded and 20 ml of the leach solution drawn out and immediately poured into a 50 ml beaker placed in a chilled bath to stop the reaction. After 10 minutes, the solution was drawn out into a centrifuge vile using a syringe, and centrifuged for 40 minutes at 2000 rev/min. The supernatant liquid was then drawn out using a syringe, filtered into a sampling vile through a 0.4 um micro filter and sent for ICP-MS (Pt and Rh) and ICP-OES (Pd) analysis at Mintek Laboratories. Experiments were duplicated and randomised.

Table 3.2: $2^3$ with 2 centre runs design matrix used for central composite experiments

| Temp/$^o$C | [$AlCl_3$]/M | HOCl/M | t = 0 mins | | t = 140 mins | |
|---|---|---|---|---|---|---|
| | | | eH/mV | pH | eH/mV | pH |
| 60 | 0.80 | 0.2 | | | | |
| 60 | 1.20 | 0.4 | | | | |
| 90 | 0.80 | 0.2 | | | | |
| 75 | 1.00 | 0.3 | | | | |
| 60 | 0.80 | 0.4 | | | | |
| 90 | 0.80 | 0.4 | | | | |
| 75 | 1.00 | 0.3 | | | | |
| 90 | 1.20 | 0.4 | | | | |
| 60 | 1.20 | 0.2 | | | | |
| 90 | 1.20 | 0.2 | | | | |

A model was formulated using Minitab 16 and 17 software and statistical analyses conducted on the data to provide insights that were then implemented in the subsequent experimental setup. Statistical analyses that were conducted were ANOVA analysis, interactions analysis, contour plots and main effects analysis.

### 3.5.5 Optimisation experiments

Compounding on all insights obtained from the experiments, optimisation was carried out by:

1. Changing the temperature range from 70 $^o$C to 100 $^o$C. This meant that even the heating method had to be altered because the water bath would not get to the required maximum level. A heating mantle, with a magnetic stirring function was used in place of the water bath.

2. The use of the mantle and magnetic stirrer also provided for a more air tight system that resulted in less loss of chlorine. The previous setup resulted in a loss of chlorine from the vessel due to a loose connection, where the overhead stirrer got into the reaction flask. The use of a magnetic stirred mantle partially eliminated this problem. $AlCl_3$ solution was also slowly added using an addition funnel, with low agitation, typically below 100 rpm, until the required temperature was reached and the total volume of $AlCl_3$ solution was added. This was also done to avoid effervescence due to rapid chlorine generation, resulting in further loss of chloride ions as $Cl_2$ gas. This change greatly reduced effervescence in the optimisation experiments.
3. The HOCl range was also changed to 0.15 M - 0.45 M based on statistical insights obtained from the previous experiments.

Figure 3.3 illustrates the new setup which was then used for the optimisation experiments.

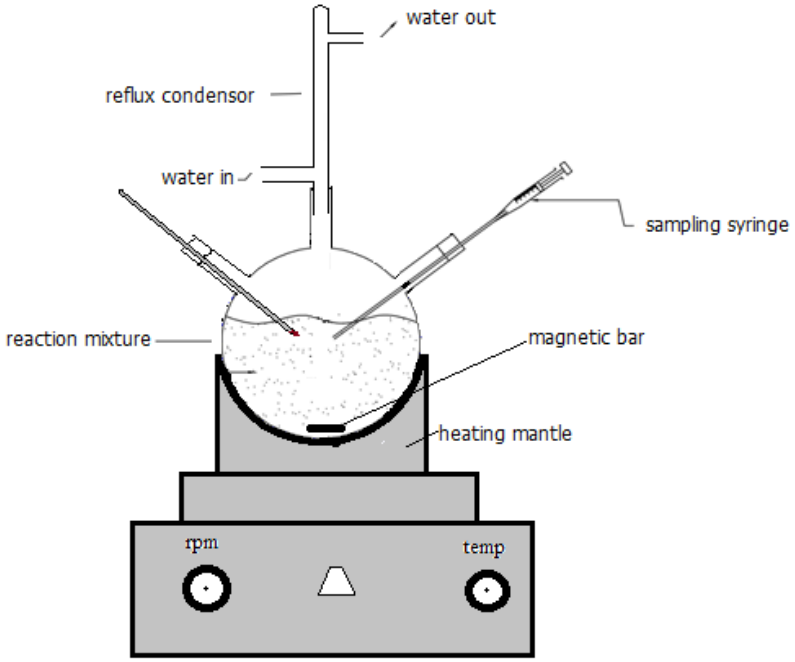


Figure 3.3: Experimental setup for optimisation experiments

Despite the above mentioned changes, the experimental method was still the same as that used in the CCD experiments. Sample collection was conducted every 35 minutes, in the same manner as in the previous section. The solutions obtained were sent for PGM ICP – MS analysis at Mintek Laboratories without dilution. The one factor at a time methodology was employed to investigate

the effects of changing parameters on yield of PGMs. Temperature was investigated at 70 $^{o}$C, 85 $^{o}$C and 100 $^{o}$C, with $AlCl_3$ and $Ca(OCl)_2$ concentrations fixed at 1.2 M and 0.3 M respectively. Whilst fixing temperature at 100 $^{o}$C and $AlCl_3$ concentration at 1.2 M, $Ca(OCl)_2$ concentration was varied between 0.15, M, 0.3 M and 0.45 M. Lastly, $AlCl_3$ concentration was investigated over 0.8 M, 1.0 M and 1.2 M whilst keeping temperature and $Ca(OCl)_2$ concentrations fixed at 100 $^{o}$C and 0.3 M respectively. All experiments were randomized and duplicated. Plots of PGM yield versus time were drawn at the different levels investigated.

### 3.5.6 Effect of solid: liquid ratio

The effect of changing solid to liquid ratio was investigated lastly. A higher S/L ratio means more solids can be leached in a given cycle, which should ideally translate to more PGMs in solution and a higher production yield. However, increasing the S/L ratio may also sacrifice PGM yield as observed in literature. The extent to which this occurs was investigated by choosing an optimum set of conditions from the previous set of experiments and repeating that experiment at two other S/L ratios. The experimental procedure was the same as that of the optimisation experiments; only without sample collection after every 35 minutes. One sample was collected at the end of the 140 minutes reaction time. The total number of S/L ratios investigated was three and these were 1 g / 20 mL, 6 g / 20 ml, and 8 g/ 20 ml. The results for the three PGMs were plotted on a yield versus S/L ratio graph. These experiments were duplicated and randomised.

## 3.6 Solvent extraction experiments

Experiments were carried out to confirm the results obtained by Nguyen et al., (2016a) for solvent extraction and recovery of PGMs from solution. The actual procedures that were followed are described in the subsequent sections.

### 3.6.1 Simulation runs for solvent extraction of Pt (IV) and Pd (II)

In order to co-extract the two PGMs into the organic phase, an excess of protons is required. The obtained PGM leach solution was therefore acidified using a volume ratio of 3:1 (pregnant leach solution: acid) varying HCl concentrations at levels of 0M, 1M, 5M, 7M and 9M. The % extraction for Pt and Pd was then consequently plotted against the HCl concentration in order to obtain an optimum HCl concentration to be used for acidifying.

750 ml of the PGM leach liquor solution from the leaching experiments was then collected and 250 mL of 5 M HCl (which was identified as the optimum) added to the PGM containing aqueous solution to acidify the PGM solution. Nguyen et al., (2016a) identified that four stages were required for 99.9% extraction of Pt (IV) and Pd (II) from an HCl solution at operating conditions of O/A volume ratio = 3/2 and 0.1 M Alamine 308 in kerosene with 5% v/v n-decanol. The optimum extraction and stripping conditions obtained by Nguyen et al., (2016a) were used for this study. An elaborate procedure, as shown in Figure 3.4, described by various authors (Türkay and Civelekoğlu, 1991), (Adu-Peasah et al., 1993), (Treybal, 2010) for using batch operations to simulate a continuous counter current process was utilised.

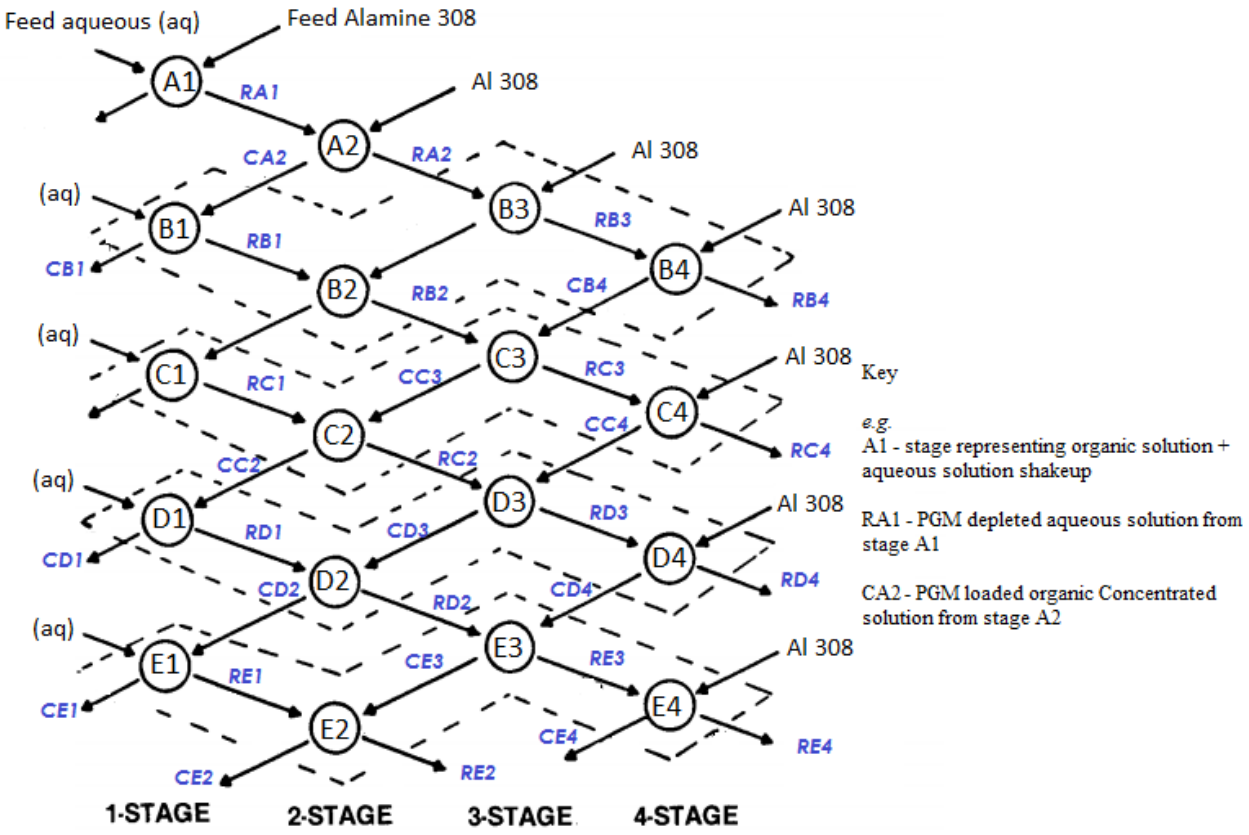


Figure 3.4: Batch simulation for 4 stage counter current continous SX system

Each circle represents a shakeup process at 300 rpm on a reciprocal shaker at room temperature for 40 minutes. 30 ml of the organic solution was contacted with 20 ml of the acidified aqueous solution containing PGMs in solution. At the end of the shaking procedure, the phases were

allowed to settle; the two solutions separated by decanting, and the raffinate and loaded organic solution subjected to further treatment. In order to simulate a continuous process, an infinite number of iterations are required. However, due to the laborious nature of the procedure and the constraint of resources, the number of repetitions was limited to four. The 20 ml aqueous solution obtained at stage E4 (labelled as RE4) in Figure 3.4 was sent for total elemental analysis (including PGM ICP-MS analysis). This procedure was duplicated.

Metal extraction was calculated using the following formula:

$$PGM\ extraction\ \% = \frac{[PGM]_{(aq)} - [PGM]_{(RE4)}}{[PGM]_{(aq)}}$$

Equation **33**

Where $[PGM]_{(aq)}$ and $[PGM]_{(RE4)}$ mean concentration of PGMs in acidified aqueous solution and in stream RE4 (as represented in Figure 3.4) respectively.

# Chapter 4 : Preliminary Leaching Results

## 4.1 Introduction

This chapter will present the results of the first section of the experimental methodology. These include the characterisation results and the preliminary leaching results, which were used to improve the methodology before optimisation of the leaching process conditions.

## 4.2 Characterisation results

The elemental composition of the spent autocatalytic converter used in the study is presented in Table 4.1 below. Samples of crushed converter were acid digested and analysed using ICP-MS. A full elemental composition for the spent autocatalytic converter (SAC) has been included in Appendix A1 (Table A1.1).

Table 4.1: Elemental composition of spent autocatalytic converter used for all leaching experiments;

| Element | Pt | Pd | Rh | Al | Ce | Zr | Others |
|---|---|---|---|---|---|---|---|
| Composition/wt. % | 0.0196 | 0.32 | 0.0229 | 9.49* | 3.751* | 14.06* | 72.3365 |

## 4.3 Results from preliminary experiment 1

The preliminary experiment was conducted according to section 3.5.1. The purpose of the preliminary run was to observe the leaching efficiency of the PGMs as a function of the initially chosen set of chemicals; $H_2SO_4$, dissolved $Ca(OCl)_2$ and $AlCl_3$. It was also meant to observe the chemical environment of the leaching solution in terms of Eh and pH, and give an indication of the time of reaction to be fixed for the subsequent experiments. The PGM leaching yield obtained from preliminary experiment 1 is presented in Figure 4.1 as a function of time. This experiment was duplicated.

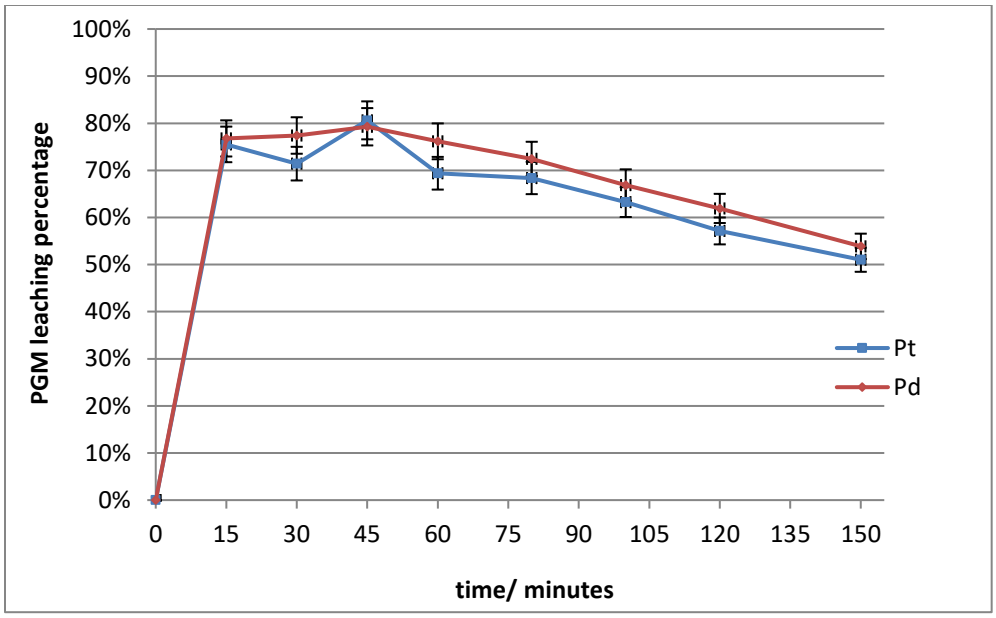


Figure 4.1: PGM leaching yield against time for preliminary leaching run 1

## 4.4 Discussion and insights obtained from Preliminary run 1

ICP-OES analysis for the PGMs failed to detect any Rh in the leach solution. This, however, did not necessarily mean that there was no Rh leached from the solid. The ICP-OES analysis used by Mintek for these analyses has a solution detection limit for Rh of 5 ppm, and any values below the limit were always reported as "< 5ppm:". Consequently, leaching percentage could not be calculated. Despite this hindrance, the results for Pt and Pd were analyzed against time and used to inform further leaching procedure. The Pt and Pd leaching yields in a solution comprising of $H_2SO_4$, $AlCl_3$ and HOCl quickly reached 75% within the first 15 minutes, followed by a slow decline in the PGM leaching extraction to around 50% at 150 minutes as shown in Figure 4.1. This fast leaching was attributed to the aggressive nature of the reaction medium, which consisted of 2.5 M $H_2SO_4$ and 1.5 M $AlCl_3$. The variations of Eh and pH for the reaction duration are presented in Figure 4.2.

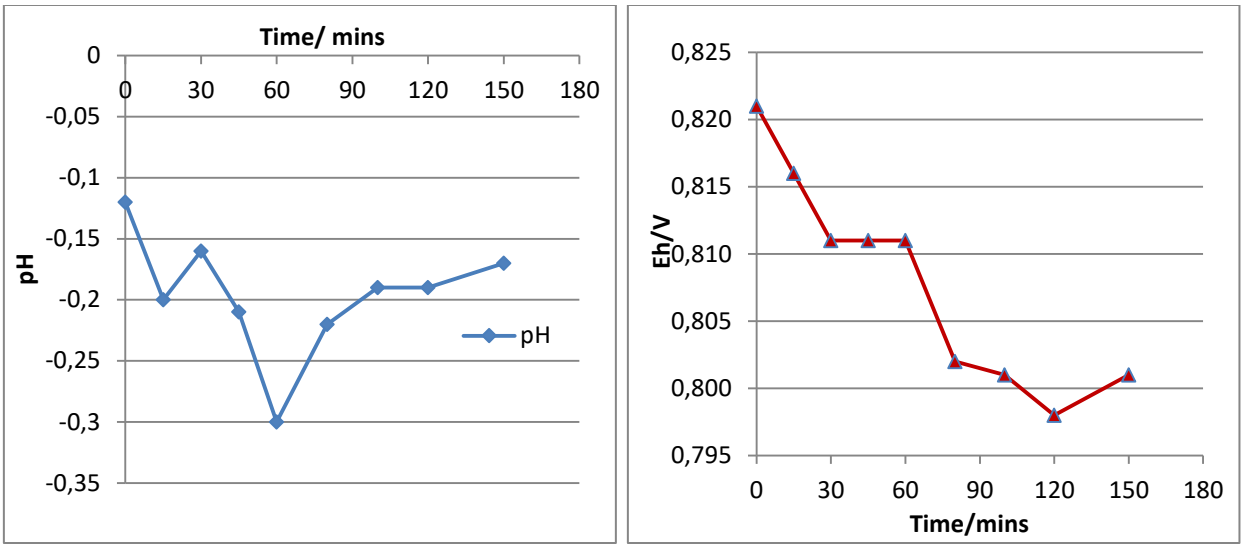


Figure 4.2: Eh and pH variation for experimental run 1

The leaching solution had a consistent negative pH reading throughout the reaction duration. At the beginning of the reaction the solution also had an excess of chloride ions. These conditions were conducive for fast leaching of the PGMs into the solution. However, the $Cl_2$ - $H_2O$ Eh – pH diagram, as shown in Figure 2.16 under section 2.9.2, illustrates that in highly acidic solutions, the aqueous and gaseous $Cl_2$ species is favored. Consequently, as the reaction proceeded, more of the chloride ions in solution were converted into the $Cl_2$ species and escaped the reactor. The experimental setup was slightly open to the atmosphere to avoid pressure build up inside the glass reactor. A yellow green gas was actually observed during the reaction, which bleached damp litmus paper, confirming the formation and escape of $Cl_2$ gas. This escaping $Cl_2$ reduced the concentration of free chloride species in the solution. The stability of PGM chloro complexes however, depends on the concentration of chloride ions in solution. With the decreasing free chloride ions resulting from the escape of chlorine gas, the PGM chloro complexes became less stable and PGMs may have precipitated back into their insoluble state. This would explain the decrease in the PGM concentration beyond the 45 minutes mark as illustrated in Figure 4.1.

Despite the leaching efficiency obtained, it was quickly determined that the conditions could not be adopted for any commercial leaching operation. The effluent solution was too acidic, with consistent negative values of pH (Figure 4.2 (a)). The use of concentrated $H_2SO_4$ at highly

oxidizing potentials provided for a very corrosive and potentially dangerous solution. Due to the operating pH, the chloride ions were converted to gaseous $Cl_2$ (as predicted by the $Cl_2 – H_2O$ Eh - pH diagram) and a lot of the chlorine gas escaped. This was undesirable because there was excessive loss of the complexing agent, and in a scaled up operation, such high chlorine generation would have grave safety concerns. Gas scrubbing to rid the effluent gas of high amounts of chlorine would also be expensive, adding to the operating and capital expenditure. Based on these observations, it was then determined that an investigation into the potential of using a combination of only $AlCl_3$ and dissolved $Ca(OCl)_2$ be done.

### 4.5 Results of titrations to determine [$AlCl_3$] and [$Ca(OCl)_2$] ranges

The use of $H_2SO_4$ was discarded based on the observations made from the previous experiment. However, upon considering the chemistry of $AlCl_3$ and dissolved $Ca(OCl)_2$ in solution, it was determined that a combination of the two, without sulphuric acid, could have the required thermodynamic potential to leach the PGMs. The scientific basis has already been presented earlier in sections 2.9.1 and 2.9.2. However, because a combination of $AlCl_3$ and dissolved $Ca(OCl)_2$ was not identified in the reviewed literature, a methodology described in section 3.5.2 was established to identify potential operating conditions (i.e. concentration ranges that could be investigated). This methodology initially sought to identify the variation of the properties for the two solutions individually and when combined. Understanding the chemistry of the individual $AlCl_3$ and HOCl solutions, and their interactions when combined, would be imperative for explaining the PGM leaching results. Figures 4.3 and 4.4 illustrate the variation of pH and Eh with concentration of $AlCl_3$ solution alone and HOCl solution alone (before any titrations).

The dissolution of $AlCl_3$ in water occurs rapidly and exothermally according to equation 34:

$$AlCl_3 \cdot 6H_2O(aq) + H_2O(l) \rightarrow Al(H_2O)_6{}^{3+}(aq) + 3Cl^-(aq) + H_2O(l)$$ Equation **34**

The $Al^{3+}$ ion is a small ion (ionic radius = 0.053 nm (Yoder, 2006)) with a high charge of + 3. The ion, therefore, has a high charge density and it readily polarises water molecules when in solution. The equilibrium between the water molecules and the ion is attained at 25 $^oC$ with a $pK_a$ value of 5 as represented in equation 35 (Chemical Rubber Company and Lide, 2003).

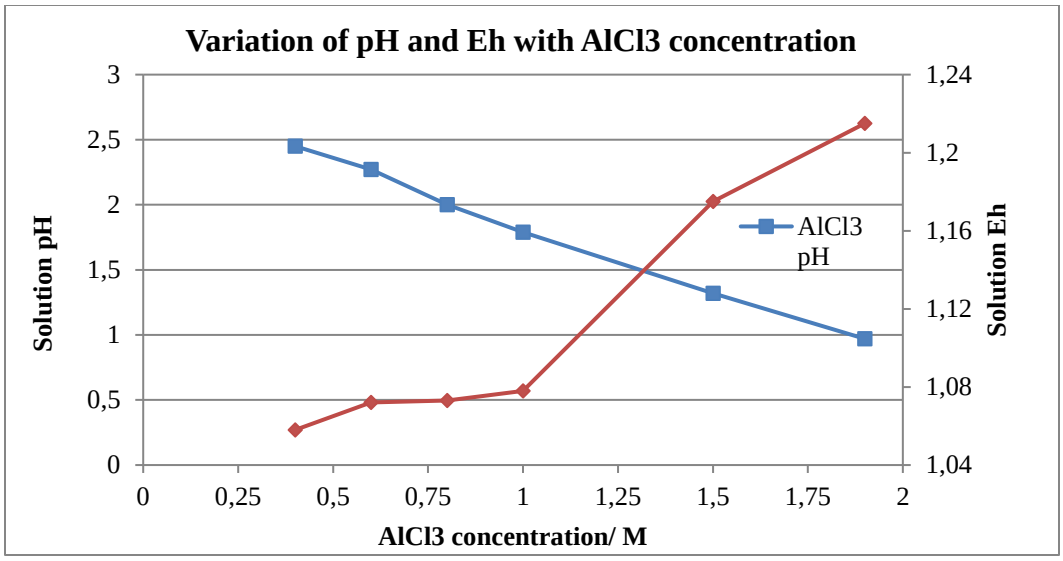


Figure 4.3: Variation of pH and Eh with $AlCl_3$ concentration

$$Al(H_2O)_6{}^{3+} + (H_2O) \leftrightarrow Al(H_2O)_5(OH)^{2+} + (H_3O)^+ \qquad \text{Equation } \mathbf{35}$$

According to equation 35, a solution of $AlCl_3$ has a low pH due to the formation of the hydroxonium ion. Increasing the concentration of $AlCl_3$ increases the concentration of $Al^{3+}$ ions, which shifts the equilibrium of equation 35 to the right, producing more of the hydroxonium ions and further decreasing the solution pH. The pH therefore becomes more acidic as shown in Figure 4.3 (blue line).

The variation of the solution Eh with concentration may be explained by considering the Nernst equation for the following water half-cell reaction in the presence of protons

$$O_2 + 4H^+ + 4\,e \leftrightarrow 2H_2O \qquad E^{\Theta} = 1.229\ V$$

The Nernst equation at standard condition of 298 K may be written as;

$$E = E^{\theta} - \frac{0.0592}{4} * (-4) * \log\,[H]^+$$

which can be simplified to

$$E = E^{\theta} + (0.0592 * \log\,[H]^+)$$

$$E = E^{\theta} + (0.0592 * -pH)$$

A decrease in the pH of the solution, as represented by the blue line in Figure 4.3, is therefore expected to make the solution more positive, according to the above relationship between E and pH. The increasing acidity (thus decreasing the pH), as a result of increasing $AlCl_3$ concentration

was probably responsible for the aqueous $AlCl_3$ solution becoming more oxidising as shown by the red line in Figure 4.3.

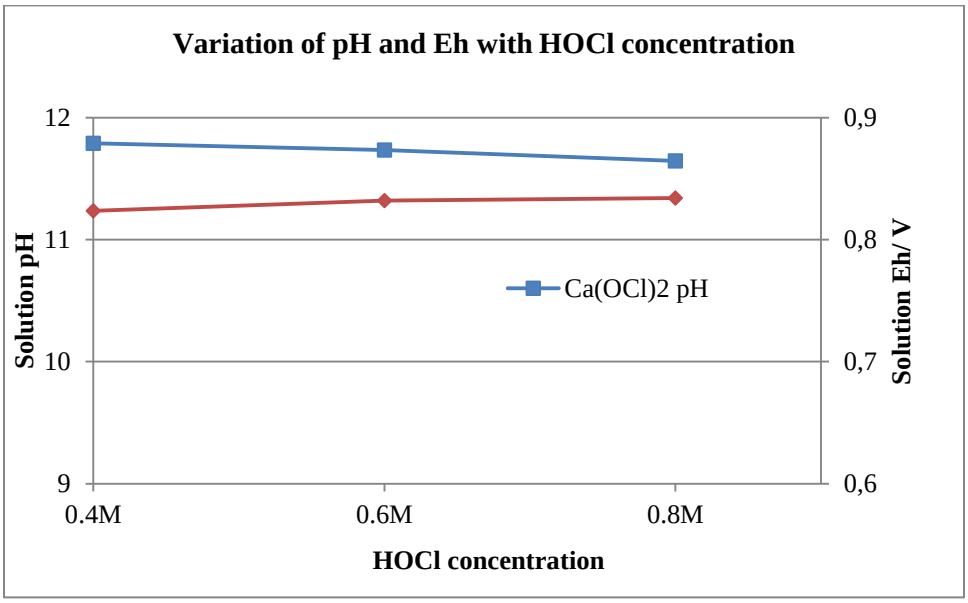


Figure 4.4: Variation of pH and Eh with HOCl concentration

Figure 4.4 shows that both the pH and Eh of a solution of $Ca(OCl)_2$ are relatively constant over the concentration range 0.4 M to 0.8 M. The dissolution of calcium hypochlorite in water is a slow reaction that occurs according to equation 36 below:

$$Ca(OCl)_2 + 2\,H_2O \rightarrow 2HOCl + Ca(OH)_2 \qquad \text{Equation } \mathbf{36}$$

HOCl is a weak acid which has an acid dissociation constant of 3.0 * $10^{-8}$ at 25 $^oC$ (Lister, 1952). However, $Ca(OH)_2$ is a strong base that has a $K_{SP}$ value of 5.02 * $10^{-6}$ (Chemical Rubber Company and Lide, 2003) at 25$^oC$. Dissolving 0.4 moles of $Ca(OCl)_2$ in a litre of water results in the formation of 0.4 M $Ca(OH)_2$, which is the same as 29.64 g/L. The maximum solubility at room temperature for $Ca(OH)_2$ is, however, 1.73g/l (obtained from the Ksp value), meaning that all the solutions that were prepared for this work resulted in $Ca(OH)_2$ concentrations that were above this saturation value. It is therefore expected that the pH of the solutions prepared should be a consistent value close to the pH of a saturated solution. The pH of all solutions obtained was relatively constant at 11.79 as shown in Figure 4.4, which is comparable to the calculated pH of 12.67 for a saturated $Ca(OH)_2$ solution.

Under these alkaline conditions, the $HOCl/OCl^-$ equilibrium illustrated in equation 37 strongly lies to the right as predicted by the $Cl_2 – H_2O$ equilibrium diagram.

$$HOCl \leftrightarrow H^+ + OCl^-$$ Equation **37**

The oxidising potential for the OCl- species, which is the dominant species under these conditions, is represented by in equation 38.

$$ClO^- + H_2O + 2e^- \leftrightarrow Cl^- + 2OH^- ; E^\theta(V) = +0.89\,V$$ Equation **38**

$$HClO + H^+ + e^- \leftrightarrow {}^1/_2\,Cl_2 + H_2O ; E^\theta(V) = +1.630\,V$$ Equation **39**

The oxidising potential for the test solutions was also relatively constant at around + 0.83 ±0.02 V, which was comparable to the predicted potential of 0.89V. However, HOCl is a better oxidant compared to the $OCl^-$ as shown in equation 39. More HOCl could be obtained by acidifying the solution into region of HOCl stability. The combination of $AlCl_3$ and HOCl in solution was therefore expected to produce favourable conditions for leaching the PGMs. This was the basis for the titrations according to section 3.5.2. The results of these titrations are presented in Table 4.2 below:

Table 4.2: Results of titrations between $AlCl_3$ and HOCl

| | | | Titrate with $AlCl_3$ | | |
|---|---|---|---|---|---|
| | | | 1 M | 0.8 M | 0.6 M |
| $Ca(OCl)_2$ = 10 ml | 0.4 M | Volume/ml | 3.75 | 5.03 | 6.97 |
| | | Final Eh | 1.369 | 1.372 | 1.373 |
| | | Final pH | 4.06 | 3.99 | 3.91 |
| | 0.6 M | Volume/ml | 4.80 | 6.70 | 10.07 |
| | | Final Eh | 1.366 | 1.373 | 1.372 |
| | | Final pH | 4.29 | 4.05 | 3.79 |
| | 0.8 M | Volume/ml | 7.30 | 8.73 | 12.80 |
| | | Final Eh | 1.367 | 1.303 | 1.361 |
| | | Final pH | 4.17 | 4.15 | 4.09 |

The end point for all titrations was chosen as the point at which the pH fell between 3.8 and 4.5. At the end point, the Eh was also recorded. This pH range was chosen because it coincided with the region of stability for all PGM chloro complexes and the HOCl species. With addition of the $AlCl_3$ solution to the HOCl solution, the Eh increased as was expected with a greater proportion of

the HOCl stabilising. Adding $AlCl_3$ to the HOCl solution reduces the pH from the alkaline conditions represented by Figure 4.4. Acidifying the solution shifts the equilibrium of equation 37 to the left, stabilising more hypochlorous acid; which has a higher oxidising potential as illustrated by equation 39. At each end point, the Eh was consistently greater than + 1.3 V, which for all the PGMs would have been too oxidising for the complexing reaction.

The optimum $AlCl_3$/HOCl volume ratio was then obtained by averaging the volumes obtained for the different $AlCl_3$/HOCl titrations carried out. A volume ratio of 7 ml $AlCl_3$: 10 ml HOCl corresponding to an $AlCl_3$/HOCl volume ratio of 0.7 was chosen for all the subsequent experiments.

A white gel, which formed for some of the titrations where $Ca(OCl)_2$ concentration was above 0.6 M, was identified as $Al(OH)_3$. This same gel was also observed in the second preliminary run. Formation of $Al(OH)_3$ gel was undesirable because it hindered efficient solid to liquid contact during leaching and also slowed down filtration after leaching.

### 4.6 Results from preliminary experiment 2 – determination of leaching time

The results from the second preliminary leaching experiment, which was duplicated, are presented in Table 4.3. As discussed in section 3.5.3, the purpose of this experiment was to fix time to be used for the subsequent central composite experiments, test out the performance of the two-reagent ($AlCl_3$ + dissolved $Ca(OCl)_2$) system for leaching and evaluate the variation in Eh and pH during the reaction. It was also meant to inform whether elemental analysis going forward was to be carried out on solids or solution. During the reaction, 10 ml samples were collected and filtered; the solids obtained were dried. Percentage leaching efficiency was calculated based on both solids and solution analyses' results. Solids obtained for each sampling point were collected and sent for analysis. Solutions at t = 15, 90, 180 and 300 minutes were also collected and sent for ICP-OES analysis. This was done for two reasons; to confirm the results obtained by each analysis method and to identify whether to send solids or solutions for the subsequent experiments to the testing laboratory. The solid samples that were collected during the reaction were however very small and therefore represented a great deal of error in analysis (the testing laboratory has a minimum mass requirement of 1g for any analyses that require digestion). The masses of the solids were

averaging ≈ less than 0.5 g. This may explain why the solid analysis failed to detect Pd and Rh, and it was subsequently rejected as an analysis method for the following experiments.

Solution analyses using ICP – OES also did not detect any Rh, for which any values of concentration below 5 ppm results were reported as " < 5ppm". This was probably because Rh is a slow leaching metal whose initial concentration in the original sample was also very low (at just 0.0229 %). ICP-OES was therefore probably unable to detect any Rh. Based on these observations, the analysis lab recommended that ICP – OES should not be used for the solution analyses, but rather employ ICP – MS for subsequent experiments, which is more precise and can detect lower Rh concentrations.

The results for the leaching preliminary run are presented in Table 4.3 below, where percentage refers to leaching efficiency of the Pt and Pd into solution. The solution analysis represents leaching efficiency calculated based on ICP – OES results and the solid analyses represents leaching efficiency based on digestion followed by ICP - OES.

Table 4.3: Leaching results from Preliminary run 2 (Solution analyses performed using ICP – OES and solid analyses performed after acid digestion followed by ICP-OES at Mintek Laboratories)

| Time /mins | Temperature/ $^{o}C$ | eH/V | pH | Solution analyses | | | Solid analyses | | |
|---|---|---|---|---|---|---|---|---|---|
| | | | | Pt | Pd | Rh | Pt | Pd | Rh |
| 0 | 57 | 1.588 | 3.06 | 0% | 0% | - | 0% | - | - |
| 15 | - | 1.4 | 3.04 | 53% | 48% | - | 53% | - | - |
| 30 | 60 | 1.32 | 3.03 | - | - | - | 54% | - | - |
| 45 | 60 | 1.28 | 3.02 | - | - | - | 49% | - | - |
| 60 | 60 | 1.25 | 3.02 | - | - | - | 48% | - | - |
| 90 | 59 | 1.254 | 3.02 | 60% | 58% | - | 58% | - | - |
| 120 | 60 | 1.218 | 2.99 | - | - | - | 51% | - | - |
| 150 | 60 | 0.745 | 3.04 | - | - | - | 58% | - | - |
| 180 | 60 | 0.739 | 3.07 | 61% | 57% | - | 59% | - | - |
| 210 | 60 | 0.741 | 3.05 | - | - | - | 61% | - | - |
| 240 | 58 | 0.745 | 3.03 | - | - | - | 61% | - | - |
| 300 | 60 | - | - | 61% | 59% | - | 61% | - | - |

Figure 4.5 shows that PGM extraction for Pt and Pd were maxima at approximately 60% and 58% (using solution analyses results) after 140 minutes. From 140 minutes, the leaching percentage was

approximately consistent with very little variation. The time of reaction for subsequent experiments was therefore set to 140 minutes.

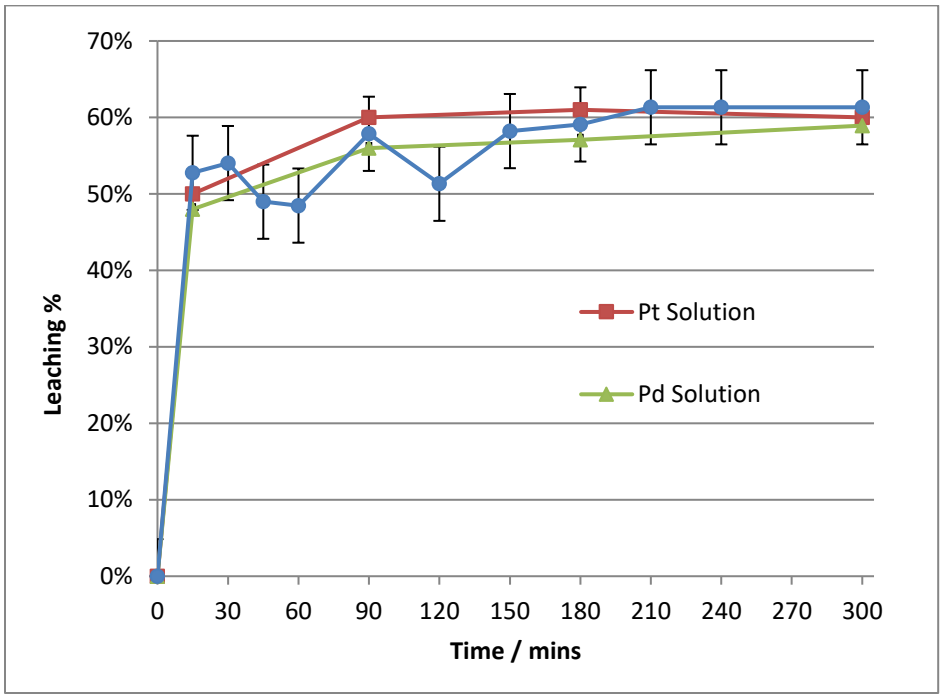


Figure 4.5: PGM yield from preliminary run 2

A white gel that formed at the end of the reaction was analysed and identified as $Al(OH)_3$. The same gel also formed during the titrations to determine concentrations of $AlCl_3$ and $Ca(OCl)_2$ as presented in section 4.5 above. At high $Ca(OCl)_2$ concentrations, the amount of $Ca(OH)_2$ in the HOCl solution is high. Addition of $Al^{3+}$ ions (in $AlCl_3$) thereby leads to the formation of the gel as a result of the reaction between the acidic $Al^{3+}$ ion and excess $OH^-$ ions. The Eh – pH diagram for the Al -$H_2O$ - Cl system is as presented in Figure 4.6 below. To avoid the formation of this gel, it was therefore determined to use lower $Ca(OCl)_2$ concentrations to minimize the amount of $OH^-$ ions available.

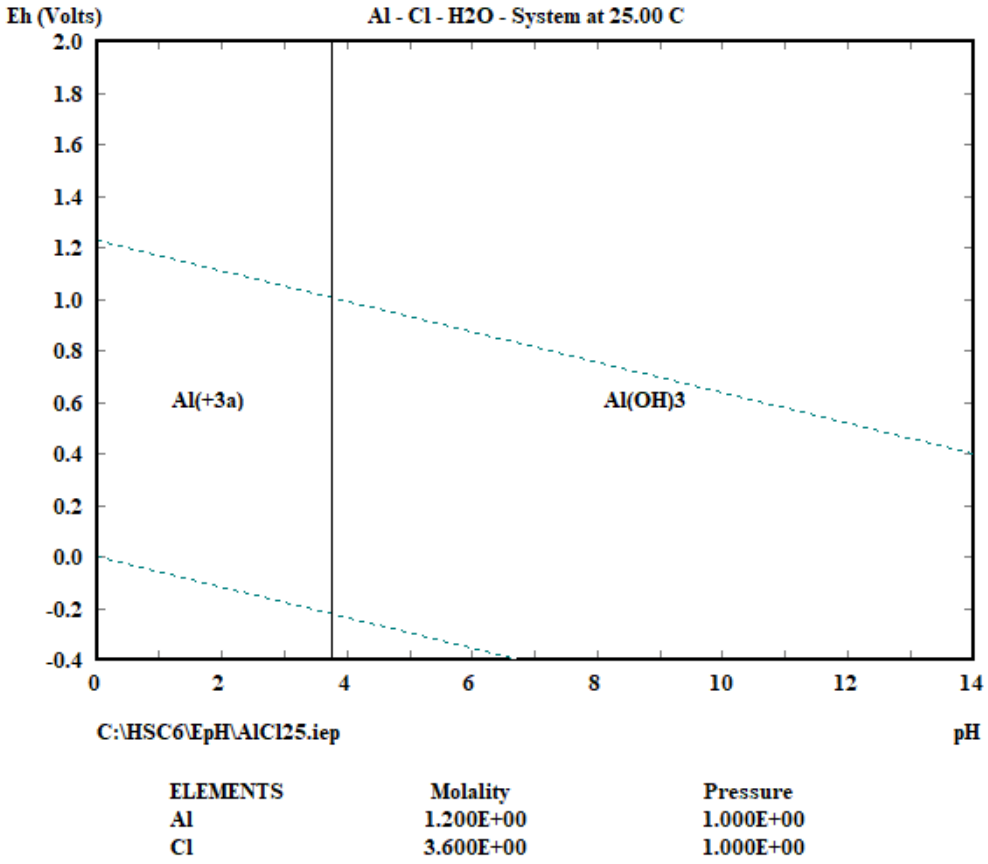


Figure 4.6: Eh – pH diagram for Al-$H_2O$-Cl system (drawn using HSC Chemistry Software)

The pH of the solution was consistent at approximately 3 throughout the duration of the reaction as shown by the red line in Figure 4.7. However, the oxidising potential of the solution decreased with time for the reaction as illustrated by the blue line. This could be attributed to $Cl_2$ escaping from the reactor. The oxidising reaction represented by the equilibrium of equation 39 produces $Cl_2$ which, if allowed to escape, reduces the concentration of HOCl and consequently the oxidising potential of the solution. $Cl_2$ escaping also reduces the chloride concentration. The combined effect of decreasing oxidising potential and chloride ions may have been responsible for the flattened part of the leaching curve from 30 minutes to the end of the reaction in Figure 4.5.

It is also worthy to mention that the removal of $H_2SO_4$ produced a more stable reaction with less chlorine generation and a higher oxidising potential because of decreased loss of $Cl_2$. The conditions prevailing in the reactor were also conducive to provide the required thermodynamic potential to leach the metals into solution as shown in Figure 4.7, up to when oxidising potential began to decrease.

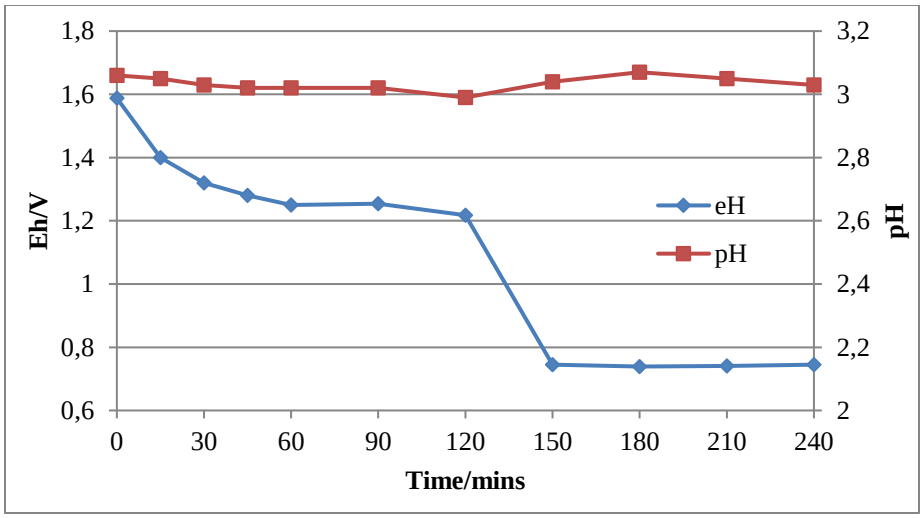


Figure 4.7: Variation of Eh and pH with time for preliminary run 2

## 4.7 Discussion of results from central composite experiments

Due to the formation of $Al(OH)_3$ at higher $Ca(OCl)_2$ concentrations observed in the preliminary experiment, it was decided to investigate PGM recovery over a lower $Ca(OCl)_2$ range (0.2 M to 0.4 M). Indeed there was no longer any gel observed for all the factor levels investigated. Results from the CCD experiments that were conducted are presented in Table 4.4 below.

Table 4.4: PGM leaching recovery from preliminary CCD experiments

| Run | Temp/°C | [$AlCl_3$]/M | HOCl/M | PGM Yield | | | t = 0 | | t = T | |
|---|---|---|---|---|---|---|---|---|---|---|
| | | | | Pt | Pd | Rh | Eh/V | pH | Eh/V | pH |
| 1 | 60 | 0.80 | 0.2 | 2% | 6% | 1% | 1.338 | 2.94 | 1.248 | 2.90 |
| | 60 | 0.80 | 0.2 | 2% | 8% | 5% | | | | |
| 2 | 60 | 1.20 | 0.4 | 34% | 45% | 3% | 1.327 | 3.04 | 1.254 | 2.86 |
| | 60 | 1.20 | 0.4 | 37% | 48% | 7% | | | | |
| 3 | 90 | 0.80 | 0.2 | 78% | 86% | 7% | 1.190 | 1.88 | 1.067 | 2.26 |
| | 90 | 0.80 | 0.2 | 80% | 84% | 10% | | | | |
| 4 | 75 | 1.00 | 0.3 | 32% | 57% | 3% | 1.304 | 2.38 | 1.089 | 2.22 |
| | 75 | 1.00 | 0.3 | 35% | 57% | 7% | | | | |
| 5 | 60 | 0.80 | 0.4 | 0% | 1% | 1% | 1.329 | 3.68 | 1.306 | 3.72 |
| | 60 | 0.80 | 0.4 | 3% | 4% | 3% | | | | |
| 6 | 90 | 0.80 | 0.4 | 33% | 46% | 1% | 1.279 | 3.20 | 0.800 | 3.93 |
| | 90 | 0.80 | 0.4 | 35% | 44% | 5% | | | | |
| 7 | 90 | 1.20 | 0.4 | 70% | 84% | 7% | 1.267 | 2.08 | 1.030 | 3.35 |

| | | | | | | | | | | |
|---|---|---|---|---|---|---|---|---|---|---|
| 7 | 90 | 1.20 | 0.4 | 83% | 80% | 10% | | | | |
| 8 | 60 | 1.20 | 0.2 | 3% | 9% | 2% | 1.326 | 2.74 | 1.288 | 2.60 |
| | 60 | 1.20 | 0.2 | 5% | 12% | 4% | | | | |
| 9 | 90 | 1.20 | 0.2 | 77% | 84% | 15% | 1.272 | 1.79 | - | - |
| | 90 | 1.20 | 0.2 | 80% | 81% | 17% | | | | |

### 4.7.1 Comparison of PGM leaching efficiencies

The first observation that stands out is the low recovery of Rh obtained at all factor combinations investigated. The maximum Rh leaching yield of 15% was very low for any economic adoption of this process. This trend in leaching efficiency of the order Pd >/≈ Pt > Rh has been observed in many of the literary works as well (Nogueira et al., 2014), (Upadhyay et al., 2013), (Rumpold and Antrekowitsch, 2012) and (Mahmoud, 2003). Nogueira et al., (2014) suggested that Pt and Pd are probably oxidised at faster rates than Rh, during the operation of the autocatalytic converter. When PGMs are in their oxidised state, they are less amenable to acid leaching (Chen et al., 2014). However, data presented by Hartley, (1991) on the order of reactivity of the PGMs in their elemental state reflects a similar order as well; of Pt >/≈ Pd > Rh. At 100 $^{o}$C the reactivity of Pt, Pd and Rh foils in saturated $Cl_2$/HCl is approximately 1, 1 and 0.1 $mg \cdot cm^{-2} \cdot hr^{-1}$. In aqua regia, at the same temperature, the reactivity is 10, 10 and <0.01 $mg \cdot cm^{-2} \cdot hr^{-1}$ for Pt, Pd and Rh. In both cases, reactivity of Pt and Pd is always more than 10 times greater than that of Rh. This illustrates that in as much as oxidation may have contributed to the lower observed Rh leaching rates during the catalysts' service life, differences in leaching rates may also be a result of the individual leaching mechanisms for the metals in acidic oxidising conditions as well.

This trend of Pt ≈/> Pd > Rh can be explained by considering the differences in the elemental leaching mechanisms for the three PGMs from a thermodynamics standpoint. The HOCl / $Cl_2$ half-cell has an oxidising potential of +1.630 V as already presented in equation 39. The standard half-cell potentials for chloride complexation of Pt, Pd and Rh are + 0.744 V, + 0.615 V and + 0.44 V as presented in equations 40 to 42. The standard half-cell potentials for formation of the Pt, Pd and Rh oxides are + 0.790 V, + 0.920 V and + 0.870 V as presented in equations 43 to 45.

$$PtCl_6^{2-} + 4\,e \rightarrow Pt + 6Cl^- \; E^\theta(V) = +0.744\,V \qquad \text{Equation } \mathbf{40}$$

$$PdCl_4^{2-} + 2\,e \rightarrow Pd + 4Cl^- \; E^\theta(V) = +0.615\,V \qquad \text{Equation } \mathbf{41}$$

$$RhCl_6^{3-} + 3\,e \rightarrow Rh + 6Cl^- \; E^\theta(V) = +0.44\,V \qquad \text{Equation } \mathbf{42}$$

$$PdO + 2\,H^+ + 2\,\text{e} \rightarrow Pd + \text{H}_2\text{O} \; E^\theta(V) = +0.790\,V \qquad \text{Equation } \mathbf{43}$$

$$PtO_2 + 4\,H^+ + 4\,\text{e} \rightarrow Pt + 2\,\text{H}_2\text{O} \; E^\theta(V) = +0.920\,V \qquad \text{Equation } \mathbf{44}$$

$$Rh_2O_3 + 6\,H^+ + 6\,\text{e} \rightarrow 2\,Rh + 3\,\text{H}_2\text{O} \; E^\theta(V) = +0.870\,V \qquad \text{Equation } \mathbf{45}$$

The standard cell potentials for the complexing of the PGMs and for the formation of the PGM oxides in a solution of HOCl/$AlCl_3$ can therefore be calculated using these oxidising potentials. The Gibbs free energy and standard cell potential for an electrochemical redox reaction are related according to the following equation;

$$\Delta G^\theta = -nFE^\theta_{cell}$$

Table 4.5 presents the calculated standard cell potentials and the corresponding Gibbs free energies for each electrochemical cell as obtained from the aforementioned standard potentials.

Table 4.5: Gibbs free energies for PGM chloro complex formation and PGM oxide formation

| | PGM Chloro – complex formation | | | PGM Oxide formation | | |
|---|---|---|---|---|---|---|
| PGM | $E^\theta_{cell}$ / V | n/mol | $\Delta G^\theta_{cell}$ / kJ/mol. | $E^\theta_{cell}$ / V | n / mol | $\Delta G^\theta_{cell}$ / kJ/mol. |
| Pt | + 0.886 | 4 | - 341.996 | + 0.710 | 4 | - 274.06 |
| Pd | + 1.015 | 2 | - 195.895 | + 0.840 | 2 | - 162.12 |
| Rh | + 1.190 | 3 | - 343.434 | + 0.760 | 6 | - 440.04 |

The formation of the chloro complexes for Pt and Pd has more negative Gibbs free energy values (-342 kJ/mol. and –195 kJ/mol.) when compared to the corresponding Gibbs free energies for the formation of their oxides (- 274 kJ/mol. and - 162 kJ/mol.) This illustrates that the formation of Pt and Pd chloro complexes is more spontaneous than that for the oxides. However, this is reversed for Rh, whose Gibbs free energy for the formation of the oxide is more negative (- 440 kJ) as compared to that of the corresponding rhodium chloro complex (- 343 kJ).

When exposed to an oxidising environment with chloride ions, Pt and Pd will readily form their chloro complexes. However, Rh is more readily oxidised as opposed to forming its chloro complex. This suggests that the leaching of Pt and Pd may occur via a single step, whilst that for Rh possibly goes through a two-step process, initially forming a passivating oxide layer followed by formation of the chloro complex. This rhodium oxide layer possibly hinders attack on the Rh metal by the leaching solution, resulting in slower leaching kinetics and low leaching efficiencies as recorded in this study and in earlier PGM leaching studies by Nogueira et al., (2014), Upadhyay et al., (2013), Rumpold and Antrekowitsch, (2012) and Mahmoud, (2003). Chen et al., (2014) presented the Gibbs free energy for the reaction of $Rh_2O_3$ with aqueous chlorine over the temperature range 0 K to 373.15 K as approximately – 50 kJ/mol. Rh chloride leaching probably occurs via a fast oxidation step (with a Gibbs free energy of - 440 kJ/mol) followed by a less spontaneous conversion of the oxide to the chloride, (with a Gibbs free energy of -50 kJ/mol.) which results in slower leaching kinetics and lower leaching efficiencies for the Rh compared to Pt and Pd. Activation energies for Pt, Pd and Rh in a NaOCl – HCl - $H_2O_2$ solution as presented by Cao et al., (2006), were 59.1 kJ/mol, 63.5 kJ/mol, and 77.9 kJ/mol. Rh clearly had a higher activation energy than Pt and Pd, which may possibly be attributed to the two-step leaching process postulated in this study. This difference in leaching mechanisms could be the reason for the low Rh leaching efficiency.

### 4.7.2 Variation of leaching environment with changing parameters

The Eh – pH characteristics for all the reactions are plotted on the standard PGM - Cl - $H_2O$ Pourbaix diagrams in Figure 4.8. The plotted Eh conditions correspond to standardised Eh values, obtained after the measured ORP values (relative to saturated Ag/AgCl) were converted to Eh values relative to SHE. This was done in an attempt to reconcile the practically recorded readings to the standardised half-cell reactions used to draw the Pourbaix diagrams. The red coloured conditions correspond to conditions for runs 3, 4, 6 and 8 where at least 30 % leaching efficiency was obtained for Pt and Pd. Conditions for run 9 were not recorded due to instrument problems. It can be seen that these points fall into the regions of stability for the PGM chloro complexes and therefore rightfully correspond to the reactions in which PGMs were leached into solution. This serves as confirmation that the conditions that were investigated were thermodynamically conducive for leaching PGMs into solution.

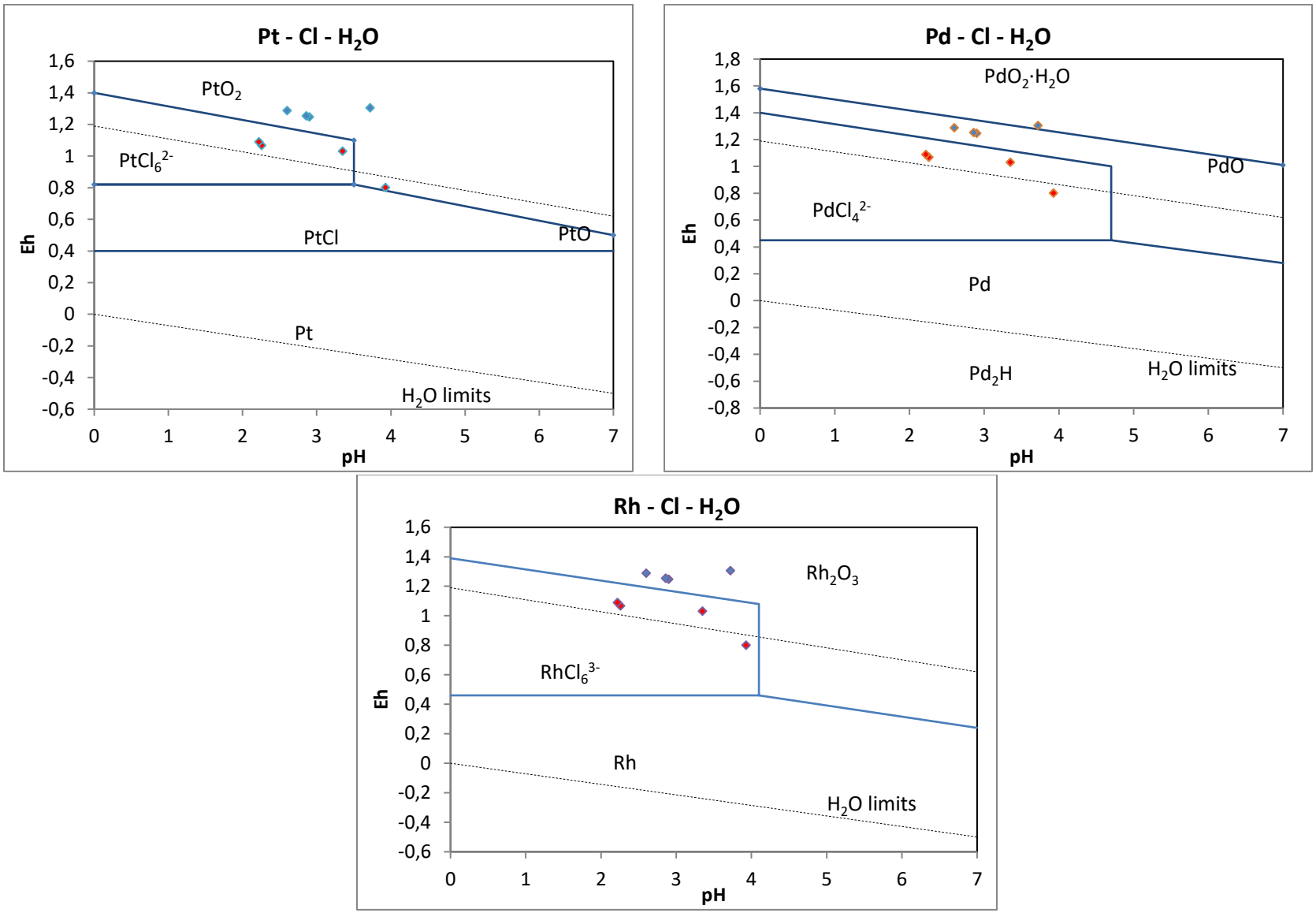


Figure 4.8: Scatter plots of Eh-pH reaction conditions on standard Pourbaix (drawn using HSC Chemistry) diagrams for CCD reactions

### 4.7.3 Statistical data analysis – selection of a suitable model

The main purpose for the preliminary CCD experiments was to investigate how PGM leaching efficiency varies with the changing leaching parameters. Development of a suitable statistical model was therefore important, and this was done using the statistical software Minitab 16.

ANOVA analysis (illustrated in table 4.6) was conducted and informed the selection of the models represented in equations 46 to 48.

$$Y_{Pt} = 0.383 + (0.281 * Temp) - (0.098 * Temp * [\mathrm{Ca(OCl)_2}]) + (0.098 * [AlCl_3]) + 0.094 * [\mathrm{Ca(OCl)_2}] * [AlCl_3] \quad \text{Equation } \mathbf{46}$$

$$Y_{Pd} = 0.464 + (0.285 * Temp) + (0.102 * [AlCl_3]) - (0.090 * \mathrm{Temp} * [\mathrm{Ca(OCl)_2}]) + 0.100 * ([\mathrm{Ca(OCl)_2}] * [AlCl_3]) \quad \text{Equation } \mathbf{47}$$

$$Y_{Rh} = 0.060 + (0.029 * Temp) + (0.020 * [AlCl_3]) - (0.015 * [\mathrm{Ca(OCl)_2}]) + (0.013 * \mathrm{Temp} * [AlCl_3]) - (0.018 * [AlCl_3] * [\mathrm{Ca(OCl)_2}]) \quad \text{Equation } \mathbf{48}$$

Table 4.6: ANOVA tables for Pt, Pd and Rh models (α = 0.05)

| | Pt | | Pd | | Rh | |
|---|---|---|---|---|---|---|
| Predictor | Coeff | P | Coeff | P | Coeff | P |
| Constant | 0.383 | 0.001 | 0.464 | 0.000 | 0.060 | 0.000 |
| Temp | 0.281 | 0.010 | 0.285 | 0.000 | 0.029 | 0.010 |
| $[AlCl_3]$ | 0.098 | 0.029 | 0.102 | 0.012 | 0.020 | 0.005 |
| $[Ca(OCl)_2]$ | -0.02 | 0.073 | -0.011 | 0.417 | -0.015 | 0.022 |
| Temp*$[AlCl_3]$ | 0.008 | 0.470 | -0.163 | 0.250 | 0.013 | 0.048 |
| Temp*$[Ca(OCl)_2]$ | -0.098 | 0.000 | -0.090 | 0.001 | -0.018 | 0.010 |
| $[AlCl_3]$*$[Ca(OCl)_2]$ | 0.094 | 0.005 | 0.100 | 0.015 | 0.001 | 0.826 |
| Temp*$[AlCl_3]$*$[Ca(OCl)_2]$ | 0.014 | 0.199 | -0.001 | 0.927 | -0.006 | 0.286 |
| $R^2$ | 99.08 % | | 98.42 % | | 86.40 % | |
| $R^2_{adj}$ | 98.44 % | | 97.31 % | | 54.71 % | |
| $R^2_{pred}$ | 97.22 % | | 97.32 % | | 76.87 % | |

Figure 4.9 illustrates the normal probability plots for the selected models, illustrating how the models fit with the observed data. Standardised residuals were subjected to normality tests and p values of 0.227, 0.163 and 0.211 for Pt, Rh and Pd models suggest that there isn't enough

evidence for deviation from normality (i.e. of the standardised residuals). As can be inferred from the graphs, the models accurately fit the observations.

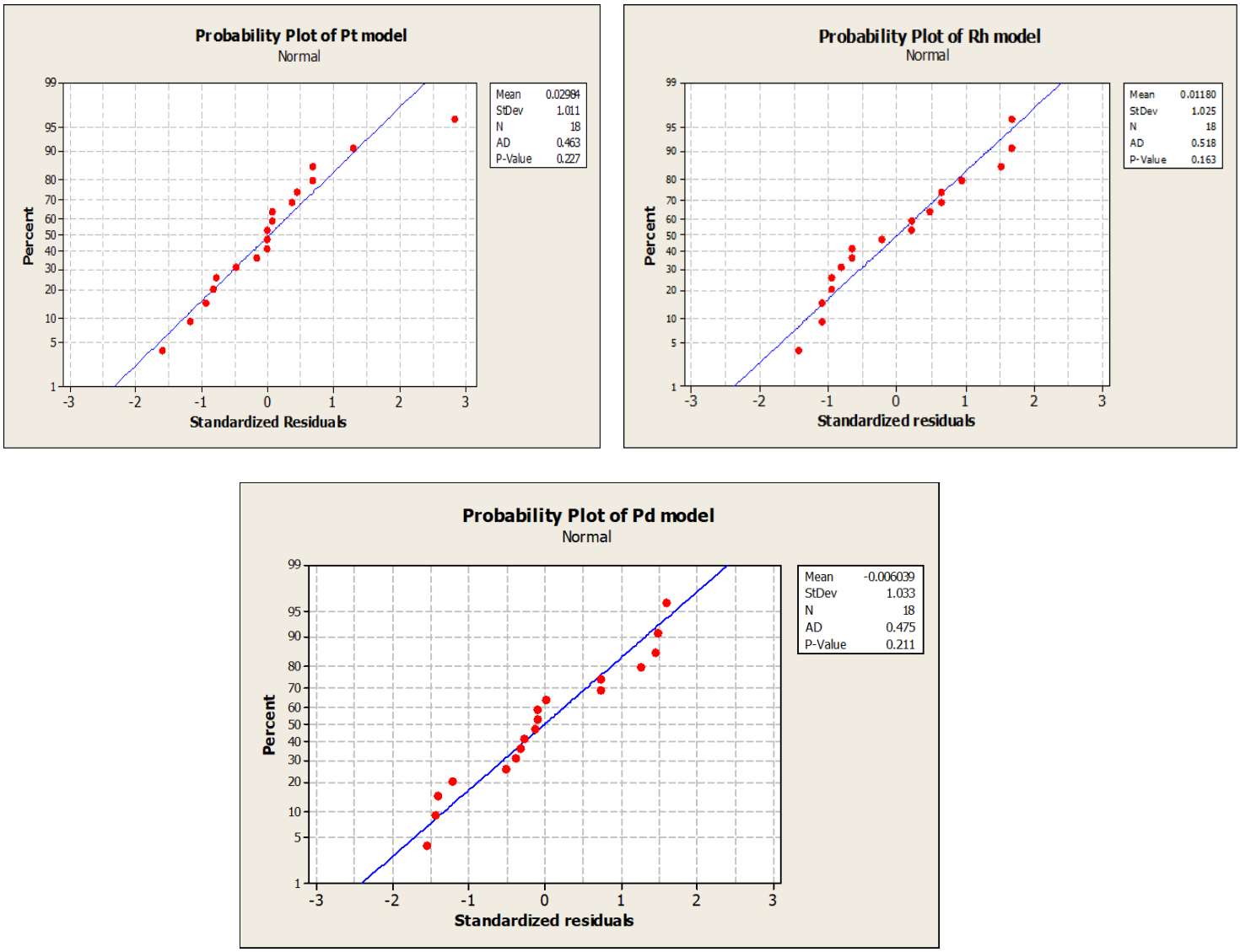


Figure 4.9: Probability plots for Pt, Rh and Pd regression models

### 4.7.4 Effects of factors

The model was then used to investigate the effects of the various factors.

#### 4.7.4.1 Effects of temperature

There was sufficient evidence at the 5% level for the Pt, Pd and Rh models respectively to prove that temperature was statistically significant on the leaching efficiency of the three PGMs. Figure

4.10, which is the main effects plot for temperature on the three PGMs' leaching yield, also corroborates this observation.

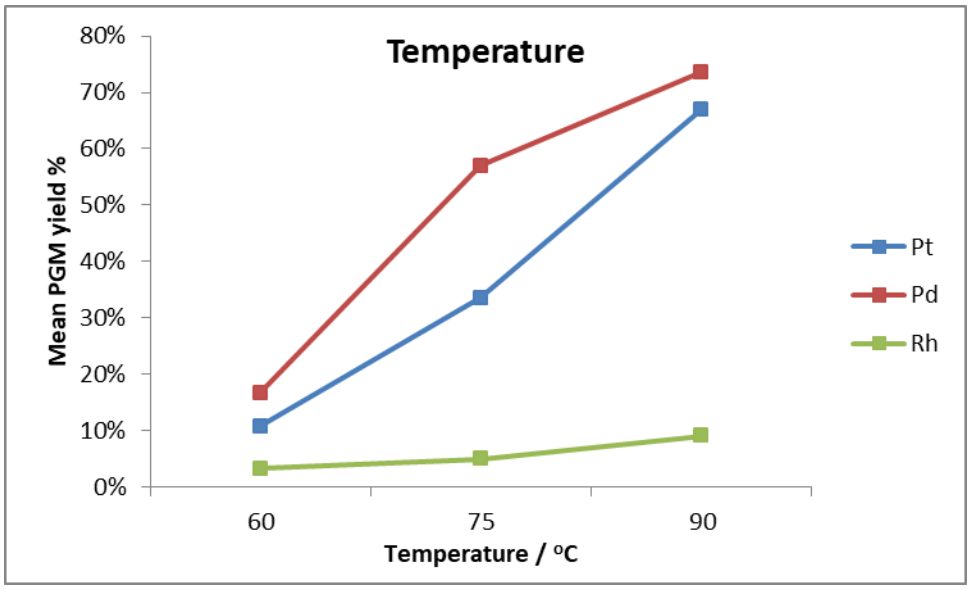


Figure 4.10: Main effects plot for temperature on the leaching of Pt, Pd and Rh.

It was quite evident, especially for Pt and Pd leaching, that increasing the temperature over the three levels that were investigated increased the average leaching yield substantially. The steep increase in leaching yield with increasing temperature for Pt and Pd means that increasing temperature even further would be expected to increase the leaching yield for the two metals. However, temperatures below the boiling point of the leaching solution were used intentionally to avoid resorting to autoclave leaching. The upper temperature limit could therefore only be below the boiling point of the reaction mixture (100 $^{o}$C).

Increasing temperature increases the average kinetic energy of the molecules in the leaching media. This therefore means more molecules now have energies above the activation energy. These increased number of molecules with higher average kinetic energies (above the activation energies) result in a high frequency of successful collisions between PGMs and chloride ions. This would explain the increase in the yield of Pt and Pd with increasing temperature.

The temperature coefficient (+0.029) for Rh was significantly lower than that for Pt and Pd (+0.281 and +0.285) as show in equations 46 to 48. The main effects plot for Rh also shows that its leaching efficiency was relatively unchanged over the temperature range investigated. These

two observations illustrate that the temperature did not have much bearing on the leaching efficiency of Rh. They may also serve as further justification of the two-step reaction mechanism for Rh, suggesting that under these unaggressive conditions, the bulk of the Rh was converted to the oxide. Llopis and Vázquez, (1964) investigated the electrochemical behaviour of Rh in an acidic oxidising solution of HCl and $HClO_4$. Based on sweeping voltammetry investigations, the authors speculated that Rh becomes passivated in such solutions, first by chemisorption of $O_2$ followed by a slow formation of $Rh_2O_3$. $Rh_2O_3$ has a corundum structure, similar to alumina crystals (Cotton, 1997). Due to this densely packed structure, it is therefore relatively unreactive rendering changes in temperature, within this range (< 90 $^oC$), practically ineffectual on its leaching yield. In order to attain acceptable leaching rates, commercial PGM refiners either employ long leach residence times, or high temperature operations under autoclave conditions to leach the PGMs, including Rh into solution (Crundwell et al., 2011). Needless to say, this observation could only be verified through a series of cyclic voltammetry tests, kinetic studies and XRD analysis of solid residue, which were all beyond the scope of this investigation.

#### 4.7.4.2 Effects of [$AlCl_3$]

The main effects plots for $AlCl_3$ concentration (Figure 4.11) showed an increase in the average Pt and Pd yield with increasing $AlCl_3$ concentration. Given that $AlCl_3$ was the acidifying agent and source of chloride ions for complexing PGMs, increasing $AlCl_3$ concentration results in a more acidic solution with an excess of chloride ions. This is therefore expected to favour the forward complexing reaction of the two PGMs, increase their rates of leaching and also the stability of the PGM chloro complexes that are formed. As expected, the coefficients for $AlCl_3$ concentration in all three models (Pt, Pd and Rh respectively) were all positive (0.098, 0.102, 0.020), indicating a positive correlation between leaching yield and $AlCl_3$ concentration.

As expected, the coefficient for Rh leaching yield was the least, which is also reflected by the main effects plot which indicated a relatively constant average Rh leaching yield over the different $AlCl_3$ concentrations. The formation of the passivating Rh oxide can also be used to explain this relatively constant profile for leaching efficiency over the $AlCl_3$ concentration range.

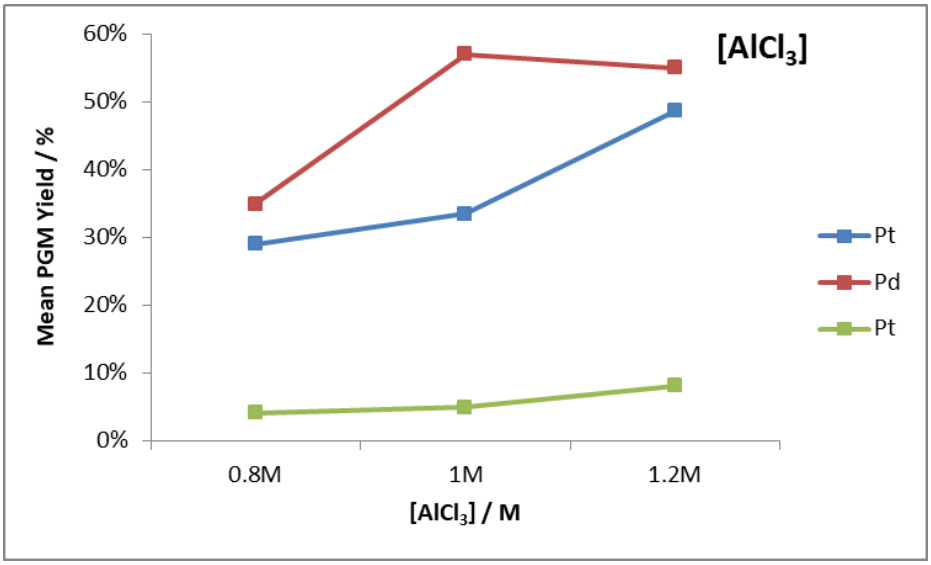


Figure 4.11: Main effects plots for [$AlCl_3$]

#### 4.7.4.3 Effects of [$Ca(OCl)_2$]

The main effects plot for the effect of $Ca(OCl)_2$ concentration on PGM yield are presented in Figure 4.12. $Ca(OCl)_2$ concentration seems to have a steep negative correlation between concentrations 0.2 M and 0.3 M, which stabilises slightly between 0.3 M and 0.4 M for the Pt and Pd models. However for Rh, the correlation is consistently negative, albeit with a very slight change. The coefficients for the three models were all negative (-0.02 , -0.011 , -0.015), suggesting a negative correlation between [$Ca(OCl)_2$] and PGM yield. At first glance, this seemed counterintuitive, as it would have been expected that the higher concentration of the oxidant should correspond to a higher PGM yield. However, the decreasing PGM yield with increasing concentration of oxidant may be attributed to the amount of $Ca(OH)_2$ which forms.

At higher $Ca(OCl)_2$ concentrations, more $Ca(OH)_2$ is left in suspension. This means when $AlCl_3$ solution is added to a solution of HOCl, more of it is first consumed by neutralising this suspended $Ca(OH)_2$. The solution is therefore not as acidic, which would result in lower PGM yield, since PGM leaching requires acidic conditions.

This effect is illustrated by considering reactions 3 and 6, which were both conducted at 90 $^oC$ and 0.8 M $AlCl_3$ solution but with different $Ca(OCl)_2$ concentrations of 0.2 M and 0.4 M. A snippet of the recoveries and reaction conditions at these concentrations has been presented in Table 4.8

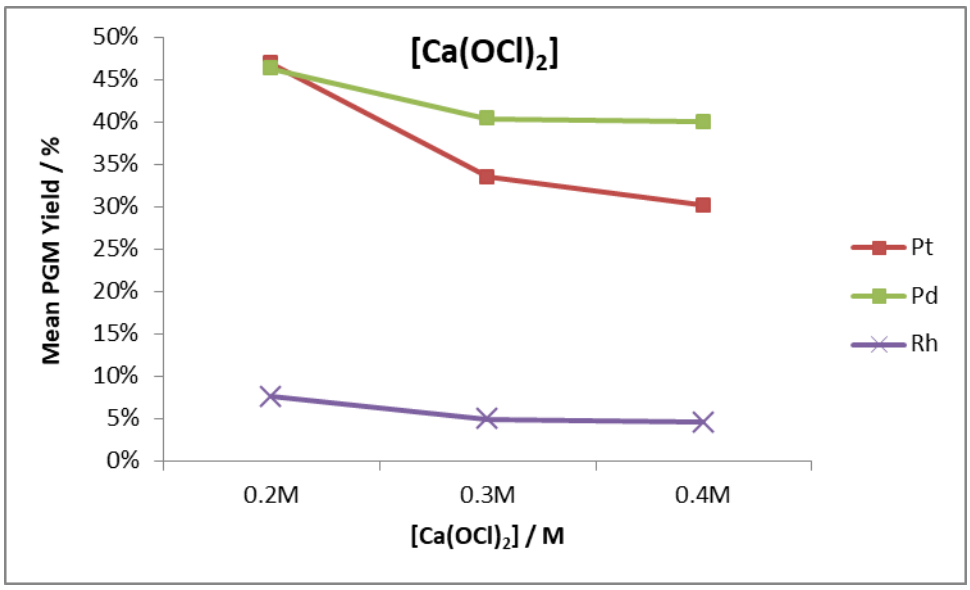


Figure 4.12: Main effects plots for $[Ca(OCl]_2$)

Table 4.7: Comparison of leaching conditions at different $Ca(OCl)_2$ concentrations

| Run | Temp/°C | $[AlCl_3]$/M | HOCl/M | PGM Yield | | | t = 0 | | t = T | |
|---|---|---|---|---|---|---|---|---|---|---|
| | | | | Pt | Pd | Rh | eH/V | pH | eH/V | pH |
| 3 | 90 | 0.80 | 0.2 | 78% | 86% | 7% | 1.190 | 1.88 | 1.067 | 2.26 |
| 6 | 90 | 0.80 | 0.4 | 33% | 46% | 1% | 1.279 | 3.20 | 0.800 | 3.93 |

It is evident that increasing the concentration of the $Ca(OCl)_2$ from 0.2 M to 0.4 M increased the starting pH of the reaction from 1.88 to 3.20. The pH at the end of the reactions was also higher at 3.93 for 0.4 M (run 6) than that for 0.2 M (run 3). The PGM yield at 0.2 M was observably higher than that at 0.4 M. Consequently, the Eh – pH conditions for run three fell within the region of thermodynamic stability of the chloro-complexes, while those for run six did not because of the high pH, giving credence to the explanation presented earlier on the effect of increased $Ca(OCl)_2$ concentration on PGM leaching.

### 4.7.5 Effects of interactions between $[AlCl_3]$ and $[Ca(OCl)_2]$

$AlCl_3$ and $Ca(OCl)_2$ are the two reagents whose properties and interactions are directly responsible for the leaching environment. The chemical reactions between the two in solution, therefore directly affects the leaching environment. The underlying theoretical chemistry has already been

presented in section 4.5. The contour plot presented in Figure 4.12 shows the leaching efficiency obtained from the leaching experiments as a function of the [$AlCl_3$] and [$Ca(OCl)_2$].

An equilibrium between the HOCl and $OCl^-$ species exists when a hypochlorite salt, or $Cl_2$ are dissolved in water. This equilibrium is affected by pH, ionic strength of solution, temperature and concentration of chloride ions. The most effective oxidant in solution is the HOCl species, which has a narrow pH range of stability. Lowering the pH of the HOCl solution by adding $AlCl_3$ solution consequently affects its equilibrium with the hypochlorite ion. The effectiveness of the leach solution to solubilise PGM as their chloro-complexes therefore relates directly to the ratio of $AlCl_3$: HOCl in the reactor as illustrated in Figure 4.12.

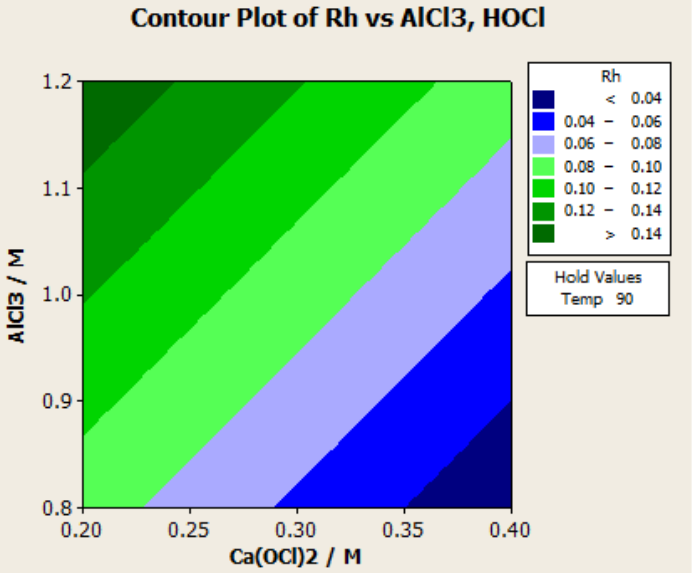


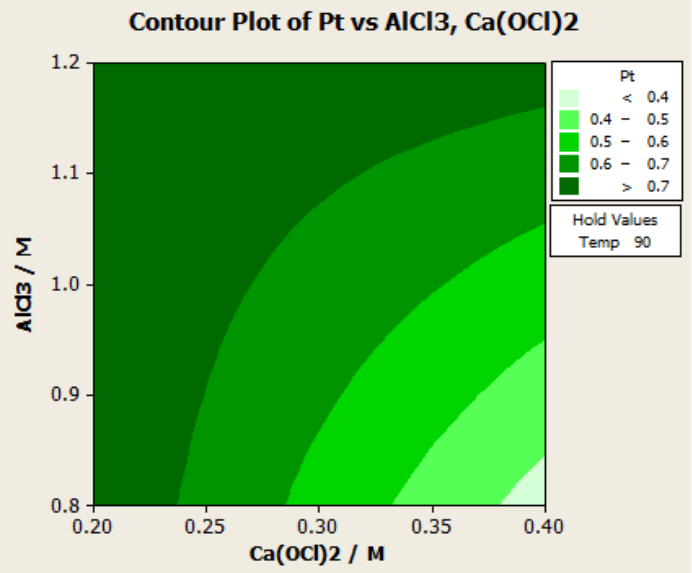


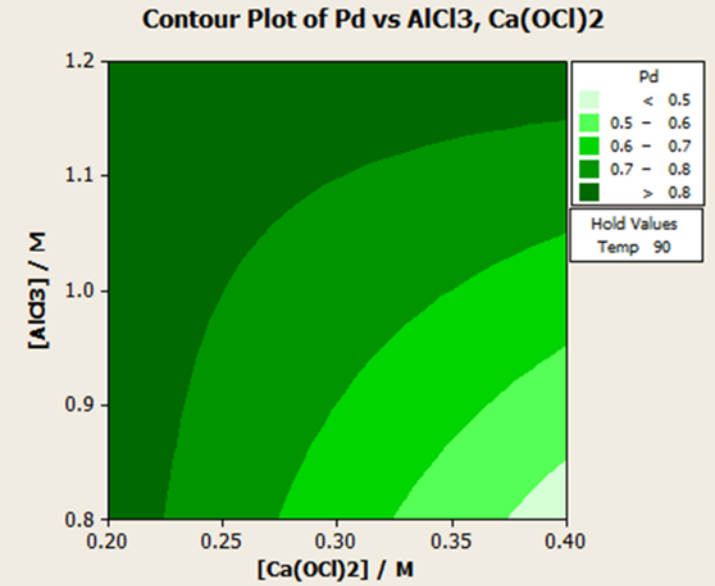

Figure 4.13: Contour Plots for the interaction of [$Ca(OCl)_2$] and [$AlCl_3$] on Rh, Pt and Pd yields

Equations 46 to 48 and table 4.6 reveal that the interaction of the 2 chemicals in solution is statistically significant. The gradient of the contours confirms what the previous data analysis revealed ; that PGM yield increases with increasing $AlCl_3$ concentration and with decreasing $Ca(OCl)_2$ concentration. Increasing $AlCl_3$ concentration makes the solution more acidic and increases the concentration of $Cl^-$ ions. This in turn increases the rate of the forward PGM complexing reaction and the stability of the PGM chloro complexes formed. The net effect is an increase in the PGM leaching yield. A lower $Ca(OCl)_2$ concentration is favourable as it also results in formation of less $Ca(OH)_2$; which means that less of the acidifying $AlCl_3$ solution is consumed by neutralising this excess $Ca(OH)_2$. The solution is therefore more acidic and more favourable for PGM leaching. A higher $Ca(OCl)_2$ concentration, and hence a higher $Ca(OH)_2$ concentration also results in formation of gelatinous $Al(OH)_3$ according to equation 49, which increases the filtration time and reduces the efficiency of the contact between the solids and the leach solution during leaching, possibly hindering PGM leaching.

$$2AlCl_3 + 3Ca(OH)_2 \rightarrow 3CaCl_2 + 2Al(OH)_3 \qquad \text{Equation } \mathbf{49}$$

## 4.8 Summary

Temperature was shown to be statistically significant, and on that basis, for subsequent experiments, the upper and lower limits for the temperature were increased. It was also observed that the interaction between $AlCl_3$ and $Ca(OCl)_2$ could be manipulated to improve PGM recoveries, especially for Rh. The $AlCl_3$ range was not changed, however, for the optimisation experiments, $Ca(OCl)_2$ range was changed to 0.15 M - 0.45 M. It was also observed that for all combinations tested, the oxidising potential of the solution decreased with time. This drop was attributed to escaping $Cl_2$ gas. The experimental setup for the optimisation runs was therefore changed to limit the escape of $Cl_2$ gas. These changes are expected to significantly improve PGM leaching yields, especially those for Rh.

# Chapter 5 : Leaching Optimisation and SX Results

## 5.1 Introduction

The results from the preliminary central composite design experiments were used to draw up the optimisation experiments. The insights obtained were used to change leaching parameters and the experimental setup in order to improve the PGM yields. The one factor at a time experimental methodology was used for the optimisation experiments.

## 5.2 Results from optimisation of leaching conditions

### 5.2.1 Effect of temperature

The effect temperature had on PGM leaching yield is presented in Figure 5.1. Readings for Rh at 70 $^{o}$C were all reported by the analysis as < 5ppm, and consequently leaching efficiency could not be calculated. Of the three PGMs, the sample was predominantly a Pd sample, containing 88% by mass of the PGMs. It is quite possible that such a high value of Pd may have affected analytical readings for the other metal ions in solution, leading to failures to detect the other two less concentrated PGMs in solution. Values of Pd leaching yield above 100% obtained in the leaching efficiency analyses were attributed to compounded experimental error between sampling and ICP analysis at Mintek. Although measures were taken to reduce evaporative losses during the reaction, leaching efficiencies above 100% may have been a result of increasing losses of the leach solution through evaporation. In such an instance, reported values would have definitely been more concentrated than they should have been had evaporative losses been contained. This may be the reason for the unstable results and higher than 100 % leaching efficiencies at temperature = 100 $^{o}$C. Notwithstanding these evaporative losses, subsequent experiments were carried out at a temperature of 100 $^{o}$C. In the follow up experiments as a result of this observation, the reaction slurry was also periodically topped up with leaching solution, to maintain its volume. However, errors that could have arisen as a result of analytical measurement could not be mitigated in any way.

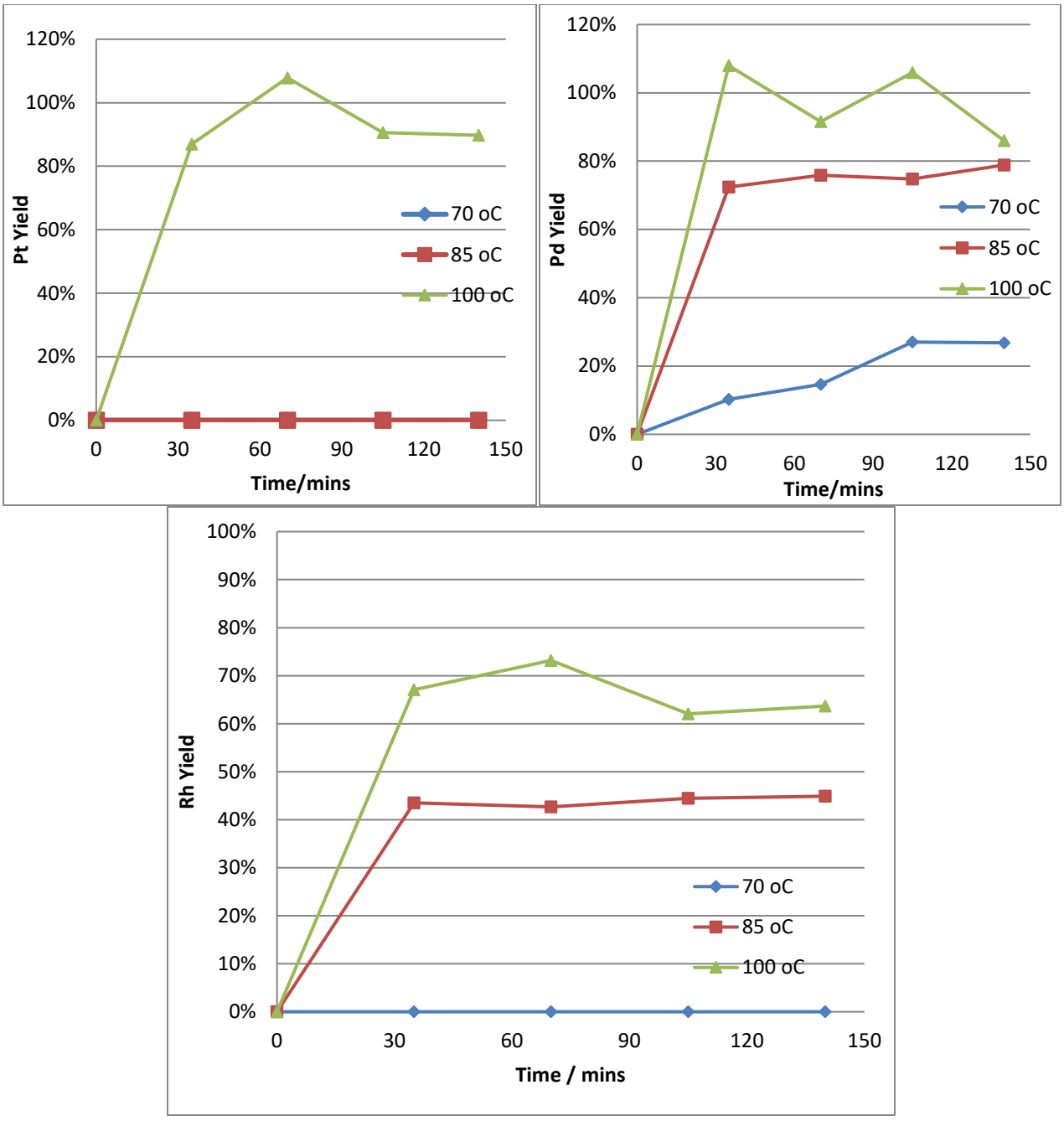


Figure 5.1: Effect of temperature on Pd and Rh yields; [$AlCl_3$] = 1.2 M, time = 140 minutes, [$Ca(OCl)_2$] = 0.3 M, S/L ratio = 1 g/ 20 ml

An increase in temperature is expected to impart more kinetic energy to the reacting species in solution. This would increase the number of successful collisions which should favour the forward complexing reaction. During the preliminary experiments, temperature was observed to be a significant factor according to the design of experiment employed. This was then confirmed in

these experiments where increasing the temperature resulted in a significantly observable increase in the leaching efficiency of the PGMs.

### 5.2.2 Effects of [$AlCl_3$] and [$Ca(OCl)_2$]

PGM yield increased with increasing concentration of $AlCl_3$ as illustrated in Figure 5.2. This confirmed the results obtained in the preliminary experiments. Maximum PGM yield was obtained at a [$AlCl_3$] value of 1.2 M.

1.2 M $AlCl_3$ concentration was therefore used for the subsequent leaching experiments. Values recorded for yields above 100% were also attributed to error between sampling and sample analysis, and the possibility of loss of solution via evaporative losses.

The effect of calcium hypochlorite concentration on Pt, Pd and Rh leaching yields has been illustrated in Figure 5.3. The effect of $Ca(OCl)_2$ concentration was more pronounced for Rh leaching than it was for Pt and Pd. Rh leaching was evidently slower at 0.45 M than at 0.15 M as depicted by the gradients of the graphs. It has already been illustrated that higher $Ca(OCl)_2$ solutions translated to more alkaline solutions, which are unfavourable for leaching PGMs. Maximum leaching was obtained at $Ca(OCl)_2$ concentration of 0.15 M. The maxima at these conditions for Pt, Pd and Rh were 91%, 100% and 74% after 105 minutes.

As mentioned in earlier chapters, the leaching apparatus was changed to obtain a more air tight reaction mixture in order to reduce the excessive loss of chlorine generated during the reaction. The $Cl^-/Cl_2$ equilibrium under acidic conditions is shifted to the right under acidic conditions, and continued removal of product favours the oxidation of chloride and its subsequent loss as chlorine. Moreover, the $HOCl/Cl_2$ equilibrium, which is also responsible for the actual oxidation reactions, also shifts to the right with mass loss of chlorine out of the system boundary. It is therefore strongly postulated that maintaining a more air tight reaction environment must have been one of the reasons why PGM leaching efficiencies in the second set of reactions were also significantly increased. In an ideal situation, whereby no chlorine is lost from the reaction vessel, it would be expected that equilibrium would be established in the reaction mixture between Cl (aq) and Cl (g). According to Majima et al., (1990) and equilibrium thermodynamic considerations by Alkan et al.,

(2005), the presence of chlorine in HCl solution produces another potent oxidising species, the $Cl_3^-$ (aq) ion. This would be expected to reduce the loss of solution oxidising potential and thereby translate to increased PGM leaching recoveries. A higher chlorine vapour pressure is also expected to maintain the $HOCl/Cl_2$ equilibrium to the left, keeping the better HOCl oxidant in solution and further maintaining oxidising conditions favourable for PGM complexation. It is therefore strongly recommended to keep a reaction medium in which none of the chlorine is allowed to escape.

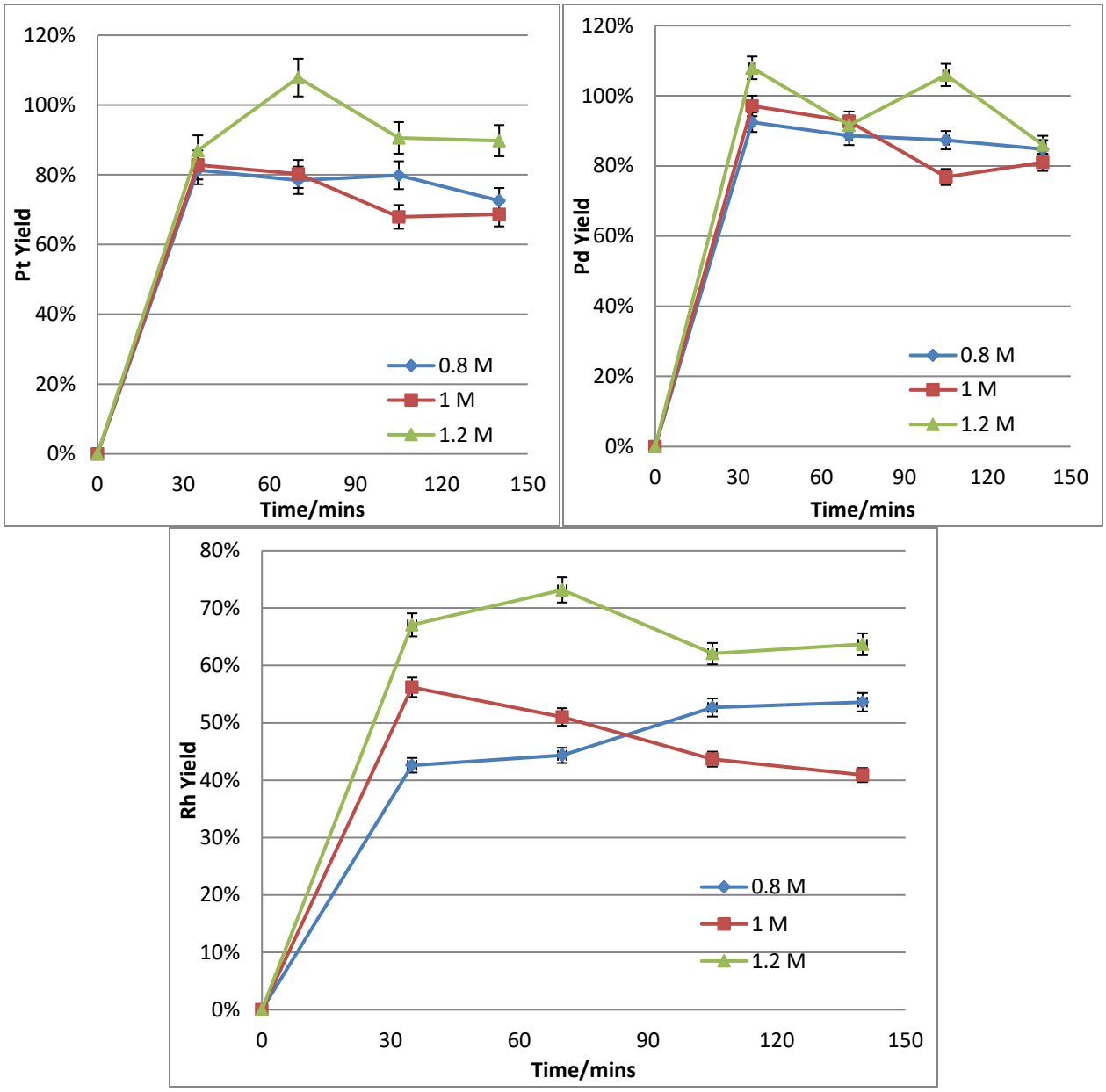


Figure 5.2: Effect of [$AlCl_3$] on Pt and Rh yields; temperature = 100 $^oC$, time = 140 minutes, [$Ca(OCl)_2$] = 0.3 M, S/L ratio = 1 g/ 20 ml

### 5.2.3 Effect of S: L ratio

The S/L ratio used in all the experiments to this point was 1g/20 ml. A decision was made to investigate the effect of changing the S/L ratio. A higher S/L ratio would be beneficial because it would improve metal production rates by allowing for leaching of more SAC per batch operation. This would translate to improved production economics.

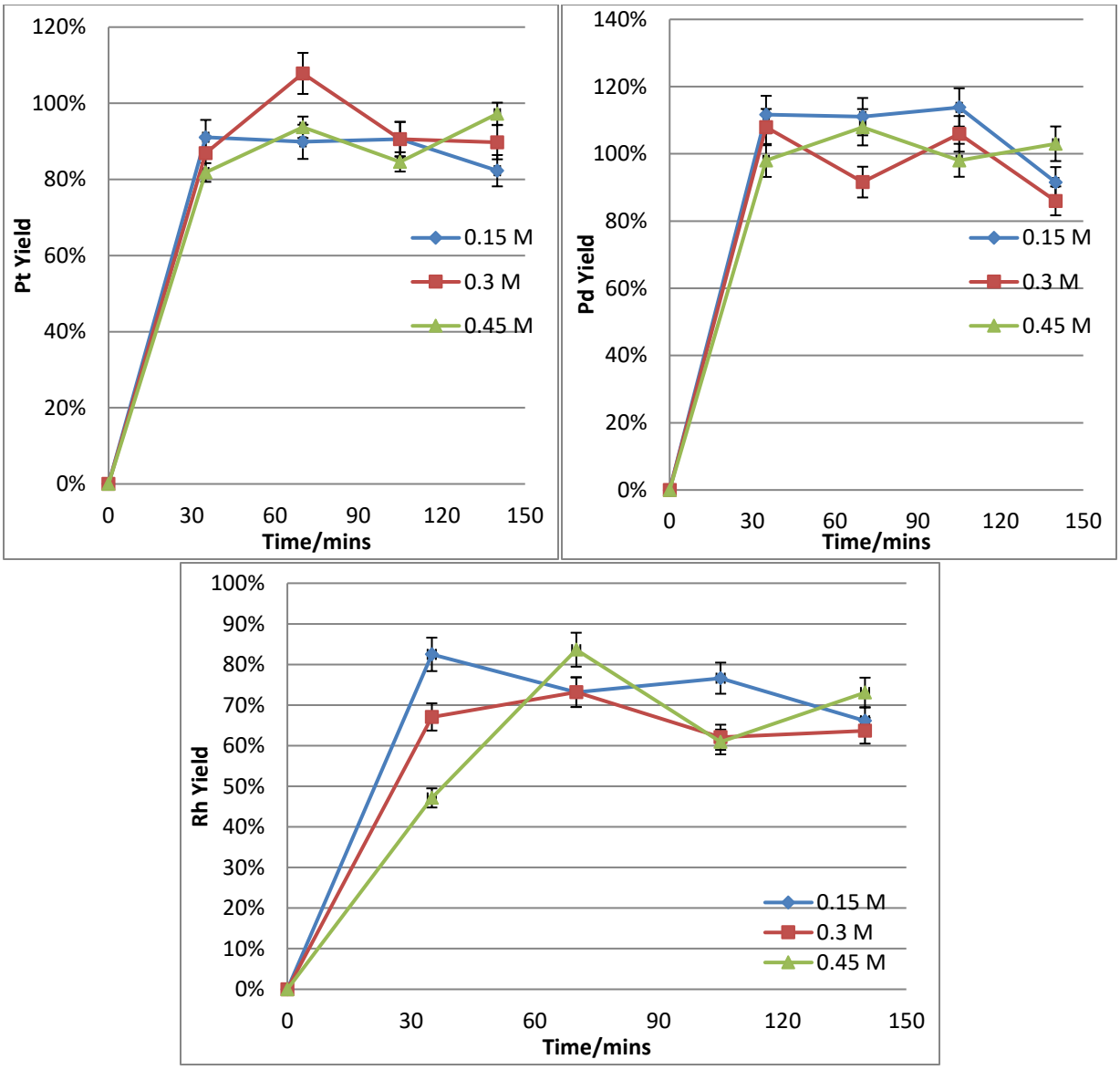


Figure 5.3: Effect of [$Ca(OCl)_2$] on Pd, Rh and Pt yields ; temperature = 100 $^oC$, time = 140 minutes, [$AlCl_3$] = 1.2 M, S/L ratio = 1 g/ 20 ml

Figure 5.4 shows the effect of changing the S/L ratio on the PGM leaching yield. PGM recoveries between 1g/10ml and 3g/10ml are comparable (Pd – 100 % vs. 86 %; Pt 100 % vs. 90 % and Rh 68 % vs. 61 %) because the pulp density is still low and mass transfer is not hindered. Beyond 3 g / 10 ml however, the effects of hindered mass transfer and re-adsorption are now enhanced, which is why the PGM yields begins to decline.

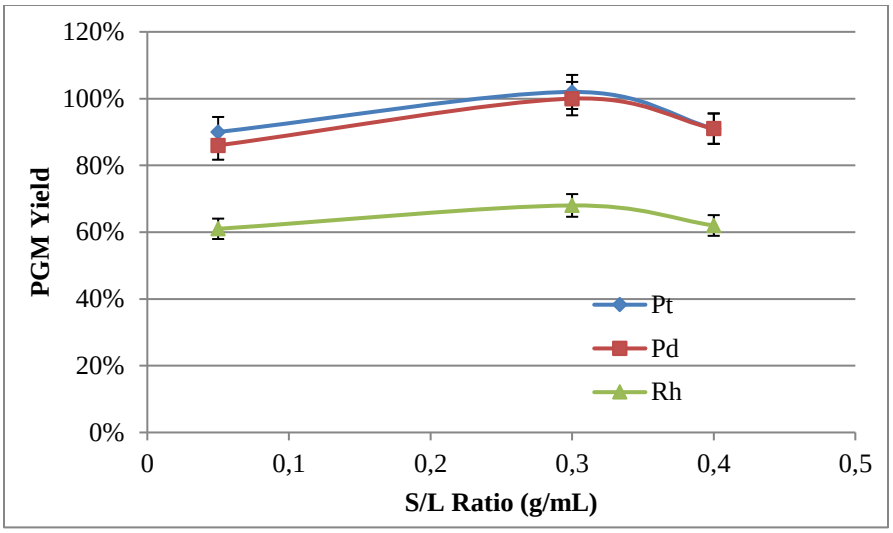


Figure 5.4: Effect of S/L ratio on PGM yields [$AlCl_3$] = 1.2 M, [$Ca(OCl)_2$] = 0.3 M, Temp = 100 $^oC$, time = 140 minutes)

In agreement with work by (Upadhyay et al., 2013), the leaching efficiency of the PGMs decreased with increasing pulp density. An optimum of 0.02 g/ml was selected by Upadhyay et al., (2013) when PGMs were leached using eletrogenerated chlorine. Kim et al., (2016) also observed a similar trend in which PGM leaching efficiency was decreasing, with an increase in the S/L ratio. When S/L ratio was increased to 0.4 g/ml the leaching efficiency greatly decreased. Optimum S/L ratio was chosen as 0.2 g/ml by Kim et al., (2016). A more recent response surface design proved the statistical significance of S/L ratio for chloride leaching at the 5% level (Hasani et al., 2017). It was shown that all three PGMs were affected by S/L ratio when it was studied within the range 0.1 g/ml to 0.5 g/ml.

In this investigation an optimum was selected as 0.3 g/ml based on recoveries of 99% for Pt and Pd, and 68% for the leaching of Rh as illustrated in Figure 5.4. Beyond this value, PGM leaching efficiency began to decrease.

The effect of S/L ratio can be attributed to re-adsorption of the PGMs onto the catalyst substrate after leaching when the pulp density is too high. Work on Pt (IV) and Pd (II) adsorption onto alumina was conducted by Ogata and Kawasaki, (2013). It was shown in this investigation that it was possible for the two metals to be adsorbed onto alumina prepared from calcination of dried

aluminium hydroxide gels. It was also shown that this adsorption competes with chloride ions. The kinetics for adsorption was quite slow (only attaining equilibrium after 50 hours) and the amount adsorbed in less than 5 hours was also quite low at less than 5 mg/g of alumina. However, when it is considered that catalytic converters contain approximately 30% – 40% by weight alumina, and there was some loss of chloride ions as $Cl_2$ from oxidation (thereby effectively reducing the chloride concentration to compete with PGMs for adsorption onto alumina surface), it is quite plausible that a greater proportion of PGMs may have subsequently re-adsorbed onto the alumina surface at higher S/L ratio. It should, however be stressed that although PGMs were adsorbed onto the alumina surface in the study by Ogata and Kawasaki, (2013), it was observed that maximum adsorption occurred at pH 5, where PGMs occur as hydrated PGM-chloro species. Leaching conditions used in this study were consistently at pH lower than 5. Nevertheless, this phenomenon of PGM re-adsorption onto alumina could be the reason for lower recoveries recorded for higher S/L ratios in this and the other cited studies.

## 5.3 Results from the experimental run at optimum conditions

PGM leaching efficiency at the optimum set of conditions is presented in Table 5.1. Pt and Pd were successfully leached into solution at the optimum conditions. However, as expected, Rh leaching was not as effective; only attaining a maximum of 68%.

Table 5.1: PGM yield at optimum operating conditions

| | | Pt | Pd | Rh |
|---|---|---|---|---|
| Leaching efficiency | | 99 % | 99 % | 68 % |
| Optimum conditions | $[AlCl_3]$ = 1.2 M, $[Ca(OCl)_2]$ = 0.3 M, Temp = 100 $^oC$, time = 140 minutes, S/L ratio = 3 g / 10ml | | | |

### 5.3.1 Leach solution after acidifying for solvent extraction runs

Solutions that were obtained from the optimisation leaching experiments were mixed together, and diluted using HCl to acidify the solution as already presented in section 3.6.1 for the solvent extraction experiments. The acidification of the solution was done in order to provide an excess of H+ ions to protonate the Alamine 308 during extraction experiments. In order to obtain a suitable HCl concentration for acidification, its effect on Pt and Pd co-extraction was investigated over HCl concentrations of 0 M (no acid) to 9 M with a fixed aqueous PGM solution: acid volume ratio

of 3:1 as already presented in section 3.6.1. This procedure was not conducted in duplicate and the results of the percentage extraction against HCl concentration are presented below.

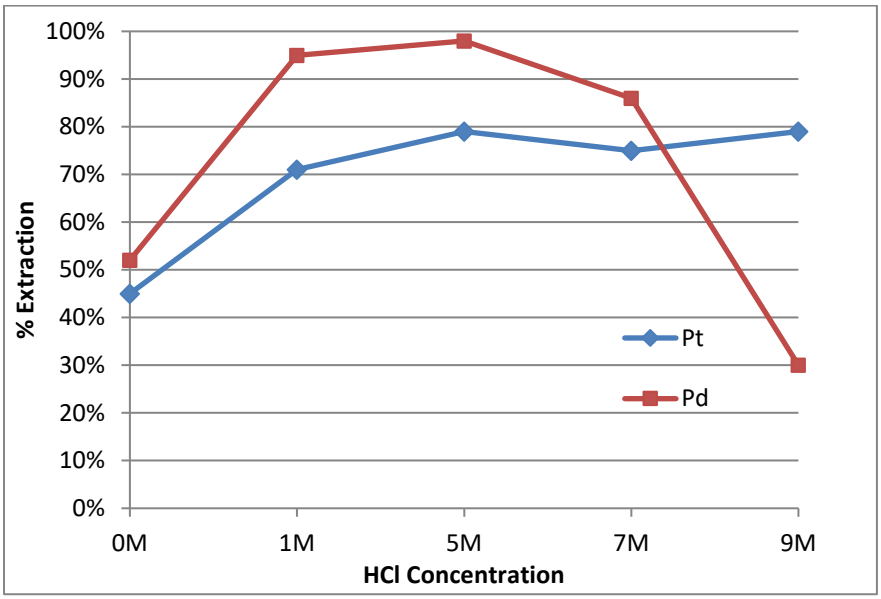


Figure 5.5: Effect of [HCl] on PGM extraction percentage ([Alamine 308] = 0.01 M in kerosene, 5 % v/v Decanol, 30 minutes shaking time at 300 rpm, 1:1 O/A volume ratio).

The extraction of Pt and Pd is directly correlated to the amount of excess $H^+$ ions available to protonate the amine complex. As such, it was expected that increasing the HCl concentration would be followed by an increase in Pt and Pd co-extraction into the organic phase. Increasing HCl concentration is also expected to increase the proportion of non-hydrated PGM chloro-complexes, which would favour Pt and Pd co-extraction into the organic phase. An HCl concentration of 5 M with an acidification volume ratio of PGM aqueous solution: acid of 3:1 was then chosen for the subsequent experiments. A stock PGM pregnant solution was prepared by mixing 750 ml of the PGM loaded solution with 250 ml of 5 M solution. The elemental composition of this resultant solution for selected elements is as presented in Table 5.2.

Table 5.2: Elemental composition of the solution

| Element | Al | Pt | Pd | Ce | Fe | Mg | Mn | Ni | Zn | Zr | La | Nd |
|---|---|---|---|---|---|---|---|---|---|---|---|---|
| Unit | g/L | ppm | ppm | ppm | ppm | ppm | ppm | ppm | ppm | ppm | ppm | ppm |
| Conc. | 13.5 | 5.33 | 100 | 67 | 119.5 | 138.5 | 533 | 15.2 | 111.5 | 0.45 | 234 | 236 |

## 5.4 Solvent extraction of Pt, Pd and Fe into the Alamine 308 organic phase

The elemental concentration of the raffinate obtained after solvent extraction of Pt and Pd into the organic phase is tabulated below, together with the percentage extraction. The methodology is as presented in section 3.6.1. The experimental run was duplicated and concentrations of the aqueous solution after the extraction are presented as $conc_1$ and $conc_2$. An average for each metal was then used for calculating % extraction of the Pt and Pd into the organic phase by using equation 33.

Table 5.3: Results for the co-extraction of Pt and Pd into Alamine 308

| Element | Pt | Pd | Al (g/L) | Ce | Fe |
|---|---|---|---|---|---|
| Conc $_{(aq)}$ (ppm) | 5.33 | 100 | 13.5 | 67 | 119.5 |
| Conc $_1$ (ppm) | 0.80 | 1.02 | 13.7 | 66.9 | 3.61 |
| Conc $_2$ (ppm) | 0.58 | 0.83 | 13.55 | 66.75 | 2 |
| Conc $_{ave}$ (ppm) | 0.69 | 0.93 | 13.6 | 66.83 | 2.81 |
| Extraction % | 87 % | 99 % | -1 % | 0 % | 98 % |

Table 5.3 presents extractions of metals into the solvent, with the Pt and Pd being the target metals. Given that Al was the most concentrated, any Al loading would be detrimental to solution purity, and hence it was imperative to track weather it loaded. Fe readily loads onto Alamine 308; hence it was also reported here to identify how much of it would load. All the other species were not included / measured because they weren't expected to load onto Alamine.

The extraction of Pt and Pd, after four stages into the organic 0.1 M Alamine was 87% and approximately 100% respectively. Co-extraction of Fe into the organic phase was also nearly 100 %. Four-stage extraction was used based on work done by Nguyen et al., (2016a) as has already been presented in the methodology section 3.6.1. It was beyond the scope of this work to redo the extraction isotherms for the two Pt and Pd complexes into Alamine 308, so the results obtained in that study were used for this section.

Alamine 308 is an anion exchange amine which extracts anion complexes after being protonated according to equation **50:**

$$R_3NH^+A^-_{(org)} + B^-_{(aq)} \leftrightarrow R_3NH^+B^-_{(org)} + A^-_{(aq)}$$ Equation **50**

The PGMs exist as chloro anion complexes (Pt as $PtCl_6^{2-}$, Pd as $PdCl_4^{2-}$ and $PdCl_5^{3-}$ ) as predicted by their speciation diagrams presented in Figures 5.6. The differences in PGM extraction are determined by differences in the ionic charge densities. The charge densities for the PGM chloro complexes are in the order $PtCl_6^{2-}$ < $PdCl_4^{2-}$ < $RhCl_6^{3-}$ < hydrated PGM chloro complexes (Nikoloski and Ang, 2014). Hydrated PGM chloro complexes are complexes in which one or more of the chloride ions have been substituted by the hydroxide ions. The amount of hydrated PGM chloro complexes increases with increasing pH of solution. Under the leach solution conditions, 100 % and approximately 96% of Pt and Pd exist as the chloro complexes $PtCl_6^{2-}$ and $PdCl_4^{2-}$ respectively.

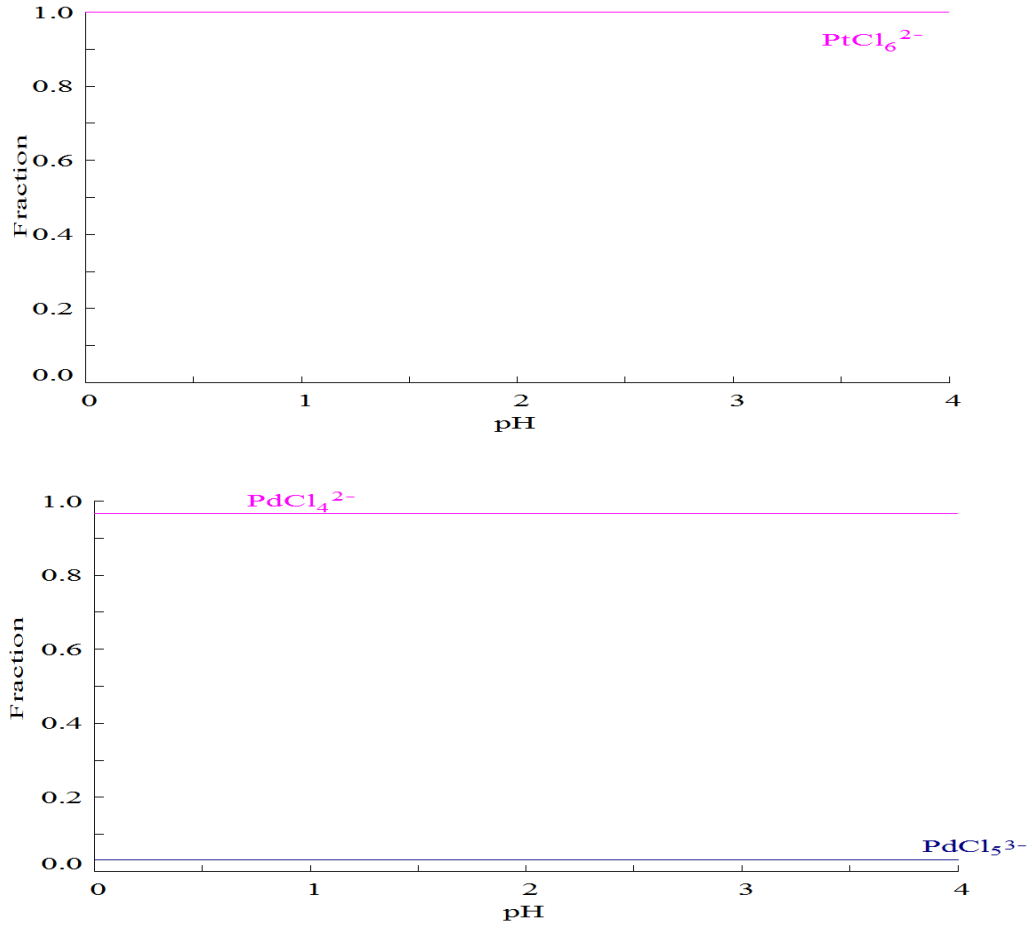


Figure 5.6: Speciation diagrams for Pt and Pd ([Cl-] = 3.37 M, [Pt] = 0.00533 mM, [Pd] = 0.1 mM, Eh = 1.078 V, Temperature = 25 $^oC$); drawn using Medusa Hydra software

The higher the charge density, the more an ion attracts water molecules around it i.e. the larger its solvation layer. This will thereby reduce coulombic interactions between the complex and the anion exchange site of the amine. In simpler terms, it reduces the effect of the attraction between the negative charge on the PGM complex and the positive charge of the protonated amine complex. Consequently, ease of extraction of the anion complex into the organic phase is of the reverse order i.e. $PtCl_6^{2-}$ > $PdCl_4^{2-}$ > $RhCl_6^{3-}$ > PGM aqua complexes.

In this investigation however, Pt extraction was lower at 87% compared to 99.6% for Pd. This was attributed to competition of the ions for loading. The Pt: Pd concentration ratio in solution was approximately 1:20 (Table 5.2). Pd would have therefore occupied a significant portion of the organic phase prior to Pt loading, leading to lower loading of Pt onto the organic solution. Furthermore, the high loading of Fe could have also hindered Pt loading onto the organic phase as well, further reducing Pt extraction from the aqueous solution.

### 5.4.1 Co-extraction of Fe into Alamine 308

Fe loading onto the organic phase was also quite high at 98%. The speciation diagram for Fe is presented below in Figure 5.6.

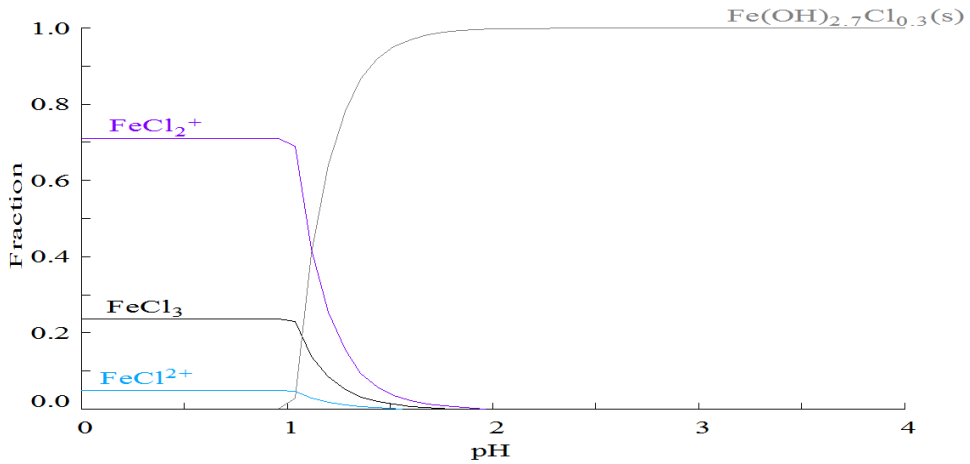


Figure 5.7: Speciation diagrams for Fe ([Cl-] = 3.37 M, [Fe] = 0.12 mM, Eh = 1.078 V, Temperature = 25 $^{o}$C) ; drawn using Medusa Hydra software

Fe exists in solution as a combination of $FeCl_2^{+}$, $FeCl_3$ and $FeCl^{2+}$ according to the speciation diagram predictions in Figure 5.7. $FeCl_3$ has been extracted using Alamine 336, another tertiary

amine with the alkyl group - $CH_3(CH_2)_7$, diluted in toluene by Lee et al., (2004). It was reported by the authors that ferric chloride is extracted by the following equation:

$$Fe^{3+}_{(aq)} + 4Cl^{-}_{(aq)} + R_3NHCl_{(org)} \rightarrow FeCl_4R_3NH_{(org)} + Cl^{-}_{(aq)} \qquad \text{Equation } \mathbf{51}$$

The presence of an excess of chloride ions around the ferric ion forms a complex which is negatively charged ($FeCl_4^-$). This ferric chloride complex then replaces the $Cl^-$ anion out of the tertiary organic salt ($R_3NHCl$) according to equation 51, forming an organometallic complex – thereby effectively extracting the Fe into the organic phase. It is therefore postulated that a similar extraction mechanism was responsible for the extraction of Fe into the organic phase in this investigation. The ferric cationic complexes; $FeCl_2^+$, $FeCl_3$ and $FeCl^{2+}$ predicted by the speciation diagrams also reacted with excess $Cl^-$ ions to form the $FeCl_4^-$ ion. The ferric chloro complex would then have reacted into the organic extractant phase as reported by Lee et al., (2004). The reactions may have proceeded according to equations **52** to **54** to form the same organometallic complex.

$$FeCl^{+}_{2(aq)} + 2Cl^{-}_{(aq)} + R_3NHCl_{(org)} \rightarrow FeCl_4R_3NH_{(org)} + Cl^{-}_{(aq)} \qquad \text{Equation } \mathbf{52}$$

$$FeCl_3 + Cl^{-}_{(aq)} + R_3NHCl_{(org)} \rightarrow FeCl_4R_3NH_{(org)} + Cl^{-}_{(aq)} \qquad \text{Equation } \mathbf{53}$$

$$FeCl^{2+}_{(aq)} + 3\,Cl^{-}_{(aq)} + R_3NHCl_{(org)} \rightarrow FeCl_4R_3NH_{(org)} + Cl^{-}_{(aq)} \qquad \text{Equation } \mathbf{54}$$

A high extraction of Fe into the organic phase has a negative effect on the desired extraction of PGMs due to increased competition between the PGM species and the ferric species, as well as contamination of the PGM solution. For this reason, Nguyen et al., (2016a) employed a TBP extraction step for Fe (III) removal prior to the co-extraction of Pt and Pd. The importance of such a stage cannot be over emphasized.

### 5.4.2 Selectivity of Alamine 308 over Al and Ce

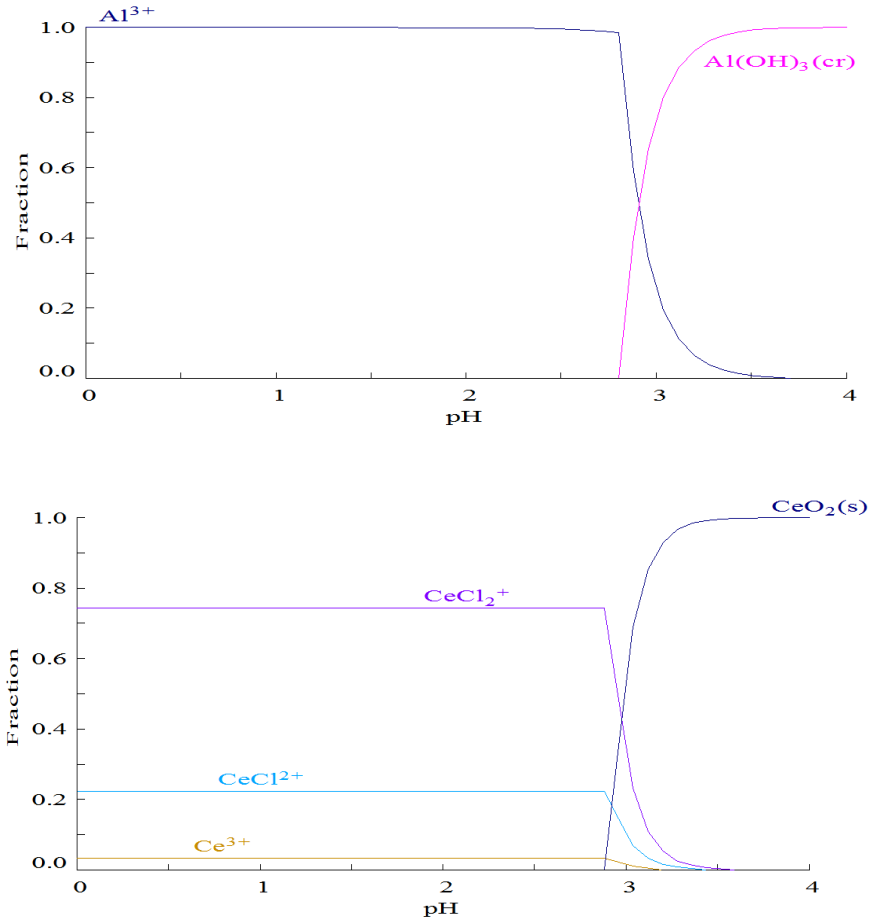


Figure 5.8: Speciation diagrams for Ce and Al ([Cl-] = 3.37 M, [Ce] = 0.067 mM, [Al] = 500 mM, Eh = 1.078 V, Temperature = 25 ºC) ; drawn using Medusa Hydra software

The speciation diagrams suggest that under the prevailing conditions, Ce and Al exist as the cation complexes $CeCl_2^{+}$, $CeCl^{2+}$, $Ce^{3+}$ and $Al^{3+}$. Alamine 308 is an anionic exchange amine and therefore the very low extractability of the Ce and Al cationic species was to be expected as there would be repulsion between the cationic species and positively charged protonated amine complex. This accounts for the very low extraction percentages into the organic phase for Al and Ce complexes.

## 5.5 Selective stripping of the organic phase

Stripping of both Pt and Pd out of the organic solution was outside the scope of this investigation and was therefore not conducted. However, Nguyen et al., (2016a) presented a selective stripping

route for the two PGMs, which entailed using a solution of 0.5 M HCl with 0.01 M Thiourea and 1 M thiourea for selective stripping of the Pt and Pd complexes respectively. Differences in charge density are again responsible for the use of different concentrations of thiourea for the two ions. The charge density for the Pd chloro complex ion is greater than that of the Pt chloro complex ion. As such, the Pd chloro complex has a higher affinity for the aqueous phase, and consequently requires a single stage 0.5 M HCl + 0.01 M thiourea contact to extract it into the aqueous phase. According to Nguyen et al., (2016a) the $PtCl_6^{2-}$ ion requires a two stage extraction into the organic phase using a higher concentration (1 M) of thiourea. In both instances, the 0.5 M HCl was to re-complex the Pd and Pt out of the organometallic complex ($R_3NH^+B^-_{(org)}$) back into their aqueous solution ions.

## 5.6 Recovery of PGMs from purified aqueous solution

Pt and Pd, after purification out of solution, may then be precipitated using saturated $NH_4Cl$ in $H_2O_2$ + HCl (for ORP and pH modification) to form $(NH_4)_2PtCl_6$ and $(NH_4)_2PdCl_2$. Given its anticipated low concentration, Rh could be scrubbed out of solution using solvent extraction or molecular recognition technology.

Tri octyl phosphine oxide was used by Mahmoud to extract approximately 95% Rh (III) out of a 2M HCl solution, after addition of $AlCl_3$ to the solution. In the leaching solution developed in this study, $AlCl_3$ is already present since it was used a leaching reagent.

SuperLig 190 has also been used successfully to recover Rh at the Tanaka Kikinzoku Kogyo KK auto catalyst recycling operation in Japan (Izatt, 2016). After purification of the Rh stream, the metal may then be recovered by cementation or precipitation as Klaus salt, prior to ignition to obtain Rh black.

## 5.7 Characterisation of leach solution after recovery of PGMs

It was an objective of this investigation to identify the potential for recovering other values from the solution to improve process economics. As such, the composition of the raffinate from the PGM solvent extraction step was obtained and is presented in table 5.4 below:

Table 5.4: Raffinate chemical composition

| **Element** | **Al** (g/L) | **Rh** | **Pd** | **Ir** | **Pt** | **Au** | **Ce** | **Ca** | **Co** | **Cu** | **Fe** |
|---|---|---|---|---|---|---|---|---|---|---|---|
| Conc (ppm) | 13.63 | 2.40 | 0.67 | - | 0.69 | - | 66.83 | 10.65 | 13.18 | 23.18 | 2.81 |
| | | | | | | | | | | | |
| **Element** | **Mg** | **Mn** | **Ni** | **V** | **Zn** | **Zr** | **La** | **Nd** | **Mg** | **Mn** | **Ni** |
| Conc (ppm) | 140.75 | 500.3 | 15.50 | 4.21 | 41.80 | 0.06 | 232.25 | 232.50 | 140.75 | 500.25 | 15.5 |

The solution had a pH of approximately -0.02 and an Eh of 1.019 V vs. the Ag/AgCl electrode at a temperature of 16.2 $^{o}$C.

### 5.7.1 Co-Metal extraction

There is a significant amount of Al in the raffinate, which may be recovered by precipitation and calcining to obtain alumina for resale to autocatalytic coaters. Rampou et al., (2017) investigated a method to recover alumina from a CFA leach liquor containing 10.1 g/L $Al^{3+}$, which involved sulphate crystallisation followed by calcining. The CFA liquor in that investigation contained the sulphate ion. However, for this work, leaching was conducted in chloride media. It could however still be worthwhile to investigate whether sulphate precipitation could be used to recover $Al^{3+}$ out of this chloride leach solution. The ionic equation for the same as was presented by the authors is given below.

$$Al^{3+} + NH_4^+ + 2SO_4^{2-} + 12H_2O \rightarrow (NH_4)Al(SO_4)_2 \cdot 12H_2O \quad \text{Equation } \mathbf{55}$$

The inherent disadvantage would be the introduction of another pollutant (the sulphate ion), which will still need to be processed downstream. The product formed can then be calcined according to equation 56 below to obtain Alumina.

$$2(NH_4)Al(SO_4)_2 \cdot 12H_2O \rightarrow Al_2O_3 + 2NH_3 + 4SO_3 + 25H_2O \quad \text{Equation } \mathbf{56}$$

By stoichiometry, 1.8 g of Alumina can be obtained for every gram of $A^{3+}$ in solution, which could actually have some commercial value to it.

Shen and Dempsey, (1998) also devised a process scheme to recover Al as Poly Aluminium Chloride (PAC). PAC is a coagulant for waste water treatment, and was synthesised by slow

addition of NaOH base at very high agitation rates. Both the synthesis of PAC and alumina would need to be investigated and evaluated for their economic viability before any commitment could be made.

### 5.7.2 Effluent treatment

The leach solution is highly acidic and as such to avoid excess consumption of neutralising reagents before disposal, the leach solution would have to be combined with solutions from other unit operations e.g. solutions obtained after precipitation of Pt and Pd. Neutralisation using a cheap base like $Ca(OH)_2$ or CaO may then be employed soon after this flow equalisation step. The other metallic constituents are also removed by hydroxide co-precipitation to form a sludge which can be safely disposed of. It is worthwhile to note that during leaching, some chlorine is generated. This chlorine may be scrubbed into a $Ca(OH)_2$ slurry. The solid residue obtained after filtering the solution from $Ca(OCl)_2$ dissolution is rich in $Ca(OH)_2$ and could therefore be used for this purpose. The remaining chloride in solution may be removed by ion exchange, before safe disposal or recycling of the process water, thereby presenting a truly environmentally and economically sustainable process for green PGM recycling.

## 5.8 Summary

PGM leaching efficiency was successfully increased from 78%, 86% and 15% to 99%, 99% and 68% for Pt, Pd and Rh respectively, by using insights obtained from prior experiments. Temperature was increased to 100 $^oC$ and optimum leaching was conducted at 0.15 M HOCl and 1.2 M $AlCl_3$. A commercially viable S/L ratio of 0.3 g/ml was selected for the operation. Furthermore, Pt and Pd were successfully extracted into the organic phase using Alamine 308, albeit with significant co-extraction of Fe into the organic solution. It was therefore recommended to remove Fe prior to solvent extraction. In order to treat the highly acidic and oxidising effluent, the inclusion of a flow equalisation tank prior to the effluent treatment plant was suggested. Lastly, effluent could be treated with neutralisation followed by dewatering to remove the sludge. Chloride content may be reduced by simple ion exchange.

# Chapter 6: Process flow sheet development

## 6.1 Introduction

The results from all tests conducted were used to develop a flow sheet and perform mass balances across the subsequent steps along the PGM recovery chain. The mass balances were used to evaluate the commercial viability of the developed lab-based process by conducting a quantitative cost benefit analysis. These results are presented in the following sections of this chapter.

## 6.2 Process flow diagram with mass balances

The mass balances were conducted on used autocatalytic converter material assaying 196 ppm Pt, 3230 ppm Pd and 229 ppm Rh. The solvent extraction results from Nguyen et al, (2016a) were used for the mass balances relating to the stripping of Pt and Pd from Alamine 308 using HCl + thiourea.

The developed process attained overall efficiencies of 85%, 97% and 67% for the metals Pt, Pd and Rh respectively. The overall recovery for Pd is comparable to the industry recovery standards (which typically range between 95% and 97%). Pt and Rh however fall short of these typical recoveries due to the inefficient extraction of Pt into the organic solvent using Alamine 308 and the very low leaching efficiency of Rh using the lixiviant system which was investigated.

A preliminary cost benefit analysis was however, subsequently conducted and compared against the prevailing cost price of the PGMs.

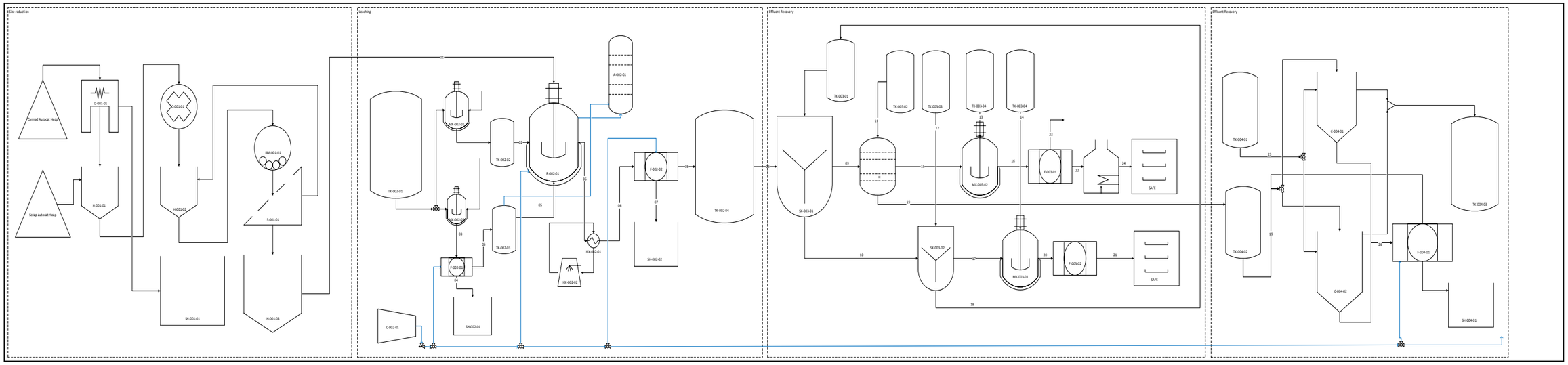


| | 1 | 2 | 3 | 4 | 5 | 6 | 7 | 8 | 9 | 10 | 11 | 12 | 13 | 14 | 15 | 16 | 17 | 18 | 19 | 20 | 21 | Pt/Pd off g | 22 | 23 | 24 | 25 | Rh Off G | effluent | solid residue |
|---|---|---|---|---|---|---|---|---|---|---|---|---|---|---|---|---|---|---|---|---|---|---|---|---|---|---|---|---|---|
| Mass flow rate/ (kg/hr) | 7.50 | 13.60 | 0.62 | 0.31 | 0.31 | 21.41 | 7.50 | 13.90 | 13.88 | 13.02 | 0.01 | 12.06 | 0.00 | 0.01 | 0.01 | 0.01 | 12.08 | 13.00 | 13.88 | 11.51 | 0.02 | 11.49 | 0.00 | 0.01 | 0.00 | 0.32 | 0.00 | 13.88 | 0.32 |
| *Volume flow rate/(L/hr)* | 0.00 | 10.50 | 0.31 | 0.00 | 0.31 | 10.81 | 0.00 | 10.81 | 10.81 | 16.21 | 0.01 | 11.35 | 0.00 | 0.00 | 0.01 | 0.01 | 11.35 | 16.21 | 10.81 | 0.00 | 0.00 | | 0.00 | 0.00 | 0.00 | 0.00 | 0.00 | 10.81 | 0.00 |
| Pt/(kg/hr) | 0.00147 | 0.00000 | 0.00000 | 0.00000 | 0.00000 | 0.00147 | 0.00001 | 0.00146 | 0.00019 | 0.00127 | 0.00000 | 0.00000 | 0.00000 | 0.00000 | 0.00000 | 0.00000 | 0.00125 | 0.00001 | 0.00019 | 0.00125 | 0.00125 | | 0.00000 | 0.00000 | 0.00000 | 0.00000 | 0.00000 | 0.00019 | 0.00000 |
| Pd(kg/hr) | 0.02423 | 0.00000 | 0.00000 | 0.00000 | 0.00000 | 0.02423 | 0.00024 | 0.02398 | 0.00024 | 0.02374 | 0.00000 | 0.00000 | 0.00000 | 0.00000 | 0.00000 | 0.00000 | 0.02351 | 0.00024 | 0.00024 | 0.02351 | 0.02351 | | 0.00000 | 0.00000 | 0.00000 | 0.00000 | 0.00000 | 0.00024 | 0.00000 |
| Rh/(kg/hr) | 0.00172 | 0.00000 | 0.00000 | 0.00000 | 0.00000 | 0.00172 | 0.00055 | 0.00117 | 0.00117 | 0.00000 | 0.00000 | 0.00000 | 0.00000 | 0.00000 | 0.00116 | 0.00116 | 0.00000 | 0.00000 | 0.00001 | 0.00000 | 0.00000 | | 0.00116 | 0.00000 | 0.00116 | 0.00000 | 0.00000 | 0.00001 | 0.00000 |
| Inert Solids/ (kg/hr) | 7.47259 | 0.03103 | 0.00000 | 0.00000 | 0.00000 | 7.50362 | 7.50362 | 0.00000 | 0.00000 | 0.00000 | 0.00000 | 0.00000 | 0.00000 | 0.00000 | 0.00000 | 0.00000 | 0.00000 | 0.00000 | 0.00000 | 0.00000 | 0.00000 | | 0.00000 | 0.00000 | 0.00000 | 0.00000 | 0.00000 | 0.00000 | 0.00000 |
| Water/ (kg/hr) | 0.00 | 10.50 | 0.08 | 0.00 | 0.08 | 10.58 | 0.00 | 10.58 | 10.58 | 0.00 | 0.00 | 10.88 | 0.00 | 0.00 | 0.00 | 0.00 | 10.88 | 0.00 | 10.58 | 10.88 | 0.00 | 10.88 | 0.00 | 0.00 | 0.00 | 0.00 | 0.00 | 10.58 | 0.00 |
| 99% $AlCl_3{\cdot}6H_2O$/ (kg/hr) | 0.00 | 3.07 | 0.00 | 0.00 | 0.00 | 3.07 | 0.00 | 3.07 | 3.07 | 0.00 | 0.00 | 0.00 | 0.00 | 0.00 | 0.00 | 0.00 | 0.00 | 0.00 | 3.07 | 0.00 | 0.00 | | 0.00 | 0.00 | 0.00 | 0.00 | 0.00 | 3.07 | 0.00 |
| $Ca(OCl)_2$/kg | 0.00 | 0.00 | 0.46 | 0.00 | 0.00 | 0.00 | 0.00 | 0.00 | 0.00 | 0.00 | 0.00 | 0.00 | 0.00 | 0.00 | 0.00 | 0.00 | 0.00 | 0.00 | 0.00 | 0.00 | 0.00 | | 0.00 | 0.00 | 0.00 | 0.00 | 0.00 | 0.00 | 0.00 |
| HOCl | 0.00 | 0.00 | 0.23 | 0.00 | 0.23 | 0.23 | 0.00 | 0.23 | 0.23 | 0.00 | 0.00 | 0.00 | 0.00 | 0.00 | 0.00 | 0.00 | 0.00 | 0.00 | 0.00 | 0.23 | 0.00 | | 0.00 | 0.00 | 0.00 | 0.00 | 0.00 | 0.23 | 0.00 |
| inerts | 0.00 | 0.00 | 0.15 | 0.15 | 0.00 | 0.00 | 0.00 | 0.00 | 0.00 | 0.00 | 0.00 | 0.00 | 0.00 | 0.00 | 0.00 | 0.00 | 0.00 | 0.00 | 0.00 | 0.00 | 0.00 | | 0.00 | 0.00 | 0.00 | 0.00 | 0.00 | 0.00 | 0.00 |
| $Ca(OH)_2$/Kg | 0.00 | 0.00 | 0.16 | 0.16 | 0.00 | 0.00 | 0.00 | 0.00 | 0.00 | 0.00 | 0.00 | 0.00 | 0.00 | 0.00 | 0.00 | 0.00 | 0.00 | 0.00 | 0.00 | 0.00 | 0.00 | | 0.00 | 0.00 | 0.00 | 0.00 | 0.00 | 0.00 | 0.00 |
| 37 %HCl/kg | 0.00 | 0.00 | 0.00 | 0.00 | 0.00 | 0.00 | 0.00 | 0.00 | 0.00 | 0.00 | 0.01 | 0.56 | 0.00 | 0.00 | 0.00 | 0.00 | 0.56 | 0.00 | 0.00 | 0.56 | 0.00 | 0.56 | 0.00 | 0.00 | 0.00 | 0.00 | 0.00 | 0.00 | 0.00 |
| *37 %HCl/L* | 0.00 | 0.00 | 0.00 | 0.00 | 0.00 | 0.00 | 0.00 | 0.00 | 0.00 | 0.00 | 0.00 | 0.47 | 0.00 | 0.00 | 0.00 | 0.00 | 0.47 | 0.00 | 0.00 | 0.47 | 0.00 | | 0.00 | 0.00 | 0.00 | 0.00 | 0.00 | 0.00 | 0.00 |
| $NH_4Cl$/kg | 0.00 | 0.00 | 0.00 | 0.00 | 0.00 | 0.00 | 0.00 | 0.00 | 0.00 | 0.00 | 0.00 | 0.00 | 0.00 | 0.01 | 0.00 | 0.00 | 0.00 | 0.00 | 0.00 | 0.00 | 0.00 | | 0.00 | 0.00 | 0.00 | 0.00 | 0.00 | 0.00 | 0.00 |
| $Pt(NH_4)_2Cl_6$ | 0.00 | 0.00 | 0.00 | 0.00 | 0.00 | 0.00 | 0.00 | 0.00 | 0.00 | 0.00 | 0.00 | 0.00 | 0.00 | 0.00 | 0.00 | 0.00 | 0.00 | 0.00 | 0.00 | 0.00 | 0.00 | | 0.00 | 0.00 | 0.00 | 0.00 | 0.00 | 0.00 | 0.00 |
| $Pd(NH_4)_2Cl_4$ | 0.00 | 0.00 | 0.00 | 0.00 | 0.00 | 0.00 | 0.00 | 0.00 | 0.00 | 0.00 | 0.00 | 0.00 | 0.00 | 0.00 | 0.00 | 0.00 | 0.00 | 0.00 | 0.00 | 0.06 | 0.00 | | 0.00 | 0.00 | 0.00 | 0.00 | 0.00 | 0.00 | 0.00 |
| $(NH_4)_3RhCl_6$ | 0.00 | 0.00 | 0.00 | 0.00 | 0.00 | 0.00 | 0.00 | 0.00 | 0.00 | 0.00 | 0.00 | 0.00 | 0.00 | 0.00 | 0.00 | 0.00 | 0.00 | 0.00 | 0.00 | 0.00 | 0.00 | | 0.00 | 0.00 | 0.00 | 0.00 | 0.00 | 0.00 | 0.00 |
| CaO/Kg | 0.00 | 0.00 | 0.00 | 0.00 | 0.00 | 0.00 | 0.00 | 0.00 | 0.00 | 0.00 | 0.00 | 0.00 | 0.00 | 0.00 | 0.00 | 0.00 | 0.00 | 0.00 | 0.00 | 0.00 | 0.00 | | 0.00 | 0.00 | 0.00 | 0.32 | 0.00 | 0.00 | 0.32 |
| $Cl^-$ | 0.00 | 0.00 | 0.00 | 0.00 | 0.00 | 0.00 | 0.00 | 0.00 | 0.00 | 0.00 | 0.00 | 0.00 | 0.00 | 0.00 | | 0.00 | 0.00 | 0.00 | 0.00 | 0.01 | 0.00 | 0.01 | 0.00 | 0.00 | 0.00 | 0.00 | 0.00 | 0.00 | 0.00 |
| $RhCl_6^{3-}$ | 0.00 | 0.00 | 0.00 | 0.00 | 0.00 | 0.00 | 0.00 | 0.00 | 0.00 | 0.00 | 0.00 | 0.00 | 0.00 | 0.00 | 0.00 | 0.00 | 0.00 | 0.00 | 0.00 | 0.00 | 0.00 | | 0.00 | 0.00 | 0.00 | 0.00 | 0.00 | 0.00 | 0.00 |
| $NH_3$ + HCl (g) | 0.00 | 0.00 | 0.00 | 0.00 | 0.00 | 0.00 | 0.00 | 0.00 | 0.00 | 0.00 | 0.00 | 0.00 | 0.00 | 0.00 | 0.00 | 0.00 | 0.00 | 0.00 | 0.00 | 0.00 | 0.00 | 0.04 | 0.00 | 0.00 | 0.00 | 0.00 | 0.00 | 0.00 | 0.00 |
| $H^+$ | 0.00 | 0.00 | 0.00 | 0.00 | 0.00 | 0.00 | 0.00 | 0.00 | 0.00 | 0.00 | 0.00 | 0.00 | 0.00 | 0.00 | 0.00 | 0.00 | 0.00 | 0.00 | 0.00 | 0.00 | 0.00 | | 0.00 | 0.00 | 0.00 | 0.00 | 0.00 | 0.00 | 0.00 |
| Alamine 308 / Kg | 0.00 | 0.00 | 0.00 | 0.00 | 0.00 | 0.00 | 0.00 | 0.00 | 0.00 | 0.55 | 0.00 | 0.00 | 0.00 | 0.00 | 0.00 | 0.00 | 0.00 | 0.00 | 0.00 | 0.00 | 0.00 | | 0.00 | 0.00 | 0.00 | 0.00 | 0.00 | 0.00 | 0.00 |
| Alamine 308 / L | 0.00 | 0.00 | 0.00 | 0.00 | 0.00 | 0.00 | 0.00 | 0.00 | 0.00 | 0.67 | 0.00 | 0.00 | 0.00 | 0.00 | 0.00 | 0.00 | 0.00 | 0.67 | 0.00 | 0.00 | 0.00 | | 0.00 | 0.00 | 0.00 | 0.00 | 0.00 | 0.00 | 0.00 |
| Kerosene / Kg | 0.00 | 0.00 | 0.00 | 0.00 | 0.00 | 0.00 | 0.00 | 0.00 | 0.00 | 11.81 | 0.00 | 0.00 | 0.00 | 0.00 | 0.00 | 0.00 | 0.00 | 11.81 | 0.00 | 0.00 | 0.00 | | 0.00 | 0.00 | 0.00 | 0.00 | 0.00 | 0.00 | 0.00 |
| Kerosene / L | 0.00 | 0.00 | 0.00 | 0.00 | 0.00 | 0.00 | 0.00 | 0.00 | 0.00 | 14.77 | 0.00 | 0.00 | 0.00 | 0.00 | 0.00 | 0.00 | 0.00 | 14.77 | 0.00 | 0.00 | 0.00 | | 0.00 | 0.00 | 0.00 | 0.00 | 0.00 | 0.00 | 0.00 |
| Decanol / Kg | 0.00 | 0.00 | 0.00 | 0.00 | 0.00 | 0.00 | 0.00 | 0.00 | 0.00 | 0.64 | 0.00 | 0.00 | 0.00 | 0.00 | 0.00 | 0.00 | 0.00 | 0.64 | 0.00 | 0.00 | 0.00 | | 0.00 | 0.00 | 0.00 | 0.00 | 0.00 | 0.00 | 0.00 |
| Decanol / L | 0.00 | 0.00 | 0.00 | 0.00 | 0.00 | 0.00 | 0.00 | 0.00 | 0.00 | 0.77 | 0.00 | 0.00 | 0.00 | 0.00 | 0.00 | 0.00 | 0.00 | 0.77 | 0.00 | 0.00 | 0.00 | | 0.00 | 0.00 | 0.00 | 0.00 | 0.00 | 0.00 | 0.00 |
| Thiourea / Kg | 0.00 | 0.00 | 0.00 | 0.00 | 0.00 | 0.00 | 0.00 | 0.00 | 0.00 | 0.00 | 0.00 | 0.62 | 0.00 | 0.00 | 0.00 | 0.00 | 0.62 | 0.00 | 0.00 | 0.00 | 0.00 | | 0.00 | 0.00 | 0.00 | 0.00 | 0.00 | 0.00 | 0.00 |

Figure 6.1: Process flow sheet and mass balances

## 6.3 Equipment List

Table 6.1: List of Equipment

| **Size Reduction Section (001)** | Equipment Type | Material of Construction |
|---|---|---|
| D-001-01 | Autocat Decanner | Carbon Steel |
| H-001-01 | Hopper | Carbon Steel |
| H-001-02 | Hopper | Carbon Steel |
| H-001-03 | Hopper | Carbon Steel |
| C-001-01 | Crusher | Carbon Steel |
| BM-001-01 | Ball Mill | Carbon Steel |
| S-001-01 | Screen | Carbon Steel |
| SH-001-01 | Solids Holder | Carbon Steel |
| **Leaching Section (001)** | | |
| TK-002-01 | Tank | Glass / titanium lined steel tanks |
| TK-002-02 | Tank | Glass / titanium lined steel tanks |
| TK-002-03 | Tank | Glass / titanium lined steel tanks |
| TK-002-04 | Tank | Glass / titanium lined steel tanks |
| MX-002-01 | Mixer | Glass / titanium lined steel reactor |
| MX-002-02 | Mixer | Glass / titanium lined steel reactor |
| R-002-01 | Reactor | Glass / titanium lined steel reactor |
| F-002-01 | Filter Press | Poly Propylene Plates, Carbon steel Frame |
| F-002-02 | Filter Press | Poly Propylene Plates, Carbon steel Frame |
| SH-002-01 | Solids Holder | Carbon Steel |
| C-002-01 | Compressor | - |
| A-002-01 | Absorber | Glass lined Steel frame |
| **PGM Recovery (003)** | | |
| SX-003-01 | SX Plant | Steel Frame, Glass lined / PP Mixer - Settlers |
| IX Plant | IX Plant | Polypropylene |
| TK-003-01 | Tank | Glass / titanium lined steel tanks |
| TK-003-02 | Tank | Glass / titanium lined steel tanks |
| TK-003-03 | Tank | Glass / titanium lined steel tanks |
| TK-003-04 | Tank | Glass / titanium lined steel tanks |
| TK-003-05 | Tank | Glass / titanium lined steel tanks |
| MX-003-01 | Reactor | Glass / titanium lined steel reactor |
| MX-003-02 | Reactor | Glass / titanium lined steel reactor |

| | | |
|---|---|---|
| MX-003-03 | Reactor | Glass / titanium lined steel reactor |
| F-003-01 | Filter Press | Poly Propylene Plates, Carbon steel Frame |
| F-003-02 | Filter Press | Poly Propylene Plates, Carbon steel Frame |
| F-003-03 | Filter Press | Poly Propylene Plates, Carbon steel Frame |
| **Effluent Treatment (004)** | | |
| TK-004-01 | Tank | Glass / titanium lined steel tanks |
| TK-004-02 | Tank | Glass / titanium lined steel tanks |
| TK-004-03 | Tank | Glass / titanium lined steel tanks |
| C-004-01 | Clarifier | Concrete |
| C-004-02 | Clarifier | Concrete |
| F-004-01 | Filter press | Poly Propylene Plates, Carbon steel Frame |

### 6.4 OPEX Estimations

The costs represented in the OPEX approximations were based on quotations obtained from bulk chemical suppliers within South Africa. All chemicals can be locally sourced from suppliers domiciled in the country. Some key assumptions that were also made are presented below:

1. A small scale operation producing 25000 oz. of PGM per year from a feedstock of 3655 ppm 3E assaying, 6 %, 88 % and 6 % Pt, Pd and Rh, with an installed production capacity of 193 tons / year in used autocats.
2. The ZAR/USD rate used for all calculations was 14.52 (as at 28 September 2018).
3. It was assumed that 5% by mass of the solvent extracting solution is added to the recycled organic stream to make up for material losses during every organic recycle.
4. It was assumed Rh could be recovered to near 100% using Superlig 190, a Rh specific extractant which has been successfully used at Tanaka Kikinzoku Precious Metal Refiners in Japan (Izatt, 2016). Stripping efficiencies for Pt and Pd were obtained from work done by (T. H. Nguyen et al., 2016a).
5. Prices for chemicals were obtained from South African Based Suppliers; Refer to Appendix B1 for screenshots and quotations from chemical suppliers
6. Cost of Kerosene for Alamine 308 was obtained from www.fuelretailers.co.za, quoted as the inland cost for kerosene

7. Cost of autocats acquisitions was pegged at 70 % of the total PGM content on the basis of prevailing Autocat Sales in the Industry (refer to Appendix C for screenshot of an industrial study carried out in 2004).
8. Selling Percentage was pegged at 95 % of total PGM content informed by one of the industry partners who were consulted during the research
9. Human Resource cost complement was assumed at 15 operators, 2 Management workers (company Head and Operations/Production Head) and 4 Administrative workers (responsible for raw material supply chain, human resources and accounting, QSHE management and research and development)
10. A 3 shift system with 5 workers per shift was assumed
11. Rentals were assumed based on data to rent a warehouse according to local prevailing rates in Johannesburg
12. In the absence of available data for solid and effluent disposal, engineering and maintenance costs and security costs, these were assumed at the student's best discretion.
13. The costs of decanning, crushing and cleaning were calculated at 5 % of the total purchase cost of converters, based on studies conducted on the pyrometallurgical recycling industry (see Appendix C, figure C.1)
14. Prices of PGMs used for cost benefit analysis are presented below, averaged for September from Johnson Matthey's pricing data for the same month.

| | | |
|---|---|---|
| Price Pt/oz. | $ | 799.50 |
| Price Pd/oz. | $ | 993.39 |
| Price Rh/oz. | $ | 2,415.60 |

Table 6.2: Income statement for the process developed

| | |
|---|---|
| **Sales** | |
| Pt | 13,075,754.97 |
| Pd | 267,740,789.92 |
| Rh | 32,025,156.52 |
| **Total Sales** | **312,841,701.41** |
| | |
| **Less Cost of Sales** | |
| Autocats acquisition | 248,303,937.96 |
| Decanning, Cleaning, Crushing | 12,516,133.46 |
| 99% AlCl3·6H2O/kg | 358,264.29 |
| Ca(OCl)2/kg | 254,193.76 |
| 37 %HCl/kg | 45,405.51 |
| Alamine 308/kg | 161,911.49 |
| Kerosene/l | 15,272.23 |
| Decanol/l | 24,943.99 |
| Thiourea/kg | 465,503.20 |
| NH4Cl/Kg | 2,278.26 |
| CaO/kg | 23,499.42 |
| Liquid waste disposal | 1,855,153.41 |
| Energy | 13,800.00 |
| Water | 18,812.23 |
| Labour | 5,160,000.00 |
| Security | 300,000.00 |
| Engineering Services | 240,000.00 |
| Rentals | 180,000.00 |
| **Less Total Expenses** | 269,939,109.21 |
| | |
| EBITDA | 42,902,592.20 |
| Less Tax 28% | 12,012,725.82 |
| EBIDA | 30,889,866.39 |

### 6.4.1 Discussion

The developed process has an EBIDA margin of 9.9 % which is quite comparable to pyrometallurgical based EBIDA margins, which are typically about 6.1 % (see appendix C, Figure C.1). The greatest cost components come from cost of catalytic converter acquisition, the human resource complement and cost of de-canning, crushing and cleaning. Optimising these cost

components would definitely be expected to improve the process economics. Detailed CAPEX estimations were beyond the scope of the research and have been presented as a recommendation in the following chapters.

Clearly, circumventing the pyrometallurgy step is expected to boost the process economics for the process. A 3 % higher margin increase per oz. is sufficient evidence to further the development through detailed costing (CAPEX and OPEX – by getting more updated quotations and more accurate estimations for the values that were estimated by the student).

This high level, stage 1 cost benefit analysis revealed that a purely hydrometallurgical process hosts a lot of potential when compared to a pyro metallurgical operation. The process, as it is in its current state, has an EBIDA margin of approximately 9% / oz. (3E) compared to the typical 6.1% / oz. (3E) for pyro metallurgical processes. It was therefore illustrated that the process can offer better financial prospects compared to existing pyro metallurgical operations. Moreover, a small 25 000 oz. (3E) / year operation with an installed capacity of just below 200 tons / year, used catalytic converters has got far more benefits outside of the financial incentives. It has the potential to increase foreign currency earnings, create jobs (skilled and unskilled, direct and indirect) and reduce the environmental damage associated with PGM supply. The benefits of PGM recycling using this purely hydrometallurgical process could far outweigh the costs associated with establishing the operation.

# Chapter 7 : Conclusions and recommendations

## 7.1 Introduction

Demand for the three PGMs has been progressively increasing over the past decade, primarily driven by the catalytic converter manufacturing industry. Consequently, the contribution of recycling to supply dynamics has also increased progressively. Pyrometallurgical flow-sheets, however, dominate the recycling industry despite the energy savings to be gained from exclusively hydrometallurgical flow-sheets. It was therefore the object of the study to develop a process for leaching PGMs from catalytic converters without resorting to a smelting step. It was also the intention of the study to identify the feasibility of recovering the PGMs from the leach solution using any one of the cost effective processes available in literature. The process developed was to be investigated for its commercial viability and the practicality of extracting and recovering other metals from the leach solution further evaluated.

PGMs where successfully leached into a solution of $AlCl_3$ and $Ca(OCl)_2$ at elevated temperatures, of approximately 95 $^oC$ to 100 $^oC$, attaining near complete PGM leaching for Pt and Pd, and a maximum of 68% for Rh leaching. It was illustrated that by keeping losses of chlorine to a minimum and reducing the concentration of $Ca(OCl)_2$, the leaching of the three PGMs could be improved from the initial 78%, 86% and 15% for Pt, Pd and Rh maxima which had been obtained in the earlier experiments. As expected, PGM leaching was very sensitive to Eh and pH variation in the solution. Temperature and S: L ratio also had a significant effect on leaching efficiencies for all three PGMs in agreement with earlier works and expectations based on scientific theory.

Pt and Pd were also loaded onto Alamine 308 dissolved in kerosene, to prove the potential of using solvent extraction for Pt and Pd co-extraction. Pt and Pd were co-extracted into the organic phase with efficiencies of 87% and 99.6% respectively. The two metals can be selectively stripped from the PGM loaded organic solution using thiourea and HCl; however this was beyond the scope of this investigation and has already been investigated elsewhere (T. H. Nguyen et al., 2016a). Using the leaching and solvent extraction results obtained from this study and those of (T. H. Nguyen et al., 2016a) for stripping, a flow sheet was developed which can attain recoveries for

Pt, Pd and Rh of 93%, 97% and 64% with a margin for excess of sales over cost of sales equal to 9.9% / oz. 3% higher than existing pyro metallurgical recycling operations. The process thus developed has a favourable return based on OPEX considerations alone. Given the high concentration of Al in solution, it was suggested that Al may be recovered as a by – product either as $Al_2O_3$, which can be sold off to converter manufacturers or as a coagulant. However, the concentrations for Ce and Zr in solution were not determined to be sufficiently high to warrant recovery out of solution. The solution which was obtained was characterised and it contained leached out base metals, was highly acidic and oxidising. Al was the highest in concentration at around 13.75 g/L. It was determined that this solution may be treated using hydroxide precipitation with a cheap base like CaO. The excess chloride ions could also be removed by chloride ion exchange. Experiments to verify these effluent treatment options were also beyond the scope of this investigation and thus were not carried out.

## 7.2 Recommendations

Based on thermodynamic considerations, it was proposed that Pt and Pd probably go through a single step leaching process where PGMs are solubilized directly into their corresponding chloro complexes. It was, however, hypothesised that Rh should probably go through a two-stage process, becoming oxidised first, followed by the slow reaction of the passive oxide layer with the chloride ions. Both hypotheses were not tested experimentally, and therefore it is recommended that further work be conducted to fully investigate the Rh leaching mechanism, with the ultimate goal of increasing the Rh leaching efficiency from the 68% obtained in this study. With this investigation, it is also recommended that a kinetic study be conducted so that the kinetics of dissolution are thoroughly understood for the purposes of process design as well.

It is also recommended that other extraction options for PGMs out of solution should also be investigated. Ion exchange or molecular recognition technology may have to be investigated and compared against solvent extraction using Alamine 308. These two extraction options have been used in other successful industrial installations and have numerous conceptual advantages over solvent extraction such as increased safety of personnel, increased stability, faster extraction, more efficient extraction schemes, lower CAPEX and OPEX and smaller space requirements. These advantages could prove more beneficial for a purely hydrometallurgical installation.

The concentration of Al in the effluent solution was significantly high, which may warrant recovery. It is therefore recommended that the potential for recovering Al be explored and its cost benefit analysis carried out. Al may be recovered out of the effluent solution as poly aluminium chloride (PAC), a commercial coagulant, by slow addition of NaOH with rapid mixing (Shen and Dempsey, 1998); or crystallised out by addition of ammonium sulphate at slightly elevated temperatures of approximately 70 $^{o}$C (Rampou et al., 2017) followed by low temperature crystallisation. Both approaches have a potential of recovering some Al. The recovery of PAC has the added benefit of reducing the chloride concentration, which may have benefits downstream regarding effluent treatment. It also produces a coagulant that can be used to treat the solution. Furthermore, the remaining solution contains the light rare earths Ce, La and Nd; which, due to their similar characteristics, may be easily extracted out of solution and precipitated as carbonates, thereby providing an alternative revenue stream.

It was also recommended that the sold residue be adequately characterised with the intention of identifying potential uses for it, e.g. in new ceramic formulations or even for reintegration into new honeycomb substrates for catalytic converters. Moreover, any recycling business case demands a solid optimised scrap supply chain. A further recommendation is therefore, an investigation into the design of a proper supply chain infrastructure for the scrap catalytic converters.

Lastly, it is recommended that a water treatment solution be developed for treating the effluent water to meet environmental discharge limits. Given the illustrated economic potential for the process, it is further suggested that a pilot plant be developed to probe the applicability of the process for PGM recovery from recycling used autocatalytic converters. It is finally recommended that conclusions drawn from these recommendations and those of this work may then be employed for the development of a business case to identify the business merit of adopting this process on a commercial scale.

# Reference List


Adu-Peasah, S.P., Diosady, L.L., Rubin, L.J., 1993. A multistage hydrocyclone/stirred-tank system for countercurrent extraction of canola oil. J. Am. Oil Chem. Soc. 70, 755–762. https://doi.org/10.1007/BF02542596

Al-Harahsheh, M., Kingman, S.W., 2004. Microwave-assisted leaching—a review. Hydrometallurgy 73, 189–203. https://doi.org/10.1016/j.hydromet.2003.10.006

Alkan, M., Oktay, M., Kocakerim, M., Copur, M., 2005. Solubility of chlorine in aqueous hydrochloric acid solutions. J. Hazard. Mater. 119, 13–18. https://doi.org/10.1016/j.jhazmat.2004.11.001

Amankwah, R.K., Pickles, C.A., 2005. MICROWAVE CALCINATION AND SINTERING OF MANGANESE CARBONATE ORE. Can. Metall. Q. 44, 239–247. https://doi.org/10.1179/cmq.2005.44.2.239

Angelidis, T.N., 2001. Development of a laboratory scale hydrometallurgical procedure for the recovery of Pt and Rhfrom spent automotive catalysts. Top. Catal. 16, 419–423.

Arenas, L.F., Ponce de León, C., Walsh, F.C., 2016. Electrochemical redox processes involving soluble cerium species. Electrochimica Acta 205, 226–247. https://doi.org/10.1016/j.electacta.2016.04.062

BASF, 2015. BASF consolidating chemical catalysts recycling and refining operations to Seneca, South Carolina, production facility [WWW Document]. URL http://www.catalysts.basf.com/p02/USWeb-Internet/en_GB/content/microsites/catalysts/news/news226+ (accessed 5.5.17).

Bergeron, M., Richer-Lafléche, M., 2011. Process for recovering platinum group metals from ores and concentrates. US7972412 B2.

Bolinski, L., 1991. Platinum and rhodium recovery from scrapped automotive catalyst by oxidative acid chloride leaching. McGill University, Montreal, Canada.

Bond, G., 2000. Relativistic Phenomena in the Chemistry of the Platinum Group Metals: Effects on coordination and chemisorption in homogenous and heterogenous catalysis. Platin. Met. Rev. 44, 146–155.

Burnham, R.F., Gibbon, A., Harry, J.E., 1985. Plasma arc furnaces. US4521890 A.

Cao, Y., Harjanto, S., Shibayama, A., Naitoh, I., Nanami, T., Kasahara, K., Okumura, Y., Fujita, T., 2006. Kinetic Study on the Leaching of Pt, Pd and Rh from Automotive Catalyst Residue by Using Chloride Solutions. Mater. Trans. 47, 2015–2024.

Chemical Rubber Company, Lide, D.R. (Eds.), 2003. CRC handbook of chemistry and physics: a ready-reference book of chemical and physical data, 84th ed. ed. CRC Press, Boca Raton.

Chen, A., Wang, S., Zhang, L., Peng, J., 2015. Optimization of the microwave roasting extraction of palladium and rhodium from spent automobile catalysts using response surface analysis. Int. J. Miner. Process. 143, 18–24. https://doi.org/10.1016/j.minpro.2015.08.007

Chen, J., Huang, K., 2006. A new technique for extraction of platinum group metals by pressure cyanidation. Hydrometallurgy 82, 164–171. https://doi.org/10.1016/j.hydromet.2006.03.041

Chen, S., Shen, S., Cheng, Y., Wang, H., Lv, B., Wang, F., 2014. Effect of O2, H2 and CO pretreatments on leaching Rh from spent auto-catalysts with acidic sodium chlorate solution. Hydrometallurgy 144–145, 69–76. https://doi.org/10.1016/j.hydromet.2014.01.018

Cieszynska, A., Wiśniewski, M., 2012. Extractive recovery of palladium(II) from hydrochloric acid solutions with Cyphos®IL 104. Hydrometallurgy 113–114, 79–85. https://doi.org/10.1016/j.hydromet.2011.12.006

Cotton, S.A., 1997. Chemistry of precious metals, 1st ed. ed. Blackie Academic & Professional, London ; New York.

Crundwell, F.K., Moats, M.S., Ramachandran, V., Robinson, T.G., Davenport, W.G., 2011. Extractive metallurgy of nickel, cobalt and platinum-group materials. Elsevier, Amsterdam ; Boston.

Dewar, K., 2012. The catalytic converter industry in South Africa, in: 5th Internation Platinum Conference. Presented at the A catalyst for change, SAIMM, Sun City, Johannesburg.

Dick, W., 2016. What is Sibanye getting for R30 billion? [WWW Document]. Moneyweb. URL https://www.moneyweb.co.za/mineweb/mining-companies-investment/what-is-sibanye-getting-for-r30-billion-2/ (accessed 5.5.17).

Dudka, S., Adriano, D.C., 1997. Environmental Impacts of Metal Ore Mining and Processing: A Review. J. Environ. Qual. 26, 590. https://doi.org/10.2134/jeq1997.00472425002600030003x

Fornalczyk, A., Kraszewski, M., Willner, J., Kaduková, J., Mrážiková, A., Marcinčáková, R., Velgosová, O., 2016. Dissolution of Metal Supported Spent Auto Catalysts in Acids. Arch. Metall. Mater. 61. https://doi.org/10.1515/amm-2016-0043

Fornalczyk, A., Saternus, M., 2009. REMOVAL OF PLATINUM GROUP METALS FROM THE USED AUTO CATALYTIC CONVERTER. Matalurgija 48, 133–136.

Glisenti, A., Natile, M.M., Carlotto, S., Vittadini, A., 2014. Co- and Cu-Doped Titanates: Toward a New Generation of Catalytic Converters. Catal. Lett. 144, 1466–1471. https://doi.org/10.1007/s10562-014-1294-5

Hageluken, C., 2017. The EU Circular Economy Package - an opportunity to improve metals recycling, in: Production and Recycling of Non-Ferrous Metals: Saving Resources for a Sustainable Future. Presented at the European Metallurgical Conference 2017, GDMB, Leipzig, Germany.

Harjanto, S., Cao, Y., Shibayama, A., Naitoh, I., Nanami, T., Kasahara, K., Okumura, Y., Liu, K., Fujita, T., 2006. Leaching of Pt, Pd and Rh from Automotive Catalyst Residue in Various Chloride Based Solutions. Mater. Trans. 47, 129–135.

Hartley, F.R. (Ed.), 1991. Chemistry of the platinum group metals: recent developments, Studies in inorganic chemistry. Elsevier, Amsterdam ; New York.

Hasab, M.G., Rashchi, F., Raygan, S., 2013. Simultaneous sulfide oxidation and gold leaching of a refractory gold concentrate by chloride–hypochlorite solution. Miner. Eng. 50–51, 140–142. https://doi.org/10.1016/j.mineng.2012.08.011

Hasani, M., Khodadadi, A., Koleini, S.M.J., Saeedi, A.H., Meléndez, A.M., 2017. Simultaneous leaching of Pt, Pd and Rh from automotive catalytic converters in chloride-containing solutions. J. Phys. Conf. Ser. 786, 012042. https://doi.org/10.1088/1742-6596/786/1/012042

Hilson, G., 2000. Pollution prevention and cleaner production in the mining industry: an analysis of current issues. J. Clean. Prod. 8, 119–126. https://doi.org/10.1016/S0959-6526(99)00320-0

Houdry, E.J., 1956. Catalytic structure and composition. US2742437 A.

Izatt, R.M. (Ed.), 2016. Metal sustainability: global challenges, consequences, and prospects. Wiley, Chichester, West Sussex.

Jha, M.K., Lee, J., Kim, M., Jeong, J., Kim, B.-S., Kumar, V., 2013. Hydrometallurgical recovery/recycling of platinum by the leaching of spent catalysts: A review. Hydrometallurgy 133, 23–32. https://doi.org/10.1016/j.hydromet.2012.11.012

Jimenez de Aberasturi, D., Pinedo, R., Ruiz de Larramendi, I., Ruiz de Larramendi, J.I., Rojo, T., 2011. Recovery by hydrometallurgical extraction of the platinum-group metals from car catalytic converters. Miner. Eng. 24, 505–513. https://doi.org/10.1016/j.mineng.2010.12.009

Johnson Matthey, 2016. Price charts. Johns. Matthey Precious Met. Manag.

Johnsson Matthey, 2017. Johnson Matthey Refining [WWW Document]. URL http://www.jmrefining.com/autocat (accessed 5.5.17).

Kasuya, R., Miki, T., Morikawa, H., Tai, Y., 2016. Dissolution of platinum in catalyst materials using hydrochloric acid: A new method based on the use of complex oxides. Miner. Eng. 87, 25–31. https://doi.org/10.1016/j.mineng.2015.10.005

Kasuya, R., Miki, T., Morikawa, H., Tai, Y., 2015. Enhanced dissolution of alkali metal platinates in dilute hydrochloric acid by addition of calcium chloride. Miner. Eng. 76, 135–140. https://doi.org/10.1016/j.mineng.2014.10.011

Kasuya, R., Miki, T., Morikawa, H., Tai, Y., 2014. Synthesis of sodium platinates and their dissolution behaviors in hydrochloric acid: Effects of lithium carbonate addition on platinate formation. Int. J. Miner. Process. 128, 33–39. https://doi.org/10.1016/j.minpro.2014.02.005

Kasuya, R., Miki, T., Morikawa, H., Tai, Y., 2013a. Synthesis of alkali metal platinates and their dissolution behavior in hydrochloric acid. J. Ceram. Soc. Jpn. 121, 884–890. https://doi.org/10.2109/jcersj2.121.884

Kasuya, R., Miki, T., Tai, Y., 2013b. Preparation of Li2PtO3 and its dissolution properties in hydrochloric acid. J. Ceram. Soc. Jpn. 121, 261–264. https://doi.org/10.2109/jcersj2.121.261

Kerr, H.D., Kulle, T.J., McIlhany, M.L., Swidersky, P., 1979. Effects of nitrogen dioxide on pulmonary function in human subjects: An environmental chamber study. Environ. Res. 19, 392–404. https://doi.org/10.1016/0013-9351(79)90064-1

Kim, M., Lee, J., Park, S., Jeong, J., Kumar, V., 2013. Dissolution behaviour of platinum by electro-generated chlorine in hydrochloric acid solution: Dissolution of platinum by electro-generated chlorine in HCl solution. J. Chem. Technol. Biotechnol. 88, 1212–1219. https://doi.org/10.1002/jctb.3957

Kim, M., Park, S., Lee, J., Choubey, P.K., 2016. A novel zero emission concept for electrogenerated chlorine leaching and its application to extraction of platinum group metals from spent automotive catalyst. Hydrometallurgy 159, 19–27. https://doi.org/10.1016/j.hydromet.2015.10.030

Kuczynski, R.J., Atkinson, G.B., Dolinar, W.J., 1995. Recovery of platinum group metals from automobile catalysts - Pilot plant operation. Minerals, Metals & Materials Society, Warrendale, Pa.

Lee, M.-S., Lee, K.-J., Oh, Y.-J., 2004. Solvent Extraction Equilibria of FeCl<SUB>3</SUB> from Hydrochloric Acid Solution with Alamine336. Mater. Trans. 45, 2364–2368. https://doi.org/10.2320/matertrans.45.2364

Levenspiel, O., 1999. Chemical reaction engineering, 3rd ed. ed. Wiley, New York.

Lillkung, K., Aromaa, J., Forsen, O., 2013. Determination of leaching parameters for the recovery of platinum group metals from secondary materials. https://doi.org/10.5277/ppmp130208

Lister, M.W., 1952. THE DECOMPOSITION OF HYPOCHLOROUS ACID. Can. J. Chem. 30, 879–889. https://doi.org/10.1139/v52-107
Llopis, J., Vázquez, M., 1964. Passivation of rhodium in hydrochloric acid solutions. Electrochimica Acta 9, 1655–1663. https://doi.org/10.1016/0013-4686(64)80092-X
Mahmoud, M.H.H., 2003. Leaching platinum-group metals in a sulfuric acid/chloride solution. JOM 55, 37–40. https://doi.org/10.1007/s11837-003-0086-y
Majima, H., Awakura, Y., Tsugui, K., Peters, E., 1990. Fundamental studies on chlorine behavior as related to zinc electrowinning from aqueous chloride electrolytes. Metall. Trans. B 21, 251–258. https://doi.org/10.1007/BF02664192
McCarthy, J., Copeland, C., Parker, L., Schierow, L.-J., 2011. Clean Air Act: A Summary of the Act and Its Major Requirements (No. RL30853). Congressional research institution.
Meyer, S., 2007. Major differences along the supply chain between b2b and b2c marketing with. Grin Verlag Ohg, Place of publication not identified.
Moon, W.-J., Na, S.-O., Oh, H.-Y., 2014. METHOD FOR RECYCLING CERIUM OXIDE. US8894733.
Multimetco, 2017. About Us | Multimetco [WWW Document]. Us. URL http://www.multimetco.com/about_us.html (accessed 5.5.17).
NextGenCat Overview [WWW Document], n.d. URL http://www.nextgencat.eu/ (accessed 7.24.17).
Nguyen, T.H., Kumar, B.N., Lee, M.S., 2016a. Selective recovery of Fe(III), Pd(II), Pt(IV), Rh(III) and Ce(III) from simulated leach liquors of spent automobile catalyst by solvent extraction and cementation. Korean J. Chem. Eng. 33, 2684–2690. https://doi.org/10.1007/s11814-016-0123-5
Nguyen, T.H., Sonu, C.H., Lee, M.S., 2016b. Separation of Pt(IV), Pd(II), Rh(III) and Ir(IV) from concentrated hydrochloric acid solutions by solvent extraction. Hydrometallurgy 164, 71–77. https://doi.org/10.1016/j.hydromet.2016.05.014
Nguyen, V.T., Lee, J., Chagnes, A., Kim, M., Jeong, J., Cote, G., 2016. Highly selective separation of individual platinum group metals (Pd, Pt, Rh) from acidic chloride media using phosphonium-based ionic liquid in aromatic diluent. RSC Adv 6, 62717–62728. https://doi.org/10.1039/C6RA09328K
Nikoloski, A.N., Ang, K.-L., 2014. Review of the Application of Ion Exchange Resins for the Recovery of Platinum-Group Metals From Hydrochloric Acid Solutions. Miner. Process. Extr. Metall. Rev. 35, 369–389. https://doi.org/10.1080/08827508.2013.764875
Nogueira, C.A., Paiva, A.P., Oliveira, P.C., Costa, M.C., da Costa, A.M.R., 2014. Oxidative leaching process with cupric ion in hydrochloric acid media for recovery of Pd and Rh from spent catalytic converters. J. Hazard. Mater. 278, 82–90. https://doi.org/10.1016/j.jhazmat.2014.05.099
Ogata, F., Kawasaki, N., 2013. Adsorption of Pt(IV) and Pd(II) by calcined dried aluminum hydroxide gel from aqueous solution system. J. Environ. Chem. Eng. 1, 1013–1019. https://doi.org/10.1016/j.jece.2013.08.011
Pickles, C.A., 2005. MICROWAVE DRYING OF NICKELIFEROUS LIMONITIC LATERITE ORES. Can. Metall. Q. 44, 397–408. https://doi.org/10.1179/cmq.2005.44.3.397
Rajiv Gandhi, M., Yamada, M., Kondo, Y., Shibayama, A., Hamada, F., 2015. Selective extraction of Pd(II) ions from automotive catalyst residue in Cl− media by O-thiocarbamoyl-functionalized thiacalix[n]arenes. Hydrometallurgy 151, 133–140. https://doi.org/10.1016/j.hydromet.2014.11.017

Rampou, M., Ndlovu, S., Shemi, A., 2017. Purification of Coal Fly Ash Leach Liquor for Alumina Recovery Using an Integrated Precipitation and Solvent Extraction Process. J. Sustain. Metall. https://doi.org/10.1007/s40831-017-0142-4

Rao, C.R.., Reddi, G.., 2000. Platinum group metals (PGM); occurrence, use and recent trends in their determination. TrAC Trends Anal. Chem. 19, 565–586. https://doi.org/10.1016/S0165-9936(00)00031-5

Rauch, S., Morrison, G.M., 2008. Environmental Relevance of the Platinum-Group Elements. Elements 4, 259–263. https://doi.org/10.2113/GSELEMENTS.4.4.259

Regel-Rosocka, M., Rzelewska, M., Baczynska, M., Janus, M., Wisniewski, M., 2015. Removal of palladium(II) from aqueous chloride solutions with Cyphos phosphonium ionic liquids as metal ion carriers for liquid-liquid extraction and transport across polymer inclusion membranes. Faculty of Geoengineering, Mining and Geology, Wrocław University of Technology, Wrocław.

Rumpold, R., Antrekowitsch, J., 2012. RECYCLING OF PLATINUM GROUP METALS FROM AUTOMOTIVE CATALYSTS BY AN ACIDIC LEACHING PROCESS, in: Platinum 2012. Presented at the Fifth International Platinum Conference, Sun City, Johannesburg.

Samouhos, M., Taxiarchou, M., Hutcheon, R., Devlin, E., 2012. Microwave reduction of a nickeliferous laterite ore. Miner. Eng. 34, 19–29. https://doi.org/10.1016/j.mineng.2012.04.005

Sasaki, H., Maeda, M., 2014. Zn-vapor pretreatment for acid leaching of platinum group metals from automotive catalytic converters. Hydrometallurgy 147–148, 59–67. https://doi.org/10.1016/j.hydromet.2014.04.019

Schön, A., Dujardin, C., Dacquin, J.-P., Granger, P., 2015. Enhancing catalytic activity of perovskite-based catalysts in three-way catalysis by surface composition optimisation. Catal. Today 258, 543–548. https://doi.org/10.1016/j.cattod.2014.11.002

Shen, Y.-H., Dempsey, B.A., 1998. SYNTHESIS AND SPECIATION OF POLYALUMINUM CHLORIDE FOR WATER TREATMENT. Environ. Int. 24, 899–910.

Sherif, F.G., 1995. Metal carbides, process for making the same and catalytic end-use. US5451389 A.

Sibanye Resources, 2017. Stillwater - Sibanye Resources [WWW Document]. URL https://www.sibanyegold.co.za/our-business/platinum/stillwater/overview (accessed 5.5.17).

Steinlechner, S., Antrekowitsch, J., 2015. Potential of a Hydrometallurgical Recycling Process for Catalysts to Cover the Demand for Critical Metals, Like PGMs and Cerium. JOM 67, 406–411. https://doi.org/10.1007/s11837-014-1263-x

Suoranta, T., Zugazua, O., Niemelä, M., Perämäki, P., 2015. Recovery of palladium, platinum, rhodium and ruthenium from catalyst materials using microwave-assisted leaching and cloud point extraction. Hydrometallurgy 154, 56–62. https://doi.org/10.1016/j.hydromet.2015.03.014

Svecova, L., Papaiconomou, N., Billard, I., 2016. Quantitative extraction of Rh using ionic liquids and its simple separation from Pd. Dalton Trans 45, 15162–15169. https://doi.org/10.1039/C6DT02384C

Treybal, R.E., 2010. Liquid extraction. Lightning Source, Milton Keynes, UK.

Türkay, S., Civelekoğlu, H., 1991. Deacidification of sulfur olive oil. II. Multi-stage liquid-liquid extraction of miscella with ethyl alcohol. J. Am. Oil Chem. Soc. 68, 818–821. https://doi.org/10.1007/BF02660594

Umicore, 2017. Spent Automotive Catalysts [WWW Document]. URL http://pmr.umicore.com/en/recyclables/spent-automotive-catalysts/ (accessed 5.5.17).

Upadhyay, A.K., Lee, J., Kim, E., Kim, M., Kim, B.-S., Kumar, V., 2013. Leaching of platinum group metals (PGMs) from spent automotive catalyst using electro-generated chlorine in HCl solution: Leaching of platinum group metals from spent automotive catalyst. J. Chem. Technol. Biotechnol. n/a-n/a. https://doi.org/10.1002/jctb.4057

Watts, J., Forrest, S.., Clarke, B., Atilan, O., 2008. Future shifts in PGM demand - the impact of technological and economic scenarios on future metal demand., in: Platinum in Transformation. Presented at the Third International Platinum Conference, SAIMM, Sun City, Johannesburg.

Willner, J., Fornalczyk, A., 2015. Dissolution of Ceramic Monolith of Spent Catalytic Converters by Using Hydrometallurgical Methods / Rozpuszczanie Monolitu Ceramicznego Zużytych Katalizatorów Na Drodze Hydrometalurgicznej. Arch. Metall. Mater. 60. https://doi.org/10.1515/amm-2015-0470

Willner, J., Kaduková, J., Fornalczyk, A., Mrážiková, A., Marcinčáková, R., Velgosová, O., 2015. Possibilities Of Metals Extracton From Spent Metallic Automotive Catalytic Converters By Using Biometallurgical Method. Arch. Metall. Mater. 60. https://doi.org/10.1515/amm-2015-0320

Yang, J., Kubota, F., Baba, Y., Kamiya, N., Goto, M., 2014. One step effective separation of platinum and palladium in a acidic chloride solution by using undiluted ionic liquids. Solvent Extr. Res. Dev. 21, 129–135.

Yoder, C.H., 2006. Ionic Compounds: Applications of chemistry to mineralogy. John Wiley & Sons, Inc., Hoboken, NJ, USA. https://doi.org/10.1002/0470075104

Zhang, C., Huang, K., Yu, P., Liu, H., 2013. Ionic liquid based three-liquid-phase partitioning and one-step separation of Pt (IV), Pd (II) and Rh (III). Sep. Purif. Technol. 108, 166–173. https://doi.org/10.1016/j.seppur.2013.02.021

# Appendices

## Appendix A: Preliminary Results

Table A1.1: Total elemental composition for PGMs in autocatalytic converter sample

| Element | **Ag** | **Au** | **Ir** | **Os** | **Pd** | **Pt** | **Rh** | **Ru** | **Al** | **Ce** | **Zr** | **As** |
|---|---|---|---|---|---|---|---|---|---|---|---|---|
| Composition (%) | 0.0 | 0.0 | 0.0 | 0.0 | 0.323 | 0.02 | 0.023 | 0.008 | 9.490 | 3.751 | 14.060 | 0.010 |

| Element | **Ba** | **Bi** | **Br** | **Ca** | **Cl** | **Cr** | **Cu** | **Fe** | **Ga** | **Hf** | **Hg** | **K** | **La** |
|---|---|---|---|---|---|---|---|---|---|---|---|---|---|
| Composition (%) | 0.018 | 0.006 | 0.002 | 0.096 | 0.002 | 0.015 | 0.044 | 0.649 | 0.004 | 0.183 | 0.001 | 0.029 | 1.104 |

| Element | **Mn** | **Mo** | **Nd** | **Ni** | **Pb** | **Rb** | **Se** | **Si** | **Sr** | **Th** | **Ti** | **Tl** |
|---|---|---|---|---|---|---|---|---|---|---|---|---|
| Composition (%) | 0.641 | 0.013 | 0.015 | 0.007 | 0.314 | 0.003 | 0.005 | 1.554 | 2.020 | 0.004 | 0.178 | 0.003 |

| Element | **U** | **V** | **W** | **Y** | **Zn** |
|---|---|---|---|---|---|
| Composition (%) | 0.002 | 0.074 | 0.004 | 0.014 | 0.253 |

## Appendix B: Screenshots of quotations obtained from Bulk Chemical Suppliers

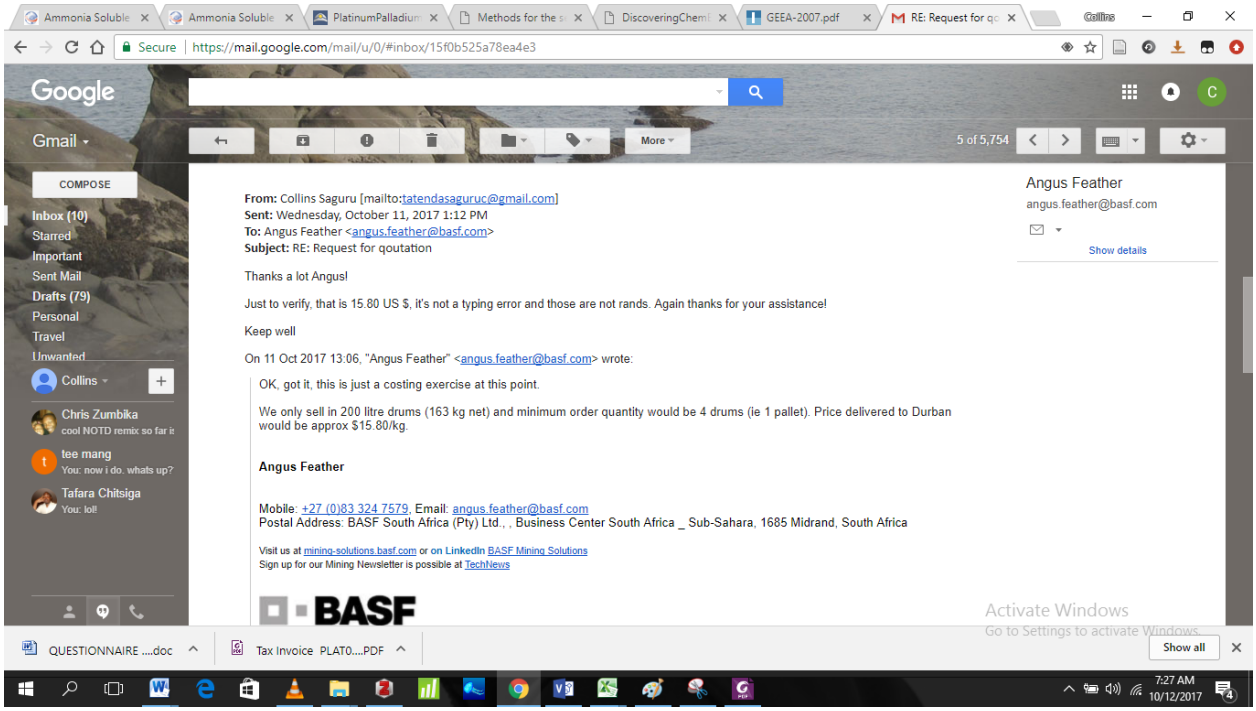


Figure B1.1: Screenshot of quotation for Alamine 308 from BASF

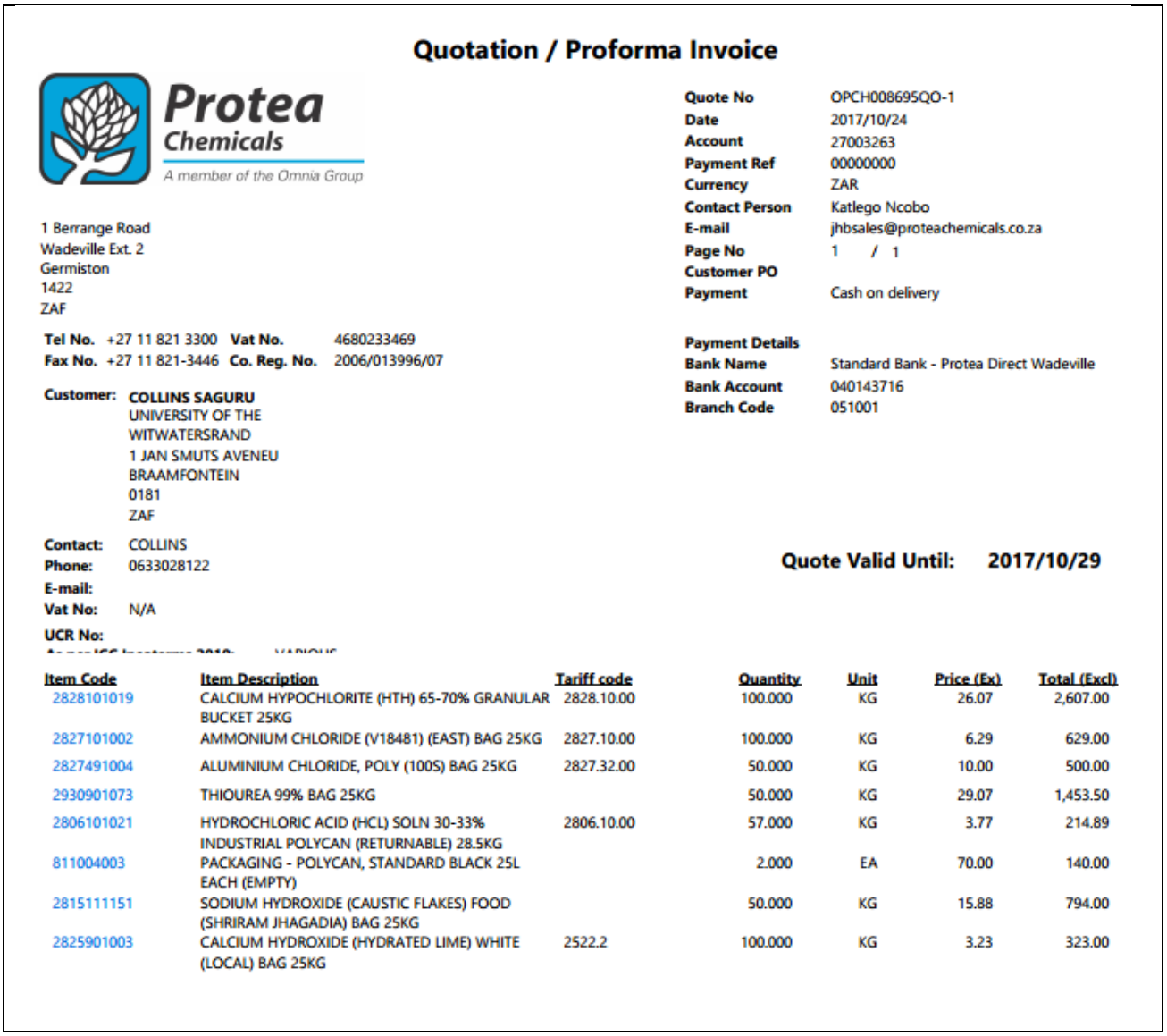

## Quotation / Proforma Invoice

Protea Chemicals
A member of the Omnia Group

1 Berrange Road
Wadeville Ext. 2
Germiston
1422
ZAF

**Tel No.** +27 11 821 3300 **Vat No.** 4680233469
**Fax No.** +27 11 821-3446 **Co. Reg. No.** 2006/013996/07

**Customer:** **COLLINS SAGURU**
UNIVERSITY OF THE
WITWATERSRAND
1 JAN SMUTS AVENEU
BRAAMFONTEIN
0181
ZAF

**Contact:** COLLINS
**Phone:** 0633028122
**E-mail:**
**Vat No:** N/A
**UCR No:**

| | |
|---|---|
| **Quote No** | OPCH008695QO-1 |
| **Date** | 2017/10/24 |
| **Account** | 27003263 |
| **Payment Ref** | 00000000 |
| **Currency** | ZAR |
| **Contact Person** | Katlego Ncobo |
| **E-mail** | jhbsales@proteachemicals.co.za |
| **Page No** | 1 / 1 |
| **Customer PO** | |
| **Payment** | Cash on delivery |

**Payment Details**

| | |
|---|---|
| **Bank Name** | Standard Bank - Protea Direct Wadeville |
| **Bank Account** | 040143716 |
| **Branch Code** | 051001 |

**Quote Valid Until: 2017/10/29**

| Item Code | Item Description | Tariff code | Quantity | Unit | Price (Ex) | Total (Excl) |
|---|---|---|---|---|---|---|
| 2828101019 | CALCIUM HYPOCHLORITE (HTH) 65-70% GRANULAR BUCKET 25KG | 2828.10.00 | 100.000 | KG | 26.07 | 2,607.00 |
| 2827101002 | AMMONIUM CHLORIDE (V18481) (EAST) BAG 25KG | 2827.10.00 | 100.000 | KG | 6.29 | 629.00 |
| 2827491004 | ALUMINIUM CHLORIDE, POLY (100S) BAG 25KG | 2827.32.00 | 50.000 | KG | 10.00 | 500.00 |
| 2930901073 | THIOUREA 99% BAG 25KG | | 50.000 | KG | 29.07 | 1,453.50 |
| 2806101021 | HYDROCHLORIC ACID (HCL) SOLN 30-33% INDUSTRIAL POLYCAN (RETURNABLE) 28.5KG | 2806.10.00 | 57.000 | KG | 3.77 | 214.89 |
| 811004003 | PACKAGING - POLYCAN, STANDARD BLACK 25L EACH (EMPTY) | | 2.000 | EA | 70.00 | 140.00 |
| 2815111151 | SODIUM HYDROXIDE (CAUSTIC FLAKES) FOOD (SHRIRAM JHAGADIA) BAG 25KG | | 50.000 | KG | 15.88 | 794.00 |
| 2825901003 | CALCIUM HYDROXIDE (HYDRATED LIME) WHITE (LOCAL) BAG 25KG | 2522.2 | 100.000 | KG | 3.23 | 323.00 |

Figure B1.2: Screenshot of quotation for Alamine 308 from BASF

## Appendix C: Screenshots of earlier study on pyrometallurgical recycling of catalytic converters

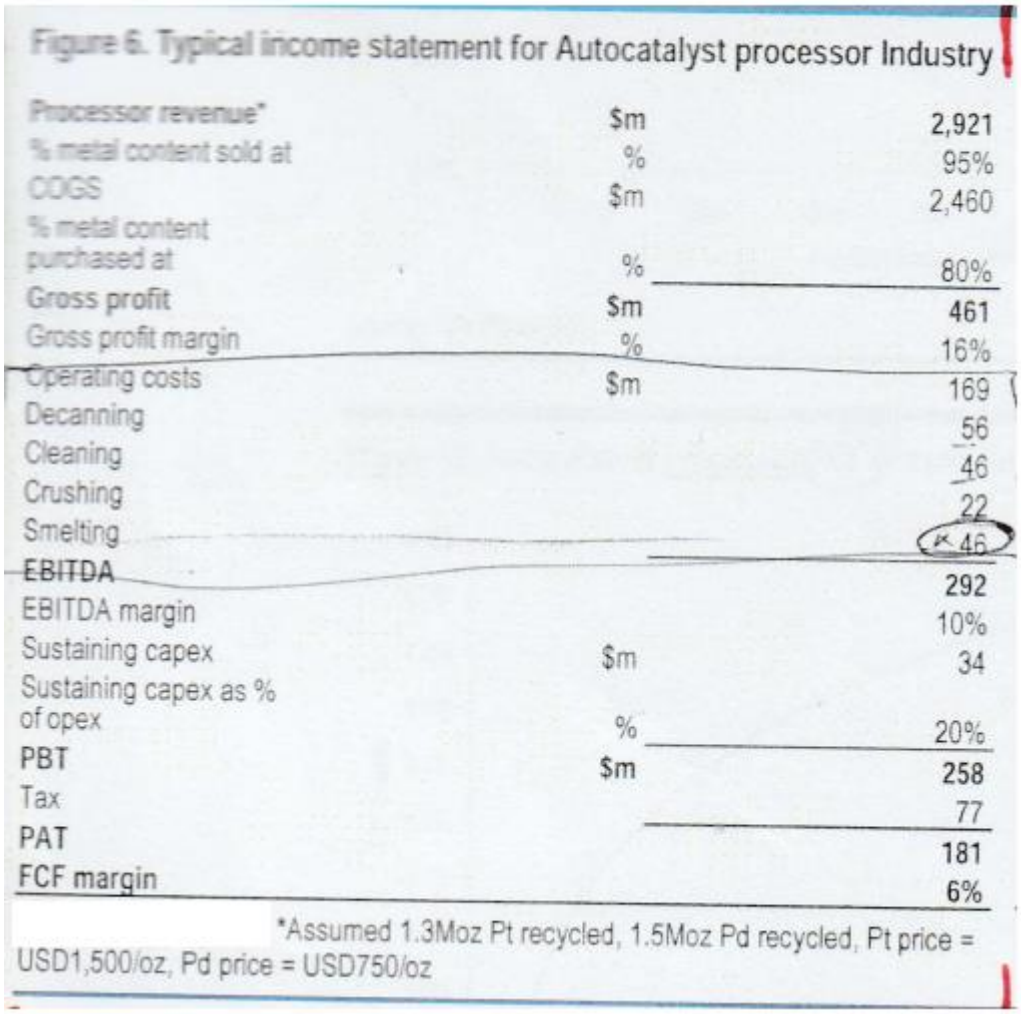

Figure 6. Typical income statement for Autocatalyst processor Industry

| | | |
|---|---|---|
| Processor revenue* | $m | 2,921 |
| % metal content sold at | % | 95% |
| COGS | $m | 2,460 |
| % metal content purchased at | % | 80% |
| Gross profit | $m | 461 |
| Gross profit margin | % | 16% |
| Operating costs | $m | 169 |
| Decanning | | 56 |
| Cleaning | | 46 |
| Crushing | | 22 |
| Smelting | | 46 |
| EBITDA | | 292 |
| EBITDA margin | | 10% |
| Sustaining capex | $m | 34 |
| Sustaining capex as % of opex | % | 20% |
| PBT | $m | 258 |
| Tax | | 77 |
| PAT | | 181 |
| FCF margin | | 6% |

*Assumed 1.3Moz Pt recycled, 1.5Moz Pd recycled, Pt price = USD1,500/oz, Pd price = USD750/oz

Figure C.1: Typical Income statement for auto catalyst processor industry

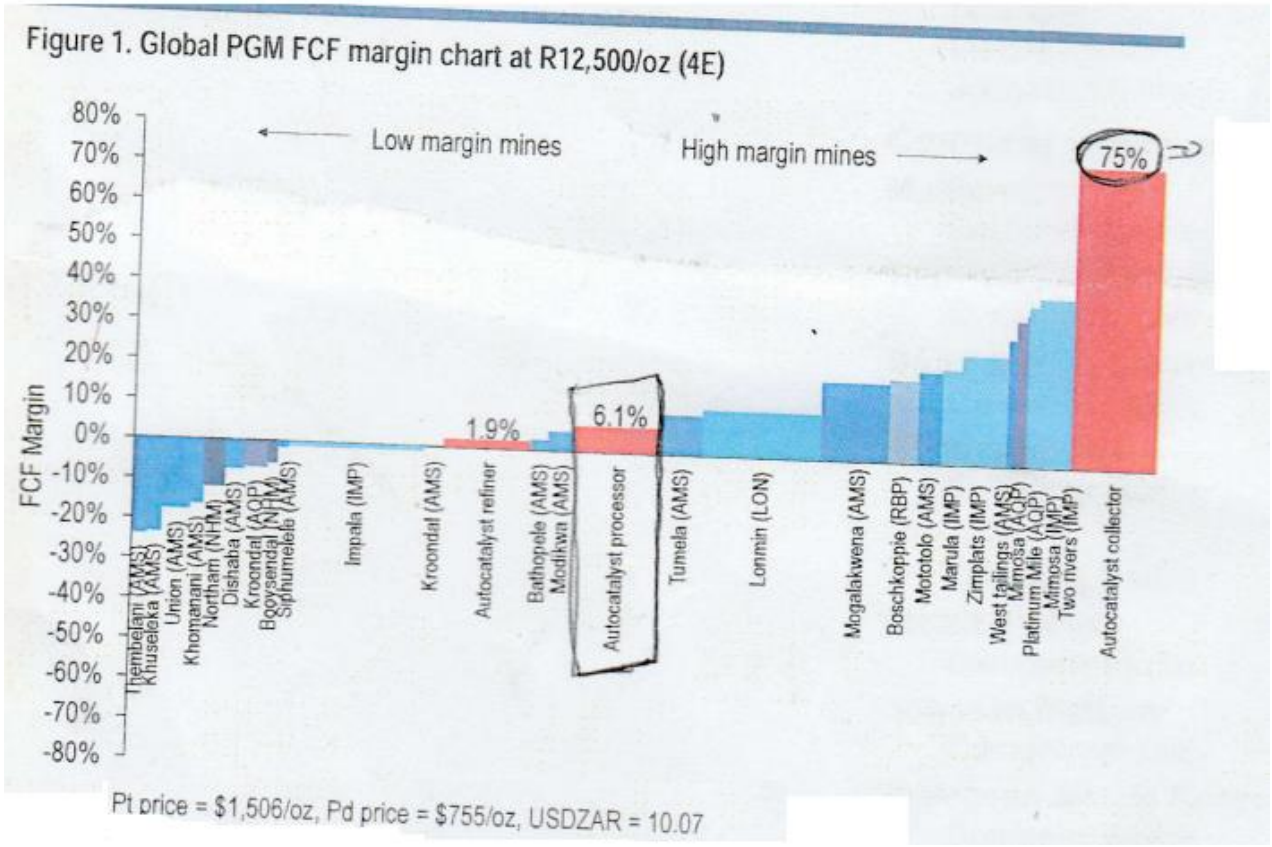


Figure C.2: Typical EBIDA margins for different entities across the PGM value chain